SIMULATING WATER AVAILABILITY IN A SPRING-FED AQUIFER WITH SURFACE WATER/GROUNDWATER FLOW MODELS, GRAND CANYON, ARIZONA

by Jeremiah S. Kobor

A Thesis

Submitted in Partial Fulfillment

of the Requirements for the Degree of

Master of Science

in Geology

Northern Arizona University

August 2004

Approved:

____
Abraham E. Springer, Ph.D., Chair

____
Diana E. Anderson, Ph.D.

____
Ronald C. Blakey, Ph.D.

ABSTRACT

SIMULATING WATER AVAILABILITY IN A SPRING-FED AQUIFER
WITH SURFACE WATER/GROUNDWATER FLOW MODELS,
GRAND CANYON, ARIZONA

JEREMIAH S. KOBOR

Previous modeling efforts suggest that groundwater abstraction from the Redwall-Muav aquifer of the South Rim of the Grand Canyon, has the potential to result in decreased discharges at springs along the South Rim. Evapotranspiration induced by recent drought conditions or reduced recharge induced by long-term climate change may also play a role in diminished spring discharge. To aid in understanding the potential impacts of diminished spring discharges on the woody riparian vegetation associated with these springs, this study presents a coupled local groundwater and surface-water flow model for the riparian aquifer associated with Cottonwood Springs and the results of trend analyses of stream gauge data from Cottonwood Springs and Indian Gardens Springs.

Repeated field observations of the extent and magnitudes of surface-water flows in conjunction with shallow-well data and existing U.S. Geological Survey gauge data, allowed for characterization of spatial and temporal water availability, and provided data with which to calibrate the model to steady-state and transient conditions. The model simulated conditions observed between March, 2003 and January, 2004 and successfully simulated surface-water flow, groundwater flow and stream/aquifer interaction at an unprecedented scale (1-m grid spacing). Fluxes in the transient model were measured along various transects to highlight longitudinal variation in surface-water and

groundwater flow and provide data for future vegetation modeling. During the spring and winter of 2003, the total flux of water was relatively constant throughout the model area and was ~60 m^3/d, and during the summer and autumn of 2003, the total flux of water decreased progressively in the downstream direction from ~60 m^3/d to ~35 m^3/d.

Statistically significant trends of decreasing discharge were observed at Cottonwood and Indian Gardens Springs since 1994. In particular, a 19% decrease in winter discharge was observed at Cottonwood Springs and a 25% decrease was observed at Indian Gardens Springs. These trends of decreasing discharge coupled with ongoing groundwater pumping and climate predictions of continuing drought suggest that there is a potential for alteration to South Rim spring-fed ecosystems over relatively short timescales.

ACKNOWLEDGMENTS

Major funding for this project was provided by a grant from Grand Canyon National Park passed through the Colorado Plateau Cooperative Ecosystem Studies Unit. This grant was financed by Fee Demonstration Funds collected at Grand Canyon National Park. Additional funding was provided by a research grant from the Geological Society of America, and scholarships from the Friday Lunch Clubbe, Montgomery and Associates, and the L.B.C. McCullough Foundation.

This project would not have been possible were it not for the support and advice provided by a host of individuals. Dr. Abe Springer was instrumental in developing the concept for this project and in obtaining funding for its execution, additionally he provided continuous and much appreciated guidance throughout the modeling and text editing processes. Dr. Diana Anderson was particularly helpful in the field, and I wish to thank her along with Dr. Ronald Blakey for editing the text and for serving on my committee. I wish to thank my collaborators on this project at the USGS in Fort Collins, Mike Scott and Pat Shafroth; I really enjoyed working with you and learned a lot throughout our collaboration, especially in the field setting. Steve Monroe at the USGS in Flagstaff was very helpful both through insightful discussions and by providing stream gauge data. I also wish to acknowledge John Rihs who served as the National Park Service Technical Representative, at Grand Canyon National Park.

Sean Welch spent hours teaching me how to survey just because he knew I needed the help, thank you. James Rumbaugh at Environmental Simulations Inc. was very generous with his time and provided much needed assistance with the modeling software. Siobhan McConnell was unfortunate enough to have to live with me throughout the thesis process, and was supportive and kind throughout, despite my reoccurring grumpiness. Many foolish souls agreed to assist me in the field (read: carry ridiculously heavy packs into the canyon during inclement weather), including Cubbie Miller, Siobhan McConnell, Eric Adams, Lanya Ross, Brandon Hugart, Armondo Lamadrid, Caroline Harris, Bill Fry, Ben Siwek, and Trent Newkirk; thanks for all your help.

TABLE OF CONTENTS

LIST OF TABLES

LIST OF FIGURES

LIST OF APPENDICES

<u>LIST OF PLATES</u>

PREFACE

Chapter 2 of this thesis was written as a manuscript for publication in a journal. The remaining chapters provide additional details of the study which may be duplicated in Chapter 2. Chapter 1 discusses the regional and local hydrogeology of the study area and summarizes previous relevant research. Chapter 3 discusses the methods used to characterize the site and collect data for model calibration and the results of the characterization. Chapter 4 summarizes the findings of the study. In order to maintain the flow of discussion while reading this thesis, the author suggests that the reader read Chapters 1, 3, and 4 separately from Chapter 2.

CHAPTER ONE

INTRODUCTION

Purpose

Since 1989, increasing population growth and water demand on the Coconino Plateau Sub-Basin of Arizona has led to the development of the Redwall-Muav aquifer of the South Rim of the Grand Canyon as a water supply, with potential abstraction rates up to 1.1 x 10^6 m^3/yr (900 ac-ft/yr). This abstraction has the potential to result in decreased discharges at the over 20 springs (Kessler, 2002) on the South Rim (Fig. 1). Such decreases will result in reduced baseflow conditions in the spring-fed channels of the Grand Canyon and larger depths to groundwater beneath the associated floodplains of these channels. These changes will alter the timing and magnitude of water available to woody riparian vegetation potentially leading to mortality of cottonwood (*Populus*), willow (*Salix*), and other riparian species. Damage to native riparian vegetation could in turn lead to negative impacts to both aquatic and terrestrial organisms. This study examines temporal trends in discharge at two South Rim Springs, and presents local, coupled, surface-water and groundwater flow models for the riparian aquifer associated with one of the smaller of the South Rim springs, Cottonwood Springs (Fig. 2). In conjunction with field data, the models provided estimates of surface-water and groundwater availability for use in the future development of a vegetation water-use model. The results were used to estimate the potential for future decreases in discharge at South Rim Springs, and associated decreases in water availability in the spring-fed riparian aquifers.

Objectives

Specific objectives of this study were to:

1) Examine existing U.S. Geological Survey gauge data to quantify temporal trends in discharge at Cottonwood and Indian Gardens Springs, and estimate future discharges by exploring the potential factors influencing the trends,
2) Characterize the topography and geology of the fluvial deposits in the riparian zone associated with Cottonwood Springs, and calculate channel morphologic parameters and hydrologic properties of the various hydrostratigraphic units,
3) Develop a conceptual water budget and characterize the spatial and temporal patterns of surface-water and groundwater availability and plant-water usage,
4) Develop both a steady-state and a transient, groundwater and surface-water flow model, and calibrate the models to observed surface-water and groundwater conditions,
5) Use the models to quantify variations in surface-water and groundwater flux in the riparian aquifer for use in future vegetation modeling,
6) Based on the results, make management recommendations regarding the potential for diminished spring discharge at South Rim Springs, and associated reductions in water availability in the spring-fed riparian aquifers.

Hydrogeologic Setting

The Coconino Plateau Sub-Basin is a Cenozoic aged, upland, physiographic province located on the southern edge of the Colorado Plateau (Fig. 1), and consists of

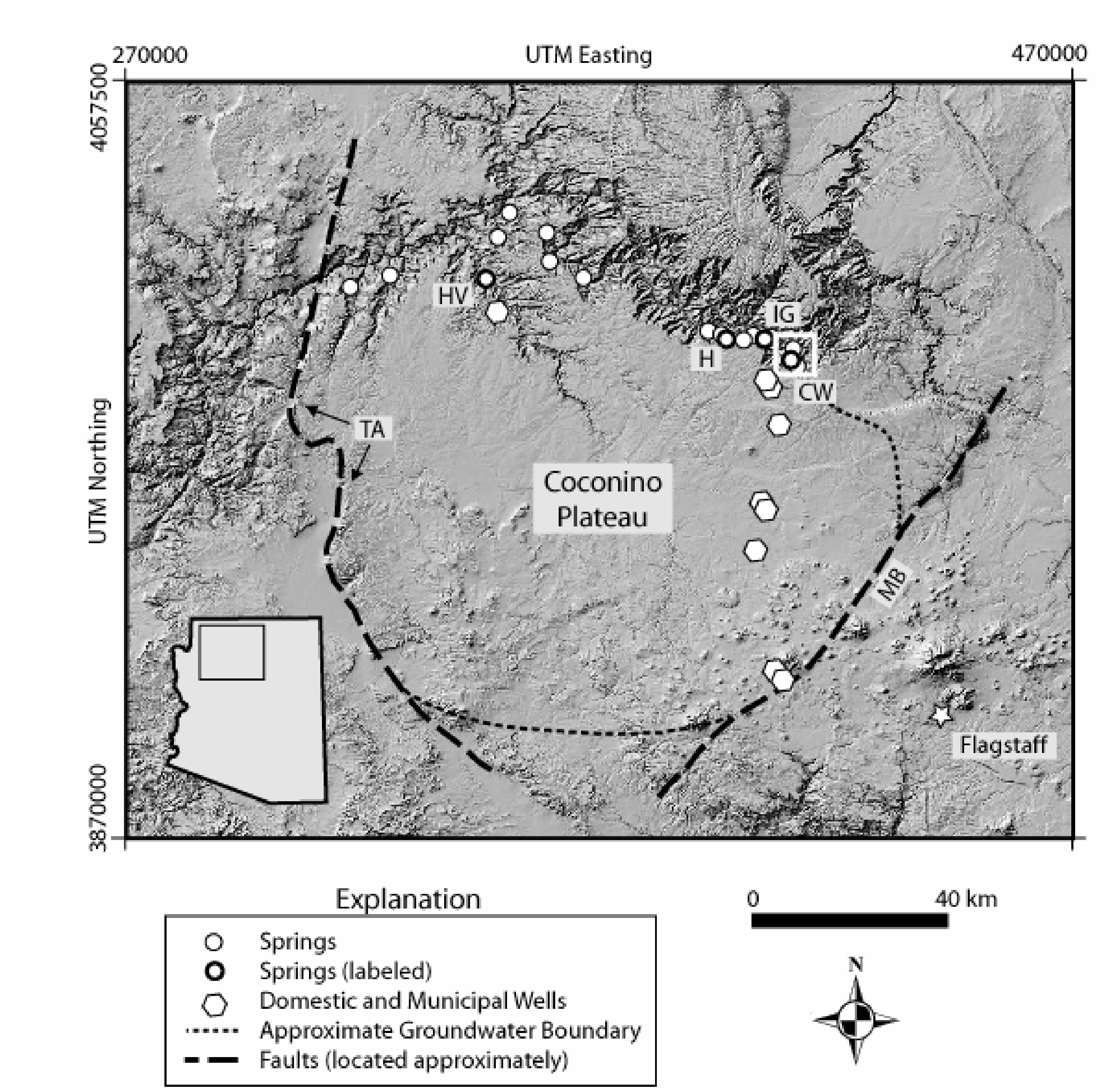

Figure 1: Map of the Coconino Plateau showing wells, springs, and regional groundwater boundaries. Abbreviations are Havasu Springs (HV), Hermit Springs (H), Indian Gardens Springs (IG), Cottonwood Springs (CW), Toroweap-Aubrey Fault System (TA), and Mesa Butte Fault (MB). The area in the white square is shown in detail in Fig. 2. Structures and groundwater boundaries after Kessler (2002). Wells after ADWR Arizona Well Registry Distribution Database 3rd ed.

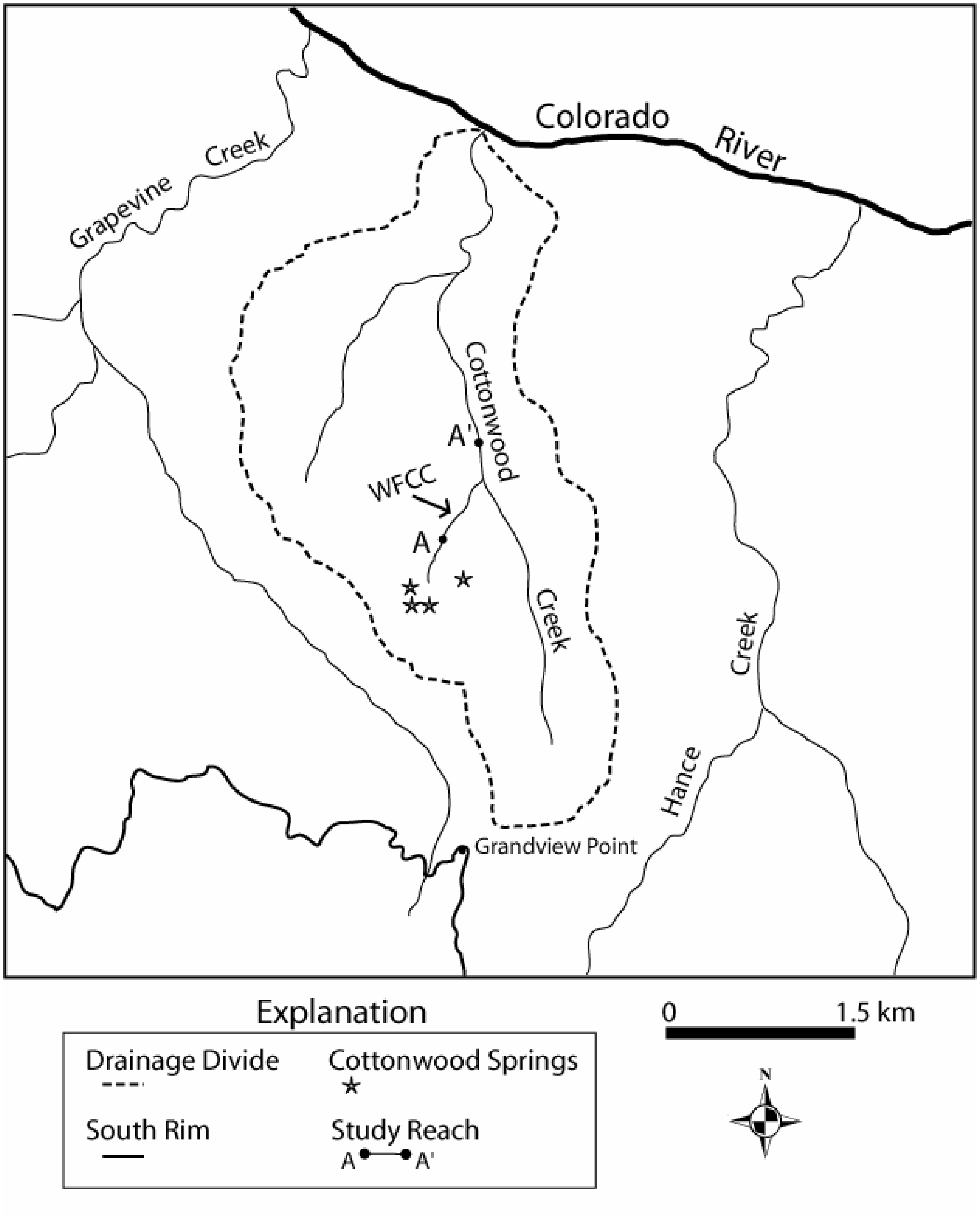

Figure 2: Map showing locations of bedrock wall source springs, principle streams, West Fork Cottonwood Creek (WFCC) and extent of the study reach at Cottonwood Springs.

relatively horizontal layers of Paleozoic strata underlain by Precambrian basement (Fig. 3). For a comprehensive treatment of these units see Billingsley and Hendricks (1989), and Beus and Morales (2003). Groundwater resources consist of perched water-bearing zones, a regional aquifer, and the regionally extensive Redwall-Muav aquifer (Bills and Flynn, 2002). Most of the streams on the plateau are ephemeral, however numerous seeps and springs support short perennial reaches in many streams.

The Redwall-Muav aquifer is composed of the water-bearing zones in the Redwall and Muav Limestones, and in the Temple Butte Formation and Devonian limestones where present (Metzger, 1961; Harshbarger & Associates, Inc., 1973). Primary porosity is low in the aquifer and secondary porosity occurs primarily as a result of dissolution enhancement along faults and fractures. Groundwater flow is thought to be controlled primarily by the numerous structural features on the plateau including the Havasu Downwarp, the Kaibab Monocline, the Aubrey Cliffs, and the Mogollon Escarpment.

Numerous springs discharge from the Redwall-Muav aquifer on the Coconino Plateau Sub-Basin along the South Rim of the Grand Canyon including Havasu Springs, Indian Garden Springs, Hermit Springs, and at least 17 smaller springs (Kessler, 2002) (Fig. 1). To the south of the Coconino Plateau, springs from the Redwall-Muav aquifer discharge to the Verde River and its tributaries (Montgomery and Associates, 1996; 1998). Most of the South Rim springs discharge from the Redwall or Muav Limestones where flow is confined by the underlying, low-permeability Bright Angel Shale (Fig. 3). Havasu Spring is an exception as it discharges from the overlying Supai Formation. The locations of the South Rim springs are largely controlled by structural features. For

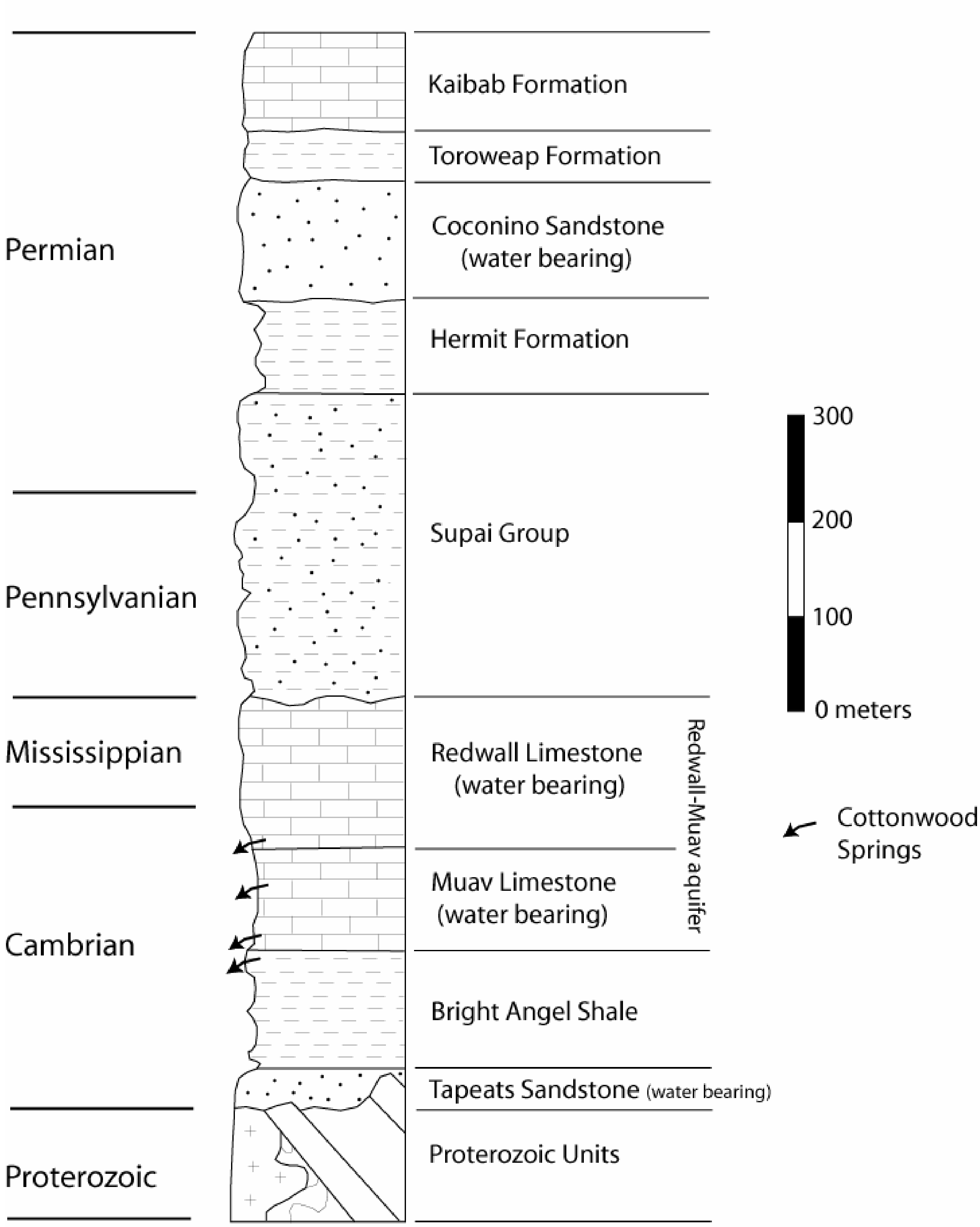

Figure 3: Generalized stratigraphic section of the Grand Canyon and Coconino Plateau, showing water-bearing units and location of Cottonwood Springs. The Redwall and Muav Limestones comprise the regional aquifer on the Coconino Plateau. Modified from Beus and Morales (2003) and Blakey (2004).

example, Havasu Springs is associated with interaction of the Havasu Downwarp and Havasu Springs Fault, Indian Gardens Springs is associated with the Bright Angel Fault, and Hermit Springs is associated with the Hermit Fault (Billingsley and Huntoon, 1983; Huntoon and Billingsley, 1996). Approximately 5.9 x 10^7 m^3/yr of water discharge from all of the springs and seeps along the South Rim of the Grand Canyon (Kessler, 2002), nearly 98% of which discharges at Havasu Springs.

Description of Aquifer Units

Muav Limestone

In the eastern Grand Canyon, the Middle Cambrian Muav Limestone is ~50 m thick and consists predominantly of thin-bedded, nodular, and mottled limestone and dolostone (Rose, 2003). The formation overlies the Bright Angel Shale and forms resistant cliffs. Additional lithologies include pebble conglomerates, fine-grained sandstone, silty limestone, and bioturbated siltstone (Middleton and Elliott, 2003; Rose, 2003). The contact with the underlying Bright Angel Shale is gradational and complex intertonguing of the two formations occurs (Middleton and Elliot, 2003).

Redwall Limestone

In the eastern Grand Canyon, the Early to Late Mississippian Redwall Limestone is ~150 m thick consists of four distinct stratigraphic members (Beus, 2003). The formation overlies the Muav Limestone and forms massive, vertical cliffs. The lowest member is the Whitmore Wash Member which consist of fine-grained dolomite (Beus, 2003). Overlying this member is the Thunder Springs Member which consists of thinly-bedded limestone and dolomite alternating with thinly-bedded chert. The overlying Mooney Falls Member consists of limestone with minor chert lenses. The upper most member is the Horseshoe Mesa Member which consists of thinly-bedded limestone with a mudstone to wackestone texture and minor chert lenses (Beus, 2003).

Previous Modeling Efforts

Several groundwater flow models have been built for the Redwall-Muav aquifer of the Coconino Plateau Sub-basin. Montgomery and Associates (1996; 1998) constructed a two-dimensional groundwater flow model and found that up to a 30% decrease in discharge at some South Rim springs may occur after 100 yrs of pumping at current abstraction rates. Wilson (2000) constructed a three-dimensional groundwater flow model with similar boundaries and parameters to the Montgomery and Associates model. These two models only simulated discharge from the three major springs, Havasu Springs, Hermit Springs, and Indian Gardens Springs. Wilson's model was expanded by Kessler (2002) to simulate discharge at 20 of the South Rim Springs. Kessler (2002) defined capture zones for and flow paths to these 20 springs using particle-tracking and capture-zone analysis. Springer and Kessler (personal communication) presented the results of transient simulations of the model and found that current pumping may lead to significant decreases in discharge of the South Rim Springs between and including those associated with the Vishnu and Bright Angel faults.

Study Site

This study focuses on one of the smaller of the South Rim springs, Cottonwood Springs. Cottonwood Springs is located near the eastern margin of the groundwater basin, between Grapevine and Hance Springs (Figs. 1-2). Like most of the South Rim springs, Cottonwood consists of a series of small springs rather than a single source, some of which are likely buried beneath recent colluvial material. Most of the ~55 m^3/day of winter baseflow exits from the middle and upper portions of the Muav Limestone. After exiting the aquifer, water enters colluvial material almost immediately, and flows subsurface for ~500 m before appearing as channelized base flow. No springs occur at the headwaters of the main stem of Cottonwood Creek (CC); instead they are located at the headwaters of a small tributary to Cottonwood Creek, referred to in this study as West Fork Cottonwood Creek (WFCC) (Fig. 2).

The small discharges and diffuse nature of the spring orifices at Cottonwood Springs, makes direct measurement of total spring discharge at the bedrock sources impossible. Because of this, the highest measured values of baseflow in the channel downstream from the colluvial subsurface reach were assumed to represent total spring discharge. These measurements indicate that spring discharge was ~38 m^3/day during the study. Despite this small discharge, dense stands of cottonwoods, willows, and other riparian species are supported along a ~1 km reach below the springs. Most of the vegetation is restricted to the reach underlain by Bright Angel Shale, as downstream of this the relatively wide floodplain formed by the weak shale gives way to an incised canyon cut into the resistant Tapeats Sandstone.

CHAPTER 2

JOURNAL MANUSCRIPT

1. Introduction

One challenge of modern water management is to provide for human water requirements without compromising the availability of water to associated ecosystems. This challenge is particularly difficult in the arid Southwestern U.S. where ~60% of all species are directly dependent on riparian areas (Tellman et al., 1997) and the water resources needed to meet an increasing water demand are scarce. In the Grand Canyon, springs are extremely significant ecologically, and more than 11 % of the flora of the region occur obligatorily or facultatively at springs, seeps or natural ponds (Stevens and Ayers, 2002). Changes to hydrologic systems due to groundwater pumping, surface-water diversions, and flow regulation by dams have resulted in the loss or alteration of much of the pre-American settlement riparian vegetation in the Southwestern U.S. (Tellman et al., 1997; Busch and Smith, 1995; Rood et al., 1995; Stromberg et al., 1996; Scott et al., 1997, 1999). Effective management and restoration of riparian ecosystems requires an interdisciplinary understanding of the dynamics between hydrologic and ecologic processes.

Numerous springs discharge from the regional Redwall-Muav aquifer of the Coconino Plateau Sub-Basin along the South Rim of the Grand Canyon, AZ (Fig. 4). This groundwater discharge provides base flow for many first-order tributaries to the Colorado River and supports dense stands of native riparian vegetation in an otherwise xeric landscape. Increasing population growth and development on the Coconino Plateau

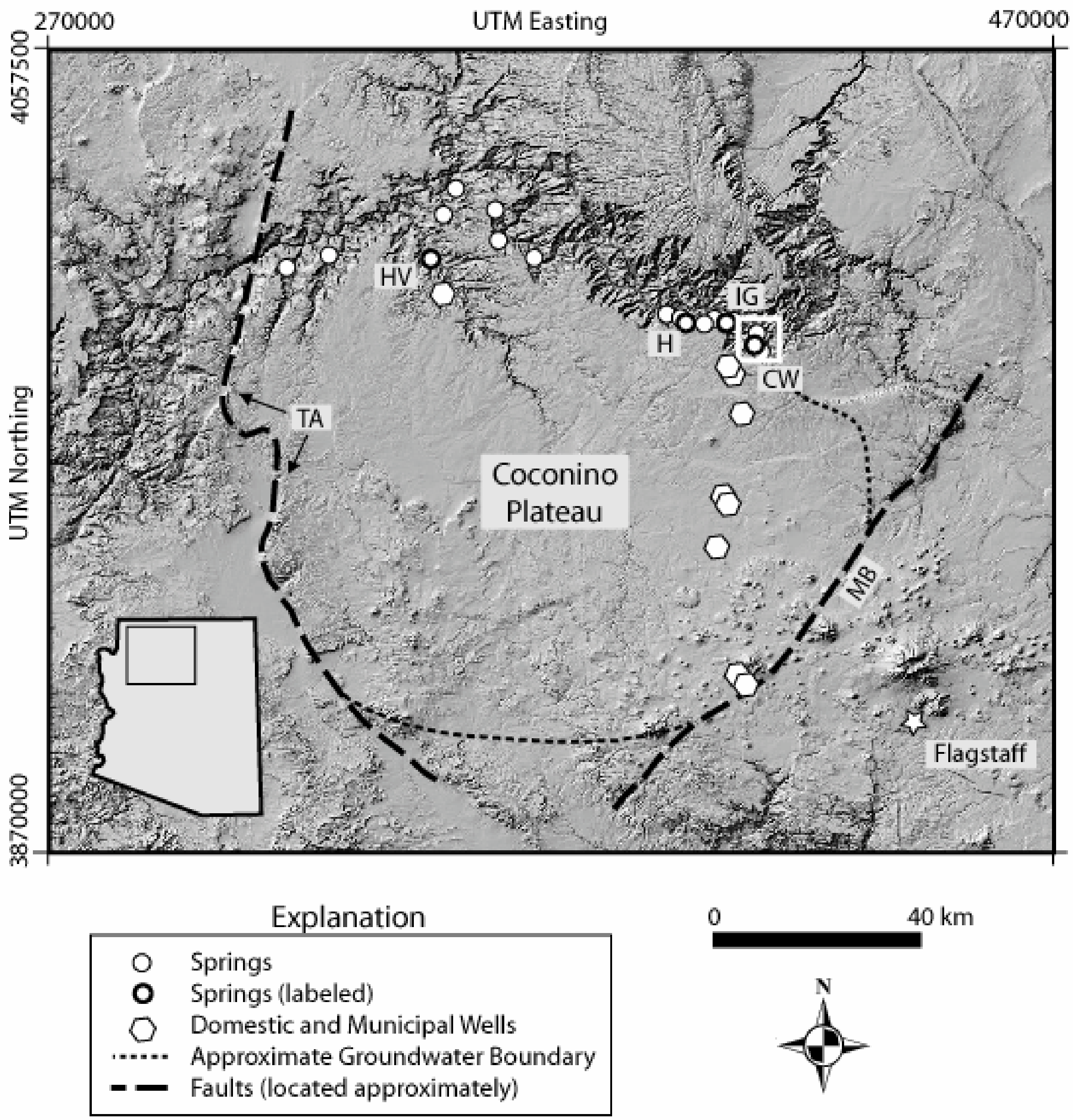

Figure 4: Map of the Coconino Plateau showing wells, springs, and regional groundwater boundaries. Abbreviations are Havasu Springs (HV), Hermit Springs (H), Indian Gardens Springs (IG), Cottonwood Springs (CW), Toroweap-Aubrey Fault System (TA), and Mesa Butte Fault (MB). The area in the white square is shown in detail in Fig. 2. Structures and groundwater boundaries after Kessler (2002). Wells after ADWR Arizona Well Registry Distribution Database 3rd ed.

led to the initial development of the Redwall-Muav aquifer as a water supply in 1989, with potential abstraction rates up to ~1.1 x 10^6 m^3/yr. The majority of this water is abstracted and used in the vicinity of Tusayan, a small community located just outside of Grand Canyon National Park, approximately 10 km south of the South Rim. As part of an Environmental Impact Statement for Tusayan growth, Montgomery and Associates (1996; 1998) constructed a transient, two-dimensional groundwater flow model for the Redwall-Muav aquifer and concluded that after 100 yrs of pumping at current abstraction rates, up to a 30% decrease in discharge may occur at the three major South Rim springs. A three-dimensional groundwater flow model was constructed by Wilson (2000), and an expansion of the model defined capture zones for and flow paths to twenty of the South Rim springs (Kessler, 2002). Springer and Kessler (personal communication) presented the results of transient simulations of the model and found that current pumping could result in significant decreases in discharge at some South Rim springs, perhaps over relatively short time scales (years).

The development of numerical modeling codes to simulate the complex process of surface water/groundwater exchange has been the topic of recent studies (Prudic, 1989; Swain and Wexler, 1996; Shibing et al., 2002). Few modelers, however, have applied these codes to simulate stream/aquifer interaction in field sites at a fine resolution, particularly in arid and semi-arid regions, and adequate simulation of stream/aquifer interaction has proven to be difficult. Bissett (1994) constructed and calibrated a surface-water and groundwater flow model for a small ephemeral stream aquifer in Golden, Colorado and found that stream/aquifer interaction was highly sensitive to the size of the model cells. Further studies applying the model codes to a diverse range of field sites are needed in order to fully test the ability of these codes to properly simulate stream/aquifer interaction.

Numerical surface-water and groundwater models provide a means of quantifying changes in water availability resulting from changing climate or human water-use. Because of the tight coupling of hydrologic and ecologic systems in arid and semi-arid riparian landscapes, riparian vegetation distributions can be largely understood in terms of moisture availability gradients (Franz and Bazzaz, 1977; Shafroth et al., 1998; 2000; Rains et al., 2004). Vegetation has been modeled as a function of elevation relative to stream stage (Franz and Bazzaz, 1977), as well as inundation duration (Auble et al., 1994; Primack, 2000; Rains et al., 2004), and depth to groundwater (Springer et al., 1999b Rains et al., 2004). These studies have focused on evaluating the vegetative response to hydrologic change resulting from changes in reservoir operation or climate, and have modeled vegetation using one or two hydrologic variables. In contrast, this study focused on evaluating the effects of diminished spring discharges potentially due to groundwater pumping or climate change, and quantified surface-water and groundwater fluxes for use in future vegetation modeling.

This study focused on the construction of local, coupled, numerical surface-water and groundwater flow models for the riparian aquifer associated with one of the smaller of the South Rim springs, Cottonwood Springs (Fig. 5). The models were calibrated to observed surface-water and groundwater conditions, and in conjunction with projections of decreasing springs discharge trends, was used to predict the impacts of diminished spring discharge on groundwater and surface-water availability in the spring-fed riparian

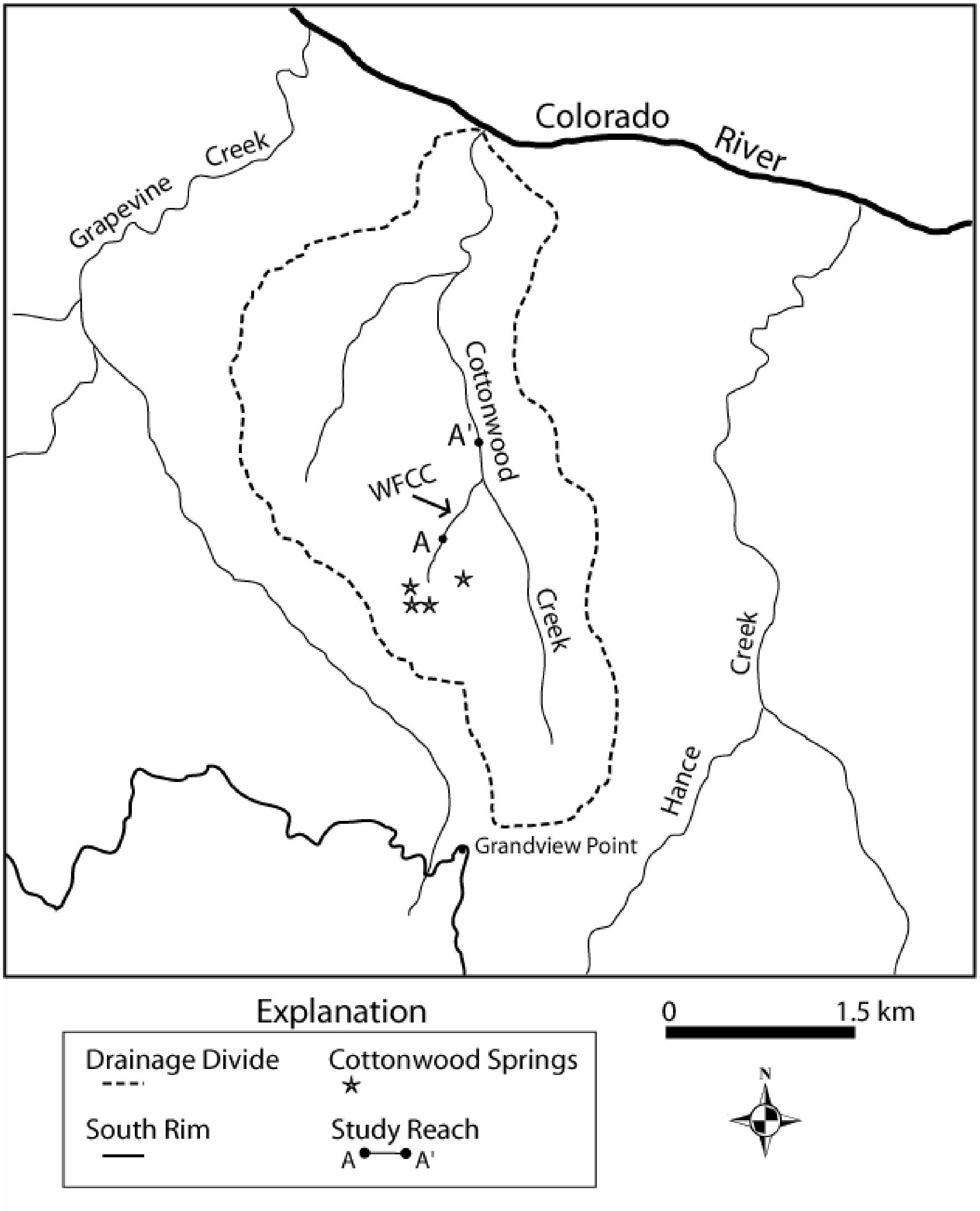

Figure 5: Map showing locations of bedrock wall source springs, principle streams, West Fork Cottonwood Creek (WFCC) and extent of the study reach at Cottonwood Springs.

aquifer. Future studies will involve the development of a vegetation water-use model, which in conjunction with the models presented here will be used to estimate the response of riparian vegetation to decreases in water availability based on various diminished spring discharge scenarios.

2. Site Description

The Redwall-Muav aquifer is located on the Coconino Plateau Sub-Basin at the southern edge of the Colorado Plateau in northern Arizona (Fig. 4). The principle water-bearing units are the Redwall and Muav Limestones, the Temple Butte Formation, and Devonian limestones where present (Metzger, 1961; Harshbarger & Associates, Inc., 1973). Primary porosity is low in the aquifer and secondary porosity occurs primarily as a result of dissolution enhancement along faults and fractures. Groundwater flow is controlled primarily by the numerous structural features on the plateau, and the regional groundwater boundary is thought to be bounded on the west by the Toroweap-Aubrey Fault System and to the east by the Mesa Butte Fault (Fig. 4) (Montgomery and Associates, 1996; 1998).

Numerous springs discharge from the northern exposure of the aquifer along the South Rim of the Grand Canyon, including Havasu Springs, Indian Garden Springs, Hermit Springs, and at least 17 smaller springs (Kessler, 2002) (Fig. 4). Along the southern exposure of the aquifer, springs discharge into the Verde River and it’s tributaries (Montgomery and Associates, 1996; 1998). Many of the South Rim springs discharge near the base of the aquifer due to the underlying Bright Angel Shale, which acts as the lower confining unit for the aquifer. The locations of the springs are largely controlled by structural features, for example, Havasu Springs is associated with interaction of the Havasu Downwarp and Havasu Springs Fault, Indian Gardens Springs is associated with the Bright Angel Fault, and Hermit Springs is associated with the Hermit Fault (Billingsley and Huntoon, 1983; Huntoon and Billingsley, 1996). Approximately 5.9 x 10^7 m^3/yr of water discharge from all of the springs and along the South Rim of the Grand Canyon (Kessler, 2002), of which nearly 98% discharges at one major spring complex, Havasu Springs.

This study focuses on one of the smaller discharge South Rim springs, Cottonwood Springs. Cottonwood is located near the eastern margin of the groundwater basin between Grapevine and Hance Springs (Fig. 5). No springs occur at the headwaters of the main stem of Cottonwood Creek; instead they are located at the headwaters of a small tributary to Cottonwood Creek, referred to in this study as West Fork Cottonwood Creek (WFCC) (Fig. 5). Like many other South Rim springs, Cottonwood consists of a series of small, distributed spring orifices rather than a single source, many of which are buried beneath recent colluvial material. Mean daily discharge is approximately 55 m^3/d, and stands of cottonwood, willow, and other riparian species are supported along an ~1 km reach below the springs.

3. Methodology

3.1 Site Characterization

Discharge data from 1994 to 2003 at U.S. Geological Survey (USGS, 2002; 2004a) stream gauges located at Cottonwood Springs (Fig. 6; Plate 1a) and

Indian Gardens Springs were collected and analyzed. Mann-Kendall statistical analyses were performed on the gauging data from Cottonwood Springs and Indian Gardens Springs to determine any significant trends in mean daily discharge during the Winter. Because the Cottonwood Springs gauge recorded days with zero discharge, an additional analysis was conducted to determine if there were any significant trends to the number of days without flow at the Cottonwood Springs gauge. Because periods of zero discharge at the gauge occurred during the growing season and a trend may represent a vegetative response to climate as opposed to a groundwater pumping induced decrease in spring discharge, the trend in the 3-day average winter discharge was analyzed such that vegetative control would be minimized. Linear regression of the winter discharge data was used to project the discharge trends into the future, and provide estimates of future discharge values. To explore the trend in climate at the site, precipitation data from stations on the South Rim (NOAA, 2004b) were compiled and mean values for a series of multidecadal precipitation regimes were calculated (Hereford et al., 2002).

A 1-meter contour interval topographic base map was produced for the site from surveying conducted with an electronic Total Station (Topcon Positioning Systems Inc., Pleasanton, CA), and used to produce a detailed geomorphic and geologic map of the study area (Fig. 6; Plate 1a). The horizontal point closure ratio of the survey was 1:12,000 and the elevation misclosure was 0.028 ft. Geologic mapping methods consisted of measuring and plotting the distances from the thalweg to various geologic contacts and interpolating between measurements to define contacts on the topographic base map. The topographic and geologic data were used in conjunction with geologic data collected

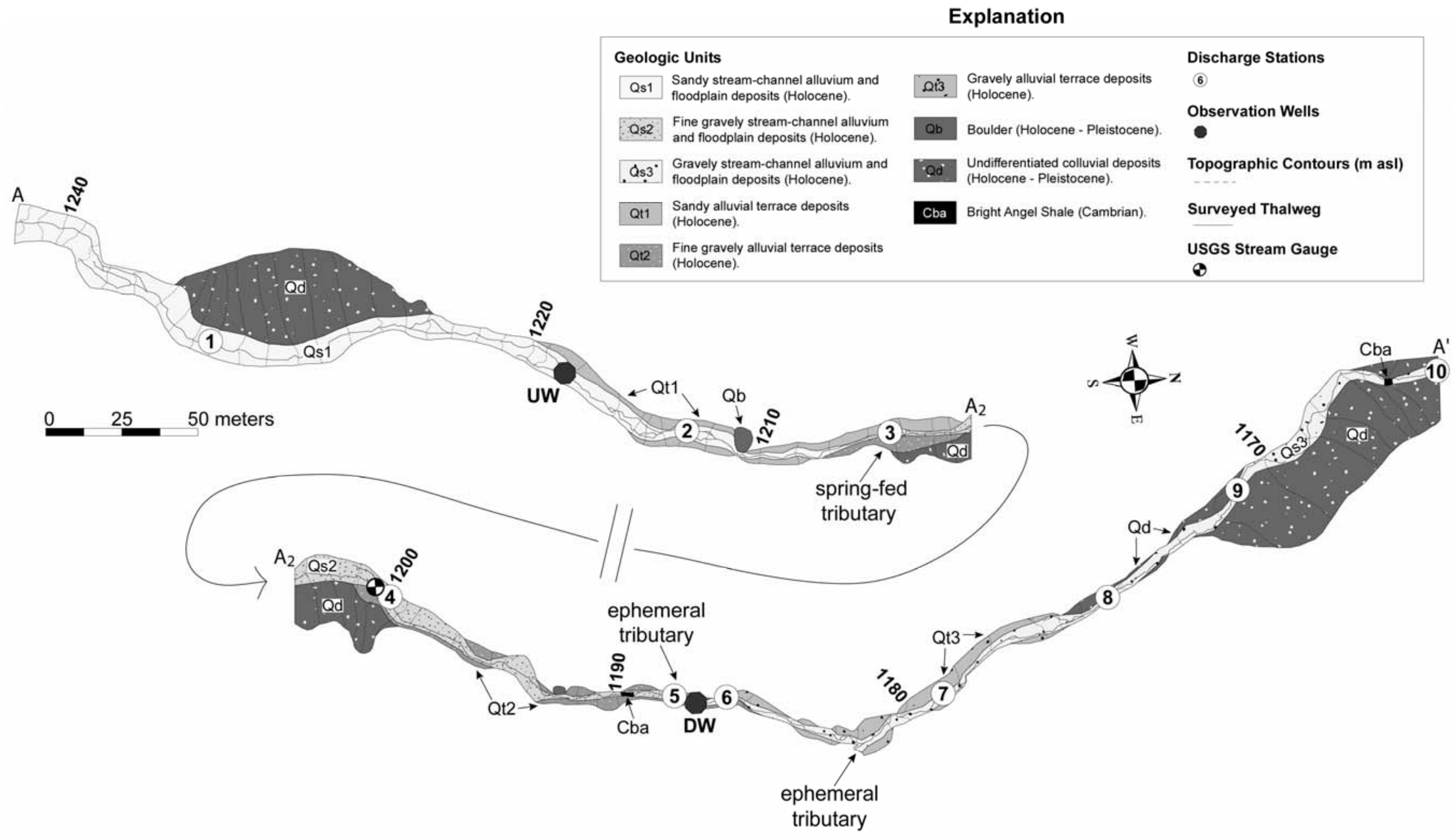

Figure 6: Topographic and geologic map of the study area at Cottonwood Springs (A - A' on Fig. 5), showing locations of discharge stations and observation wells (contour interval is 1 meter).

at depth to construct two generalized geologic cross-sections perpendicular to the main channel and one section longitudinal to the channel.

To characterize the seasonal range of water availability, twelve field visits were made to the site between February, 2003 and April, 2004. Stream discharge was measured on these visits at 8-10 locations in the channel using a v-notch weir, and the extent of dry and flowing reaches was mapped. Two shallow observation wells were installed in the channel bed and equipped with pressure transducers (Solonist, Waterloo, Ontario) which recorded water-levels at 15-minute intervals from July, 2003 to April, 2004.

3.2 Water Budget

A conceptual water budget for Cottonwood Springs was constructed using stream gauging data (USGS, 2002; 2004a), precipitation data from stations at Grand Canyon Village, AZ and Phantom Ranch, AZ (NOAA, 2004a; 2004b), pan evaporation data from stations throughout Arizona (WRCC, 2001), vegetation data (Scott and Shafroth, unpublished data) in conjunction with literature ET values, and stream discharge measurements taken during this study.

3.3 Surface and Groundwater Modeling

Groundwater flow was simulated using the modular, three-dimensional, finite difference groundwater flow model MODFLOW-2000 (McDonald and Harbaugh, 1984; Harbaugh et al., 2000). Surface flow was routed and surface water/groundwater interactions were simulated with a stream flow routing package (Prudic, 1989), and an evapotranspiration package was used to simulate plant water usage. Groundwater Vistas v.3.45 (Environmental Simulations Inc., Reinhold, PA) was used with MODFLOW-2000 for pre- and post-processing. The Link-Algebraic Multigrid (LMG) solver (Mehl and Hill, 2001) was used with default settings. An evenly spaced grid composed of 1-m by 1-m square grid cells was constructed for the ~10,000 m^2 model area (Fig. 7; Plate 1b). The choice of cell size was determined by the scale and accuracy of available data (survey data, gauging data) and the desired detail of the model output. The aquifer was modeled as a single layer of variable thickness with constant hydraulic properties with depth.

A steady-state groundwater and surface-water flow model was constructed to simulate the maximum water availability condition and to provide an initial hydraulic head distribution for the transient simulation. The model was calibrated to field data collected on March 21, 2003. This date was chosen because it represents the earliest date of data collection and the date on which the highest water availability conditions were observed. Calibration was accomplished by varying the hydraulic conductivity values and distributions and streambed conductance values within a reasonable range based on field observations and literature values. Additionally, different types of boundary conditions were examined for the upstream and downstream ends of the model.

Five of the ten discharge stations were selected as discharge calibration targets (see Fig. 6 and Plate 1a for locations). The targets were chosen based on the number of observations at the station and to provide spatial representation of model area. Residuals were calculated as the difference between the observed discharge at each target and the simulated discharge in the corresponding model stream reach. The goodness-of-fit was

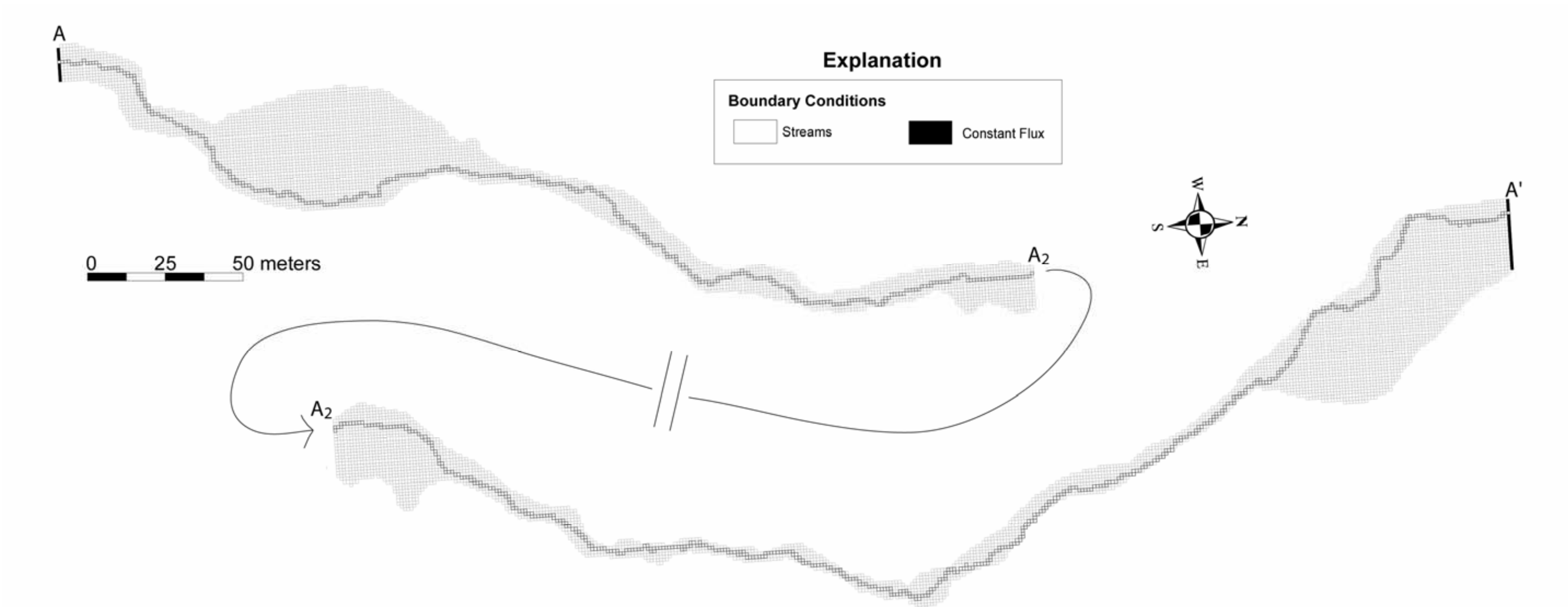

Figure 7: Entire grid layout, orientation, and model boundary conditions of Cottonwood Springs model (A-A' on Fig. 5). Grid cells are 1m x 1m.

evaluated based on the standard that residual values should be less than 15% of the range of observed values:

$$[(Q_{obs}) - (Q_{sim})] / (Q_{obs}) < 0.15 \quad (1)$$

where Q_{obs} is the range of observed, or measured discharges, and Q_{sim} is the simulated discharge.

The model was also calibrated to the observed extent of dry and flowing reaches. The goodness of fit for this calibration was evaluated by tallying the number of stream cells where the correct flow condition was not correctly simulated (flow vs. no flow). The uppermost 25 reaches were not evaluated due to boundary effects observed at the upstream end of the model. The goodness-of-fit was evaluated based on the standard that the correct flow condition should be simulated in a at least 80% of the stream cells:

$$(N_c) / (N_t) > 0.8 \quad (2)$$

where N_c is the number of correctly modeled stream cells and N_t is the total number of stream cells.

To simulate seasonal variability at the site, a transient model was constructed with six time steps varying between 36 and 85 days corresponding to the interval between field visits between April 26, 2003 and January 16, 2004 (Table 1). Calibration data for the transient simulation consisted of measurements of the extent of surface flows and stream discharge taken every 5-8 weeks at five locations. The goodness-of-fit was evaluated using the standards described above for the steady-state model. Additionally, the transient model was calibrated to water-level measurements from two observation wells (see Fig. 6 and Plate 1a for locations). Residuals were calculated as the difference between the observed head at each well and the simulated head in the corresponding

Table 1: Temporal framework for the transient model showing the length of each stress period used in MODFLOW. Dates are the ending date of each stress period and correspond to the dates of field visits.

Stress Period	Number of Days	Date
Initial Condition	50	3/21/2003
1	36	4/26/2003
2	42	6/7/2003
3	43	7/20/2003
4	54	9/12/2003
5	41	10/23/2003
6	85	1/16/2004

model cell. The goodness-of-fit was evaluated based on the standard that residual values should be less than 5 cm. The six time steps used in the transient model captured the seasonal range of water availability, and limited the computational time of the transient simulation.

3.3.1 Model Boundaries

The model area is underlain by bedrock of the Bright Angel Shale (Figs. 8-9), and the contact between bedrock and the unconsolidated fluvial deposits of the riparian zone was used as the lower model boundary**.** This boundary was simulated with a constant-flux (no flow) boundary because in comparison to the fluvial deposits, the Bright Angel Shale is relatively impermeable and vertical movement of water across this boundary is expected to be minimal in the absence of data indicating significant fracturing. Because of the difficulty in obtaining data constraining the potentiometric surface beneath the coarse-grained colluvial deposits near the steep headwaters of WFCC, and because most of the multiple spring orifices are buried beneath colluvium, it was not possible to model this system beginning at the sources (individual spring orifices). Instead a large headcut in the channel of WFCC located above the point where the highest measured discharges were recorded in the channel was chosen as the upstream boundary of the models. This boundary was simulated with a constant-flux boundary (Fig. 7; Plate 1b). The downstream boundary of the models was chosen to include a wide variety of vegetation and water availability zones needed to fully characterize the site. This boundary was simulated with a constant-flux boundary to represent the groundwater flow exiting the model area through shallow alluvium (Fig. 7; Plate 1b).

The lateral boundaries of the models were chosen to represent the major break in topographic slope associated with the hillslope/valley transition. This break in slope generally occurs at the contact between fluvial deposits of the riparian zone and adjacent colluvial hillslope material. In portions of the study area the major break in topographic slope occurs part way into the colluvial deposits, and in these locations some colluvial material was included in the model area (Fig. 6; Plate 1a). In these areas, the colluvial deposits have been eroded by surface runoff associated with steep, low-order tributaries, and in some locations form strath terraces. In a few locations, the lateral limit of xeroriparian vegetation (Scott and Shafroth, unpublished data) was used to define the lateral extent of the colluvial material included in the model area. Inspection of bedrock outcrops in and near the channel indicates that the Bright Angel Shale tends to develop a

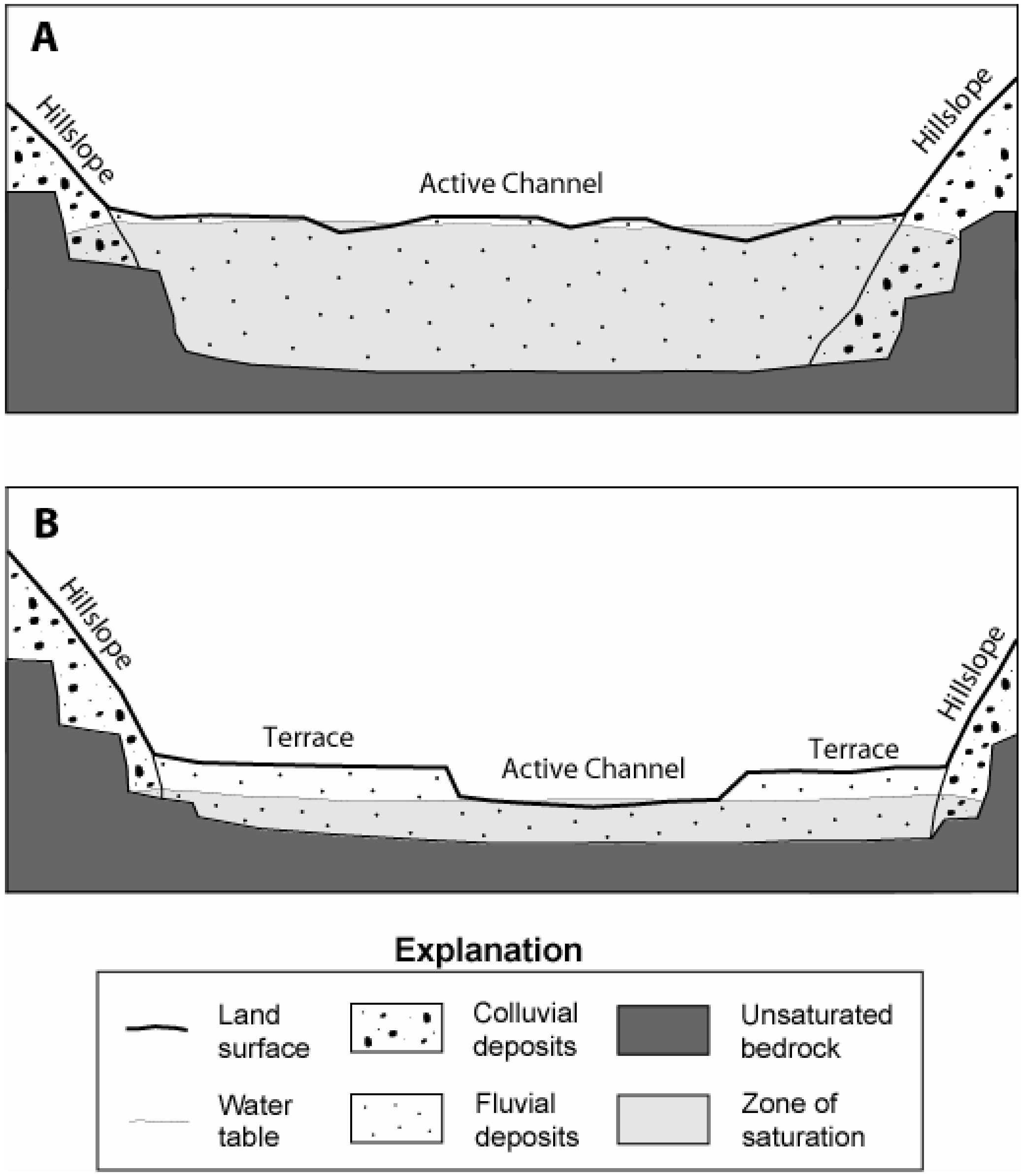

Figure 8: Conceptual diagrams of the deposits at Cottonwood Springs oriented perpendicular to the channel. Diagrams are roughly to scale, and the width is approximately 12 m. (A) upstream section characterized by deeper alluvial fill, multiple channels, and lack of fluvial terraces. (B) downstream section characterized by a single channel, shallower alluvial fill, and paired fluvial terraces.

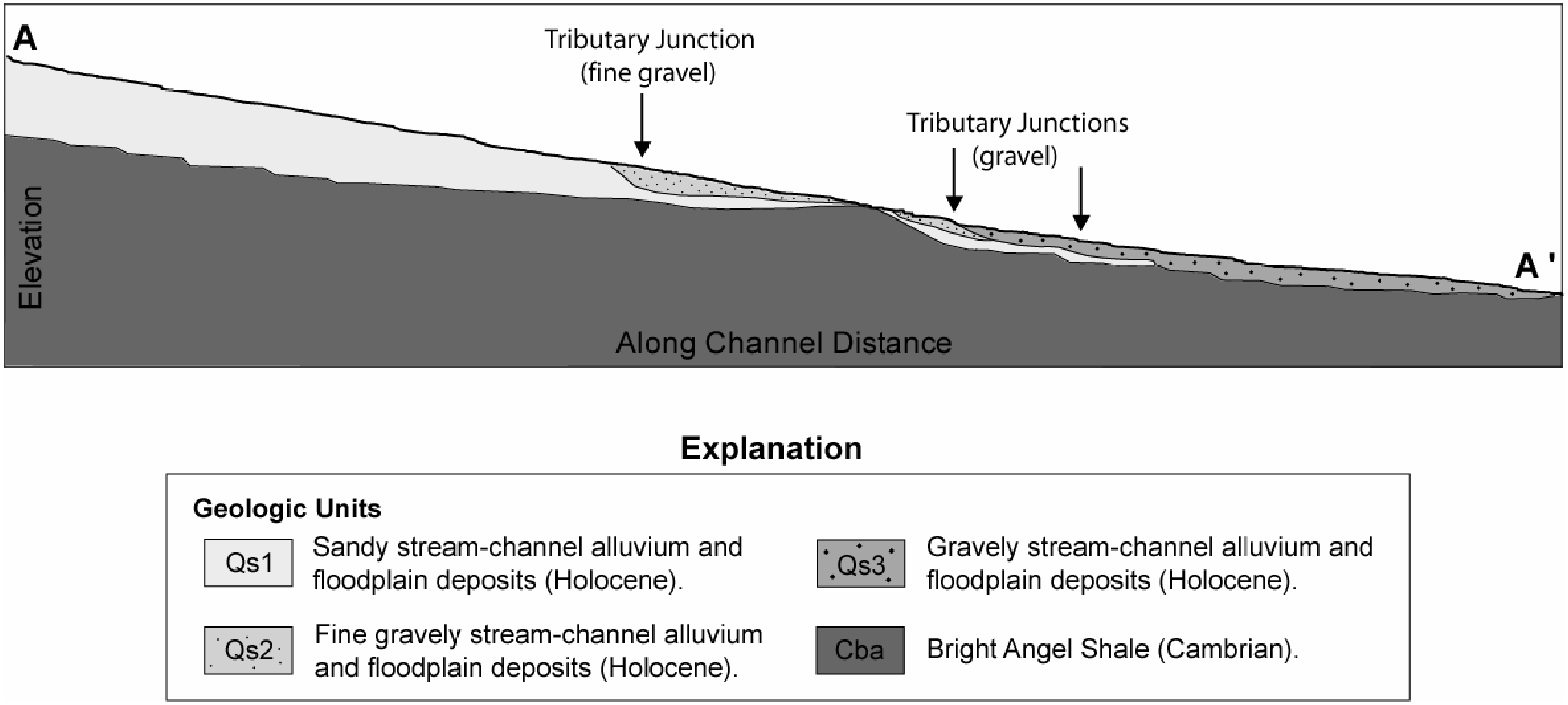

Figure 9: Conceptual diagram of the fluvial deposits at Cottonwood Springs oriented longitudinal to the main thalweg of the channel (A to A' as indicated on Fig. 5). Locations of major tributary junctions that serve as sediment sources are shown. Land surface represents surveyed topographic data and the diagram is roughly to scale with 2X vertical exaggeration and a total along-channel distance of 860 m.

terrace-like topography and that the bedrock topography likely mimics the surface topography such that bedrock is relatively planar beneath the valley bottom and very steep beneath the valley slopes (Fig. 8). From these observations, it was concluded that most of the water is confined to the region of the fluvial deposits and locally the beveled colluvial deposits, and because most of the riparian species of interest are also confined to this region, this was defined as the lateral model boundary and it was simulated as a constant-flux (no flow) boundary.

Surface water/groundwater interactions were simulated with head-dependent boundary conditions. Cells containing these boundary conditions were added to the models by importing an ArcView (ESRI, Redlands, CA) shapefile (AVS) of the surveyed thalweg of the channel into Groundwater Vistas as a base map (Fig. 7; Plate 1a). Reaches were numbered in sequential order from upstream to downstream. Channel slopes were measured from the survey data in ArcView approximately every 5 meters, and input into the appropriate stream cells (Appendix A, Tables 11-38). Manning's roughness coefficients (n) were based on field observations from three distinct reaches. Channel widths were interpolated between measured channel cross sections, and channel lengths for each cell were measured in ArcView (Appendix A, Tables 11-38). The distribution of streambed hydraulic conductivity (K) values was set based on the geologic mapping, and values were set to be 10% higher than the underlying aquifer material; K generally decreases with depth beneath unconsolidated streambed deposits. Stream stage and discharge were assigned as constant values for the upstream-most reach, and streamflows were routed to downstream reaches by treating the stream cells as head-dependent flux boundaries (Fig. 7; Plate 1b).

3.3.2 Model Parameters

The surveyed elevation data were interpolated in ArcView using an inverse distance weighted interpolation scheme (Fig. 6; Plate 1a). The resulting surface was then imported into Groundwater Vistas and set as the upper surface of the models. Using measured depths to bedrock, fluvial thicknesses were subtracted from the original elevations of the survey data along the thalweg of the channel and interpolated using an inverse distance weighted interpolation scheme. Only thalweg points were used such that the resulting surface has topography only longitudinally to the channel and is relatively flat laterally away from the channel. This surface was then imported into Groundwater Vistas as a bottom surface for the models.

An AVS containing the mapped geologic units was imported as a base map into Groundwater Vistas. K zones were then established to correspond with the mapped geologic units (Fig. 10; Plate 1c). The fluvial terraces are incisional features and field evidence suggests that their sediment characteristics are indistinct from the adjacent active channel deposits except in the upper 10 cm where recent high flow events have deposited slackwater deposits of fine sand and silt. Thus, the terraces were lumped with the active channel deposits for the purposes of defining K zones. Initial values for the various K zones were determined from grain-size analyses using an empirical relationship (Shepherd, 1989) and from previously published estimates from similar materials (Masch and Denny, 1966; Davis, 1969; Sykes et al., 1982; Adams and Gelhar, 1992; Pang et al., 1998; Woessner et al., 2001) (Table 2); final values were adjusted during calibration. Vertical to horizontal anisotropy is expected in fluvial deposits, thus a vertical K equal to 10% of the horizontal K was used.

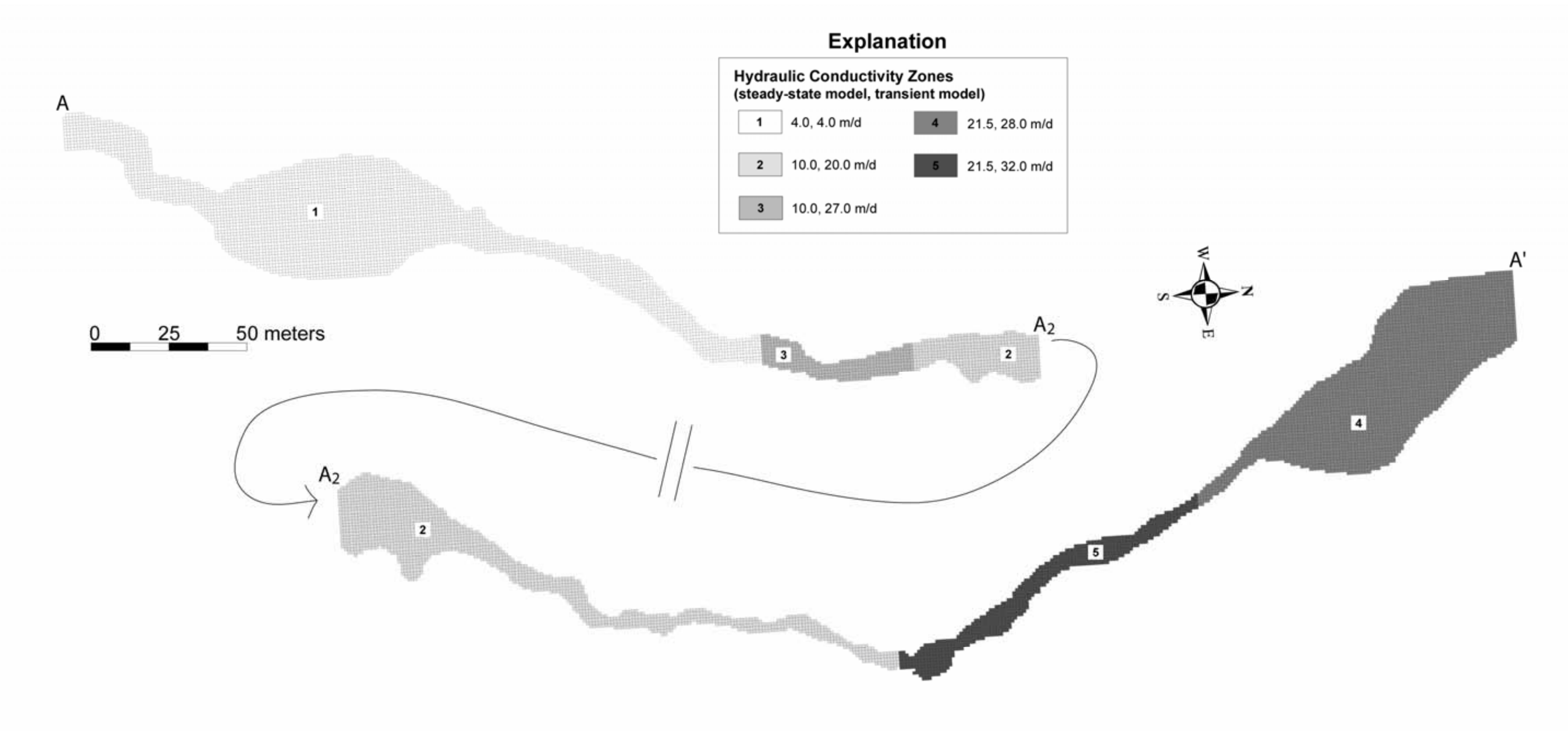

Figure 10: Distribution of hydraulic conductivity (K) zones in Cottonwood Springs model (A - A' on Fig. 5). Rates listed in legend are for the steady-state model and the transient model respectively.

Table 2: Summary of grain-size characteristics and hydraulic conductivity estimates for Cottonwood Springs deposits. Methods used to determine the d_{50} grain-size are gs (grain-size analysis) and pc (pebble counts). See Fig. 6 and Plate 1a for distribution of deposits.

Unit	d_{50} (mm)	Method	Empirical Estimate (m/d)	Range of Published Estimates (m/d)	References
Qs1	0.1	gs	3.1	0.00017 - 43	Davis, 1969; Sykes et al., 1982
Qt1	0.1	gs	3.1	0.00017 - 43	Davis, 1969; Sykes et al., 1983
Qs2	2.3	gs	540	0.86 - 8040	Adams and Gelhar, 1992; Woessner et al., 2001
Qt2	2.9	gs	790	0.86 - 8040	Adams and Gelhar, 1992; Woessner et al., 2001
Qs3	31	pc	-	8.6 - 10400	Masch and Denny, 1966; Pang et al., 1998
Qt3	29	pc	-	8.6 - 10400	Masch and Denny, 1966; Pang et al., 1998
Qd	37	pc	-	8.6 - 10400	Masch and Denny, 1966; Pang et al., 1998

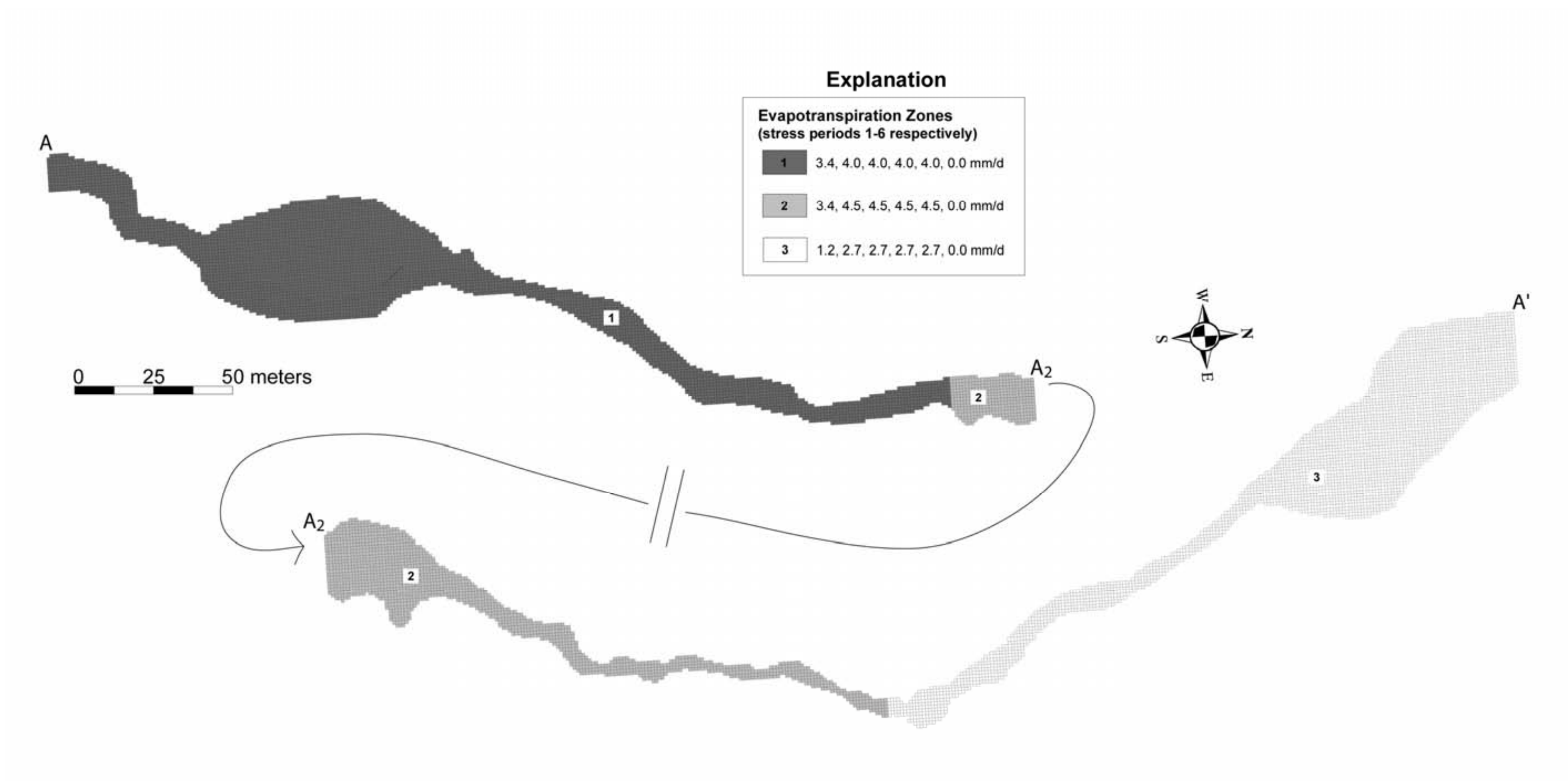

Figure 11: Distribution of evapotranspiration (ET) zones in Cottonwood Springs model (A - A' on Fig. 5). Rates listed in legend are for stress periods 1 through 6 respectively.

Table 3: Average growing season ET rates for Cottonwood Springs model ET zones based on vegetation mapping by Scott and Shafroth (unpublished data) and literature values. See Fig. 11 and Plate 1d for distribution of ET zones.

ET Zone	Dominant Species	Av. Growing Season ET Rate (m/day)	References
1	Willow	0.0042	Robinson, 1970
2	Cottonwood	0.0045	Dahm et al., 2002
3	Mesquite	0.0024	Sammis, 1972; Ball et al., 1995

Three evapotranspiration (ET) zones corresponding to three zones with distinct vegetation assemblages were defined based on vegetation mapping on digital orthophoto quadrangles (Scott and Shafroth, unpublished data) (Fig. 11; Plate 1d). Previously published estimates of ET from similar vegetation assemblages were used to establish initial rates for the ET zones (Table 3). Final values were adjusted during calibration.

3.3.3 Fluxes

To delineate spatial variations in water availability in the study area for use in future vegetation modeling, groundwater flux in the transient model was measured along transects oriented perpendicular to the hydraulic gradient and covering the width of the model. Surface-water discharge in the stream boundary cell corresponding to the position of the transect was added to the groundwater flux to determine the total flux of water at various locations in the model area.

4. Results

4.1 Site Characterization

Most of the ~55 m^3/day of discharge at Cottonwood Springs, discharges from the middle and upper portions of the Muav Limestone. After exiting the aquifer, discharge enters colluvial material almost immediately, and flows subsurface for ~500 m before appearing as channelized base flow. Most of the springs occur at the headwaters of WFCC, a small tributary to Cottonwood Creek (Fig. 5), and many of the spring orifices are buried beneath recent colluvial material.

The small discharges and diffuse nature of the spring orifices at Cottonwood, makes direct measurement of total spring discharge impossible. Because of this, the highest measured values of base flow surface-water discharge downstream from the colluvial subsurface reach were inferred to represent a minimum estimate of total spring discharge. Despite the low discharge of 50 to 60 m^3/day, dense stands of cottonwoods, willows, and other riparian species are supported along an ~1-km reach below the springs. Most of the vegetation is restricted to the reach underlain by Bright Angel Shale, because downstream of this the relatively wide floodplain formed in the weak shale gives way to an incised canyon cut into the resistant Tapeats Sandstone.

The number of days with zero discharge at the Cottonwood Springs gauge increased from 0 in 1995 to 177 in 2003, a statistically significant tend (Mann-Kendall $p = 0.0025$) (Fig. 12). Plots of low 3-day mean winter discharge indicate that an ~19% decrease in base flow discharge has occurred between 1995 and 2001 at Cottonwood Springs gauge (Fig. 13a) (Mann-Kendall $p = 0.0054$), and a decrease of ~25% was observed at Indian Gardens Springs gauge between 1994 and 2001 (Fig. 13b) (Mann-

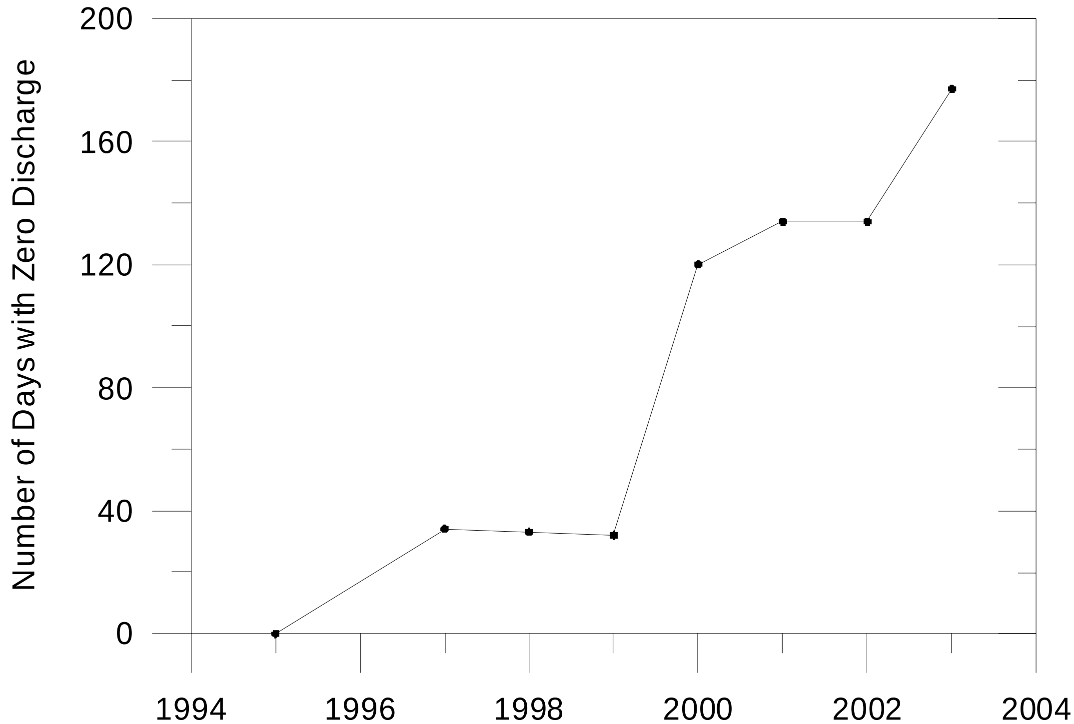

Figure 12: Trend analysis of the number of days with zero discharge at Cottonwood Springs gauge. Data from the USGS, (2002, 2004a).

Kendall p = 0.068). This evidence suggests that there has been a decrease in discharge at these springs since at least 1994. Projection of the trend in low winter discharge at Cottonwood Springs indicates that if discharge continues to decrease at the current rate, low winter baseflow at the USGS gauge may decrease to as low as ~8 m^3/day by the year 2020 (down from ~23 m^3/day in 1994) (Fig. 14).

Superimposed on annual precipitation totals at stations on the South Rim from 1903 to 2002 are mean values calculated for a series of multidecadal precipitation regimes recognized in data throughout the Colorado Plateau (Fig. 15). These precipitation regimes show a period of above-average precipitation from 1905 to 1941 (mean = 426 mm), followed by a period of below-average precipitation from 1942 to 1977 (mean = 351 mm), and a second wet period from 1978 to 1998 (mean = 484 mm).

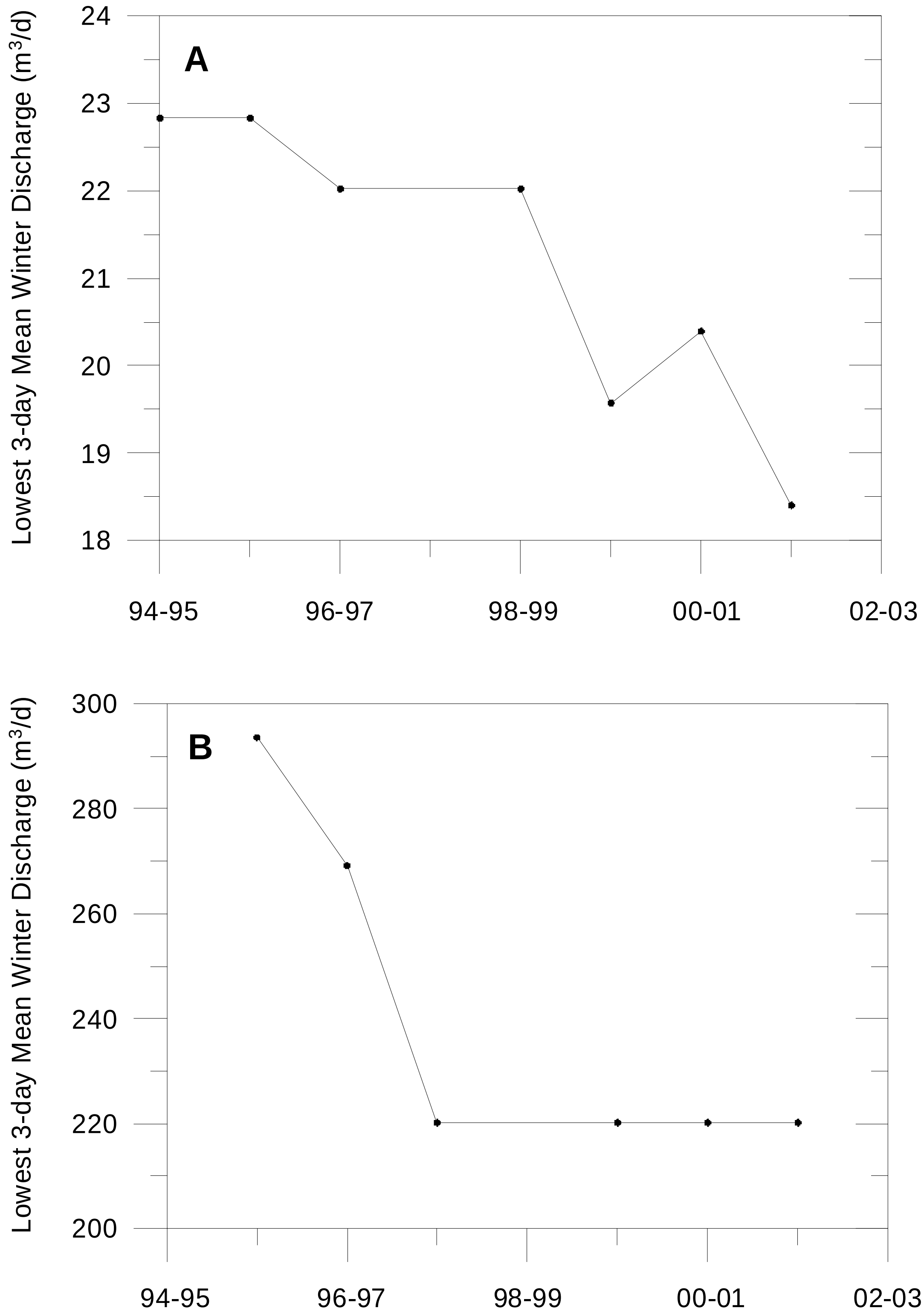

Figure 13: Trend analysis of low 3-day mean winter discharge (December 1 – February 7) at Cottonwood Springs gauge (A) and Indian Gardens Springs gauge (B). Data from the USGS (2002).

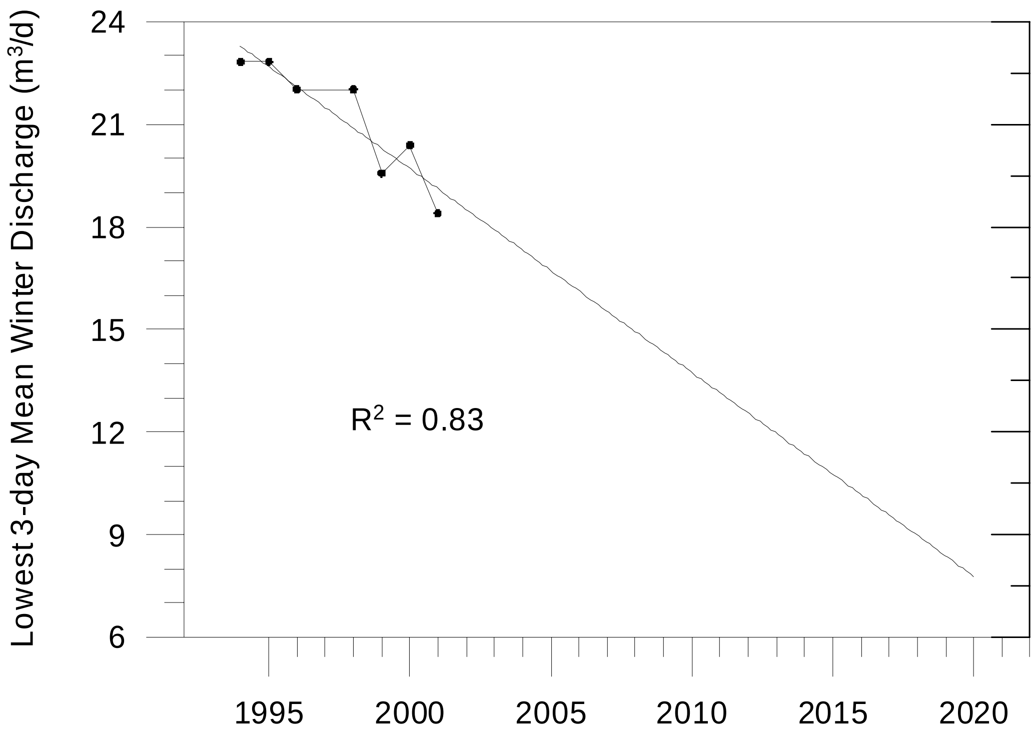

Figure 14: Projection of the trend in low 3-day mean winter discharge (December 1 – February 7) at Cottonwood Springs gauge through the year 2020. Data from the USGS (2002).

These alternating wet and dry cycles are thought to be related to Pacific Decadal Oscillation (PDO) conditions (Zhang et al., 1997). In particular, warm phases of the PDO are associated with El Nino conditions and are thought to result in increased winter precipitation in the Southwestern U.S., while cool phases of the PDO are associated with La Nina conditions and decreased winter precipitation (McCabe and Dettinger, 1999). Some workers have suggested that the below average annual precipitation totals recorded since 1998 (mean value 1999-2003 = 349 mm) (Fig. 15) reflect the recent transition into a dry cycle and this hypothesis is supported by PDO data (e.g. Hereford et al., 2002). If this recent climate change is responsible for the observed discharge trends, it is

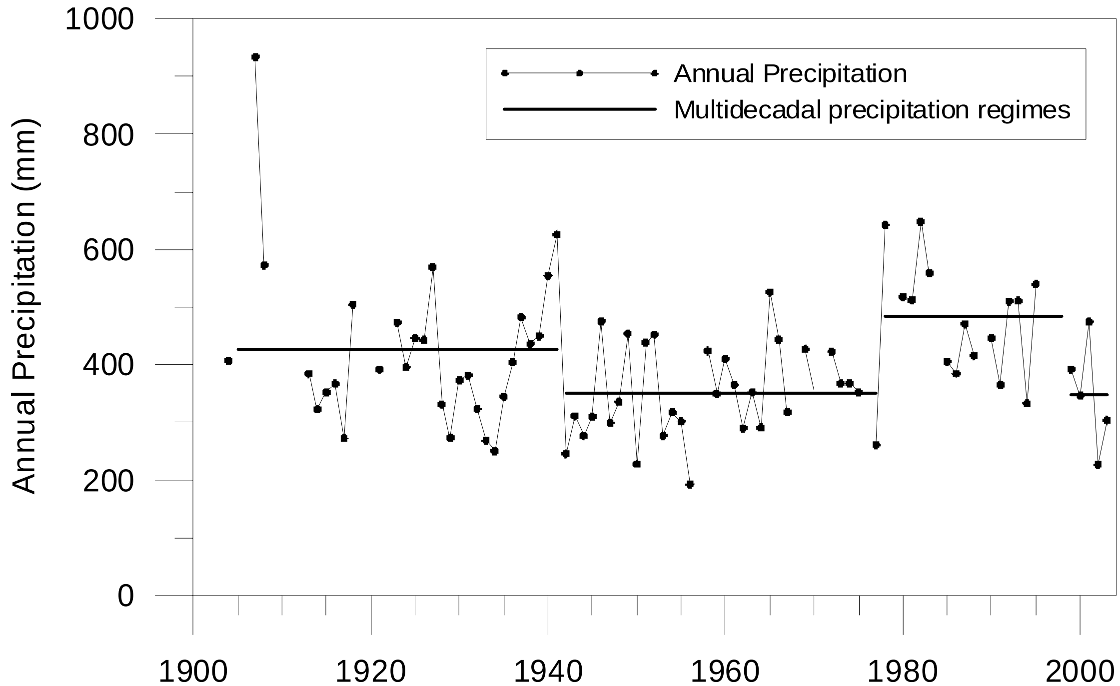

Figure 15: Total annual precipitation at the South Rim of the Grand Canyon (NOAA, 2004b) and mean multidecadal precipitation (1905-1941, 1942-1977, 1978-1998) (Hereford et al., 2002).

reasonable to expect the trend to continue until 2020 as these precipitation regimes typically last for 10-30 yrs (Hereford, et al., 2002).

The Bright Angel Shale underlies the fluvial deposits in the riparian area and acts as a lower confining unit for the riparian aquifer (Figs. 8-9). Laterally, water is confined primarily to the valley bottom area as adjacent to this area, a steep topographic break in slope occurs which is mimicked in the underlying bedrock topography (Fig. 8). The fluvial deposits were mapped as active channel deposits and a series of fluvial terraces, which are paired in places (Figs. 6 and 8; Plate 1a). The sediment characteristics of the active channel deposits are indistinct from those of adjacent fluvial terraces, owning to the incisional genesis of these features. The only significant variations occur in the upper 10 cm of the terraces, where recent high-flow events have deposited slackwater deposits of fine sand and silt. Because this portion of the terraces remains unsaturated during the base- flow conditions simulated with the models, the terraces were combined with the active channel deposits as a single hydrostratigraphic unit (Fig. 10). Longitudinally, however, significant variations in sediment characteristics occur which required differentiation into three major units with sediment size increasing from fine sand to fine gravel to coarse gravel in the downstream direction (Figs. 6 and 9; Plate 1a). The transitions in sediment size occur at tributary junctions, and presumably result from tributary input of sediment from varying source areas.

4.2 Conceptual Water Budget

Sources of inflow to the study area included flows derived from upstream springs that entered as either surface-water inflow or groundwater inflow at the upstream end of the study area, surface-water and groundwater inflows derived from other sources including runoff, and recharge from direct precipitation. Because direct measurement of total spring discharge from the multiple, buried spring orifices upstream of the study area was not possible, maximum base flow measurements from the site taken between February, 2003 and April, 2004 (~1600 m^3/mo) (Adams, unpublished data) were inferred to represent the minimum contribution of inflow from all of the spring orifices. At the upstream end of the study area, stream discharge was zero throughout the year, thus all of inflow contribution from the springs entered the study area as groundwater inflow (Table 4).

With the exception of one small spring orifice feeding a small tributary near the upstream end of the study area, no spring orifices were located at the headwaters of any of the tributaries entering the study area, and no contributing surface-water discharge was observed over the observation period in any of the tributaries. Therefore, groundwater and surface-water inflows from anywhere except at the upstream end of the study were initially presumed to be negligible except during runoff events. South Rim springs generally do not show significant variations in discharge on a seasonal scale (USGS, 2004b), thus a constant groundwater inflow was assumed (Table 4). Because the models do not begin at the bedrock spring orifices, some ET likely occurs up gradient of the model area, thus some seasonal variation in groundwater inflow is reasonable although difficult to quantify.

Using precipitation data from the South Rim and from Phantom Ranch along the Colorado River (NOAA, 2004b), average annual precipitation at the site was estimated to be ~0.3 m/yr. Assuming that 1-5% of the precipitation that falls over the study area (10,000 m^2) recharges directly, approximately 2.0-15.0 m^3 of direct recharge occurs monthly (Table 4). The majority of this recharge is associated with monsoon storms and is thus, concentrated in the summer months (Table 4). The remaining precipitation was assumed to be runoff, which due to the coarse substrate and steep gradients presumably moves through the system over relatively short time periods (hours to days). Episodic flash flood events drive sediment production and transport through the system and occur once every few years to as often as several times a year, generally associated with summer monsoon storms. Short-term fluctuations in water storage and availability occur from these events, and the stoichastic nature of runoff events at this site presumably leads to variable recharge rates. Direct recharge is two orders of magnitude less than

Table 4: Monthly water budget for Cottonwood Springs riparian aquifer based on observations taken between February, 2003 and April, 2004.

	Winter	Summer
Inflows (m^3/mo)		
Groundwater	1600	1600
Surface water	0	0
Recharge	0	17
Outflows (m^3/mo)		
Groundwater	1600	1000
Surface water	2	0
ET	45	600

groundwater inflow, and recharge during runoff events is highly episodic and presumably short-lived. Therefore, the models evaluated base flow conditions, and did not include recharge. During seasons with several runoff events, recharge is probably a significant portion of the water budget, and further study of the effects runoff events is warranted.

Sources of outflow include surface water, groundwater, and ET. Base flow measurements of stream discharge near the downstream end of the study area were used to quantify the volume of streamflow exiting the study area (Table 4). Data from stations in northern Arizona with similar elevation and climate, indicate that the average winter pan evaporation rate is ~0.004 m/d, and applied over the ~4% of the study area that is open water, this represents a winter ET rate of 30-60 m^3/mo (Table 4). Because winter ET is two orders of magnitude less that groundwater inflow, winter ET was not included in the steady-state model. Thus, the volume of groundwater exiting the study area during winter was presumed to equal the portion of the total inflow not measured as surface-water discharge. Some leakage into the underlying bedrock may occur, however these

Table 5: Water budget for the steady-state model of Cottonwood Springs riparian aquifer.

Source	In (m^3/d)	Out (m^3/d)	Out - In
Groundwater Flux	38.0	39.6	1.6
Stream/Aquifer Leakage	713.0	711.7	-1.3
Total	751.0	751.3	0.03 %

volumes are difficult to quantify, and in the absence of data indicating significant fracturing of the bedrock, would presumably be small. Three ET zones were defined using vegetation mapping (Scott and Shafroth, unpublished data) and literature values. When applied over the corresponding model areas, an average growing season ET rate of 500-700 m^3/mo was calculated (Table 4). Lower values are expected during the beginning and end of the growing season and higher values are expected during the peak of the growing season.

4.3 Steady-State Model

The steady-state model was calibrated to hydraulic heads and stream discharge values observed on March 21, 2003. The model converged with a water budget error of -0.03%, and a groundwater influx of 38.0 m^3/d (Table 5). Streamflow influx at the upstream-most stream reach was 16 m^3/d for a total influx of water of 54 m^3/d. This estimate is consistent with the conceptual water budget estimate of total inflow of 50 to 60 m^3/d. Although observed surface-water discharge was zero at the upstream boundary

Table 6: Results of steady-state calibration. (A) Observed and simulated discharge values of discharge targets showing residuals and residual values as a percentage of observed values, (B) Number of stream cells modeled correctly (flow vs. no flow) based on field observation and the number of correct cells as a percentage of the total number of cells. See Fig. 6 and Plate 1a for station locations.

A

	Observed discharge (m^3/d)	Simulated discharge (m^3/d)	Residual Value	% Error
Station 2	37.6	37.7	0.1	0.3
Station 4	4.0	5.0	1.0	2.6
Station 7	27.8	26.8	1.0	2.7
Station 8	27.9	30.4	2.5	6.7
Station 9	3.0	0.0	3.0	8.0

B

Number of correct cells	Number of incorrect cells	Number correct as % of the total
838	83	90.1

of the model, adding water in the stream was necessary to successfully calibrate the model in downstream reaches. Total outflow at the base of the model area was 54 m^3/d, consistent with the conceptual water budget estimate that outflow approximately balances inflow in the winter. The residuals of observed and simulated discharge values at five locations ranged from 0.3 to 8.0%, well within the target of <15% (Table 6a). The flow condition (flow vs. no flow) was simulated correctly in 90.1% of the stream cells (Table 6b), meeting the target of >80%.

4.4 Transient Model

The transient model was calibrated to stream discharge data and stream flow/no flow data for stress periods 1-6, and to water-level data for stress periods 3-6. The model converged and water budget errors ranged from –0.52% to 0.15% for each stress period. The highest error occurred in stress period 1, and in subsequent stress periods errors progressively decreased, reaching a low of 0.01% in stress period 4. Groundwater influx was 39.5 m^3/d in all stress periods (Fig. 16a), and surface-water flux in the upstream-most reach was 18 m^3/d for stress periods 1-5 and at 22 m^3/d for stress period 6. Total inflow in all stress periods was ~60 m^3/d, consistent with the conceptual water budget estimate that 50-60 m^3/d enters the model area throughout the year. Although streamflow was not observed at the upstream portion of the study area, the solution was much more stable with some surface-water discharge. To account for this discrepancy, the model results were not evaluated in the upper-most 25 stream cells in both the steady-state and transient models. Total outflow at the base of the model ranged from 33-36 m^3/d in stress periods 2 through 5 to 60-71 m^3/d in stress periods 1 and 6 (Fig. 16b).

Evapotranspiration removed ~19 m^3/d in stress period 1, ~25 m^3/d in stress periods 2 through 5, and 0.0 m^3/d in stress period 6 (Fig. 16b). This represents a total annual ET value of 5100 m^3 and an average growing season ET rate of ~600 m^3/mo, in close agreement with the conceptual water budget estimate. During stress period 1, ~29 m^3/d entered storage and ~0.5 m^3/d was removed from storage (Fig. 16). In all other

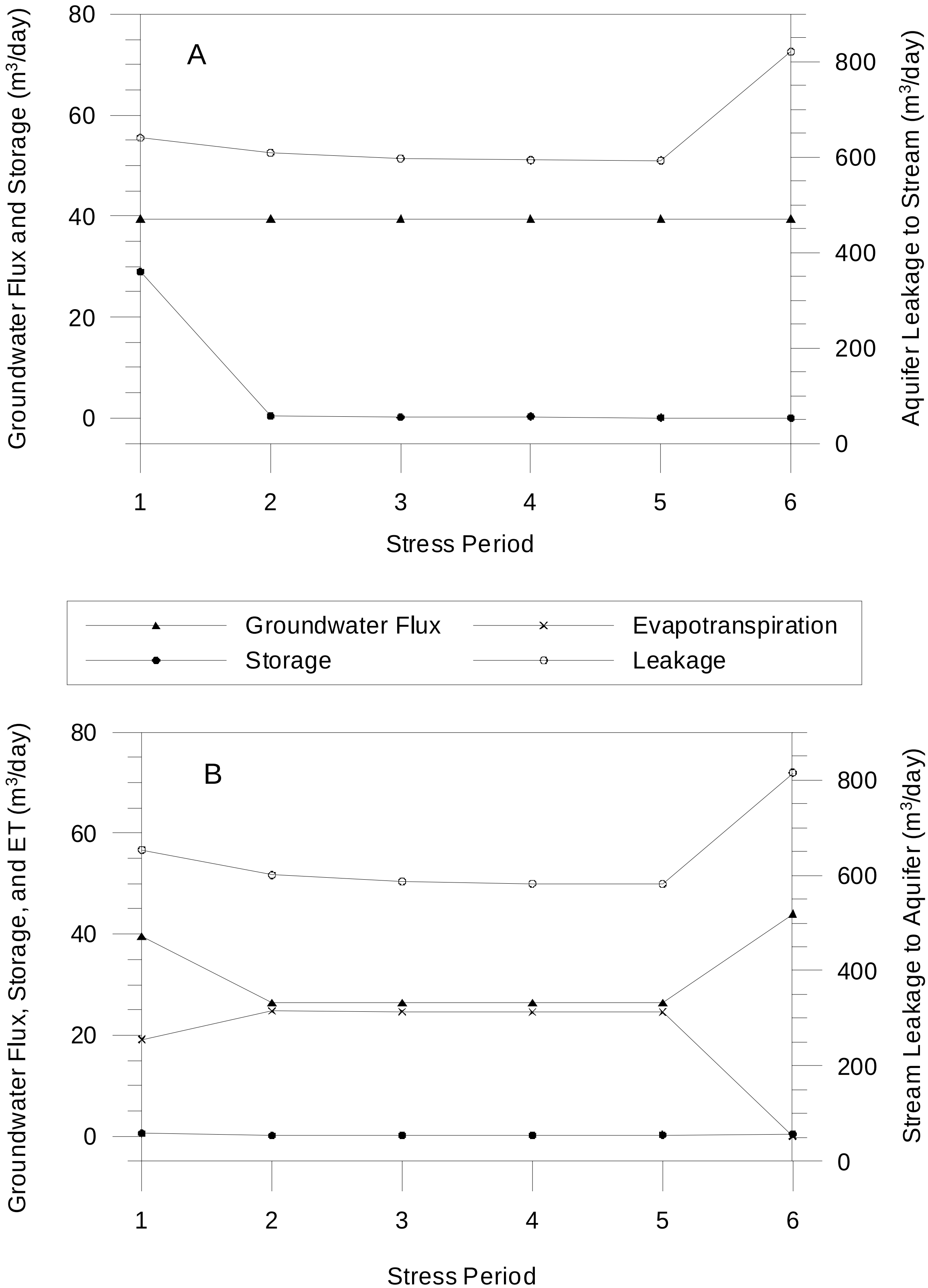

Figure 16: Water budget for the transient model of Cottonwood Springs riparian aquifer showing inflows (A) and outflows (B) for stress periods 1 to 6.

stress periods, storage was a very small portion of the budget (<1%). In stress periods 1 through 4, there was a small net gain in storage while in stress periods 5 and 6 there was a small net loss in storage (Fig. 16).

To calibrate the transient model, values of K slightly higher than those used in the steady-state model were necessary. K in zones 2 and 3 was increased by a factor of 2-3, and in zones 4 and 5 was increased by a factor of ~1.5. The values of K were similar to the estimates from the conceptual model for both numerical models, and variation of K over relatively short timescales is not unreasonable. Springer et al. (1999a), for example, found that K varied an order of magnitude over a period of months in reattachment bars along the Colorado River following a flood event.

The residuals of observed and simulated discharge values at five locations ranged from 0-14% for stress periods 1 through 5 (Table 7). These values were within the target of <15%, and were lowest at station 4 and highest at station 8. Residuals for stress period 6 ranged from 4-56% (Table 7). The target was not met at station 4 where the simulated value was too low, or at stations 7 and 8 where simulated values were too high (Table 7). The correct flow condition (flow vs. no flow) was simulated in 58-85% of the stream cells (Table 8). The target of >80% was met for stress periods 1 and 6, however percentages were too low for stress periods 2 through 5. The small percentages in stress periods 2-5 resulted from too few stream cells going dry during the growing season. Thus, the percentages were higher during those stress periods where more of the channel should be flowing (2 and 5) and were lower during the driest periods (3 and 4) (Table 8). The residuals for the water-level calibration in stress periods 3-6 ranged from 1-10 cm at the upstream well (UW) and from 2-4 cm at the downstream well (DW) (Table 9). These

Table 7: Transient discharge calibration showing observed and simulated discharge values, residual values and percent errors for stress periods 1 through 6. See Fig. 6 and Plate 1a for station locations.

Stress Period	Station Number	Observed discharge (m^3/d)	Simulated discharge (m^3/d)	Residual Value	% Error
1	2	16.2	13.6	2.6	6.9
	4	0.7	0.0	0.7	1.9
	7	2.0	0.0	2.0	5.3
	8	2.1	7.5	5.4	14.4
	9	0.0	0.0	0.0	0.0
2	2	0.0	0.0	0.0	0.0
	4	0.0	0.0	0.0	0.0
	7	0.0	0.0	0.0	0.0
	8	0.0	4.8	4.8	12.9
	9	0.0	0.0	0.0	0.0
3	2	0.0	0.0	0.0	0.0
	4	0.0	0.0	0.0	0.0
	7	0.0	0.0	0.0	0.0
	8	0.0	3.4	3.4	8.9
	9	0.0	0.0	0.0	0.0
4	2	0.0	0.0	0.0	0.0
	4	0.0	0.0	0.0	0.0
	7	0.0	0.0	0.0	0.0
	8	0.0	2.7	2.7	7.2
	9	0.0	0.0	0.0	0.0
5	2	0.0	0.0	0.0	0.0
	4	0.7	0.0	0.0	0.0
	7	0.0	0.0	0.0	0.0
	8	0.0	2.6	2.6	6.8
	9	0.0	0.0	0.0	0.0
6	2	33.1	30.3	2.8	7.4
	4	10.6	0.0	10.6	28.2
	7	11.0	18.8	7.6	20.2
	8	5.3	26.3	21.0	55.9
	9	1.3	0.0	1.3	3.5

Table 8: Transient calibration showing the number of correctly simulated (flow vs. no flow) stream cells and the number correct as a percentage of the total for stress periods 1 through 6. See Fig. 6 and Plate 1a for station locations.
Error!

Stress Period	Number correct	Number incorrect	Number correct as % of total
1	757	164	82
2	570	351	62
3	544	377	59
4	531	390	58
5	579	342	63
6	784	137	85

Table 9: Transient water-level calibration showing observed heads, simulated heads, and residual values for stress periods 3 through 6. See Fig. 6 and Plate 1a for well locations.

Stress Period	Well Name	Observed Head (m)	Simulated Head (m)	Residual Value (m)
3	DW	1186.92	1186.95	0.03
	UW	1217.71	1217.81	0.10
4	DW	1186.94	1186.96	0.02
	UW	1217.76	1217.80	0.04
5	DW	1186.94	1187.97	0.03
	UW	1217.79	1217.80	0.01
6	DW	1187.01	1187.05	0.04
	UW	1217.90	1217.86	0.04

values were all within the target of <5 cm, except at well UW during stress period 3 where the simulated water-level was too high.

4.5 Sensitivity Analysis

Over a narrow range of grid-cell dimensions (0.5-1.0 m), the model was insensitive to grid-cell size. Grid-cell size has been shown to influence surface water/groundwater interaction (Bissett, 1994), and grid-cell sizes larger than 1-m would likely result in large model changes. The model was relatively insensitive to the value of the storage coefficient, and little effect was observed when varying this parameter between 0.15 and 0.35. The model did not converge with large changes in K. Stream discharges were moderately sensitive to small changes in K. The simulation was strongly influenced by the ET rates because ET accounts for a large portion of the water budget. The model failed to converge with higher ET rates.

The model was relatively insensitive to the choice of the lower boundary condition, and significant changes were not observed when leakage across the lower boundary into a second model layer representing the bedrock was allowed in varying amounts. The model was highly sensitive to the choice of boundaries at the upstream and downstream ends of the model, and the solution was much more stable using constant flux boundaries as apposed to constant head boundaries. Small changes in the values of the constant flux boundaries had a minimal effect on the simulation, however changes in excess of 10% produced large changes. Streamflow values in the model were highly sensitive to the streambed conductance term. Numerous longitudinal changes in streambed conductance resulted in a lack of model convergence, and the solution was much more stable using a constant value of conductance.

4.6 Fluxes

During the steady-state simulation of the wettest observed conditions on March 21, 2003, total flux of water through the model area remained relatively constant and approximately ~60 m^3/d. During the simulation of the driest observed conditions on July 20, 2003 (stress period 3), groundwater flux varied from 15-50 m^3/d and surface-water flux varied from 0-40 m^3/d (Fig. 17). Longitudinal changes in the gaining and losing nature of the stream resulted in many large changes in the relative proportions of surface-water and groundwater flux through the model area. The total flux of water in the upstream portion of the model was ~60 m^3/d and decreased progressively down to ~35 m^3/d in the downstream portion of the model (Fig. 17). The values decreased steadily except for in a small area near meter 300 where slight downstream increases occurred locally. The rate of decrease was higher in upstream areas and lower in downstream areas (Fig. 17). The longitudinal decrease in flux was the result of high rates of ET progressively removing increased volumes of water in the downstream direction.

5. Summary and Discussion

Discharge trend analyses indicated that statistically significant decreasing trends in stream discharge have occurred at USGS gauging stations at Cottonwood and Indian Gardens Springs since at least 1994. The number of days with zero discharge at Cottonwood Springs increased from 0 in 1995 to 177 in 2003. This increase may

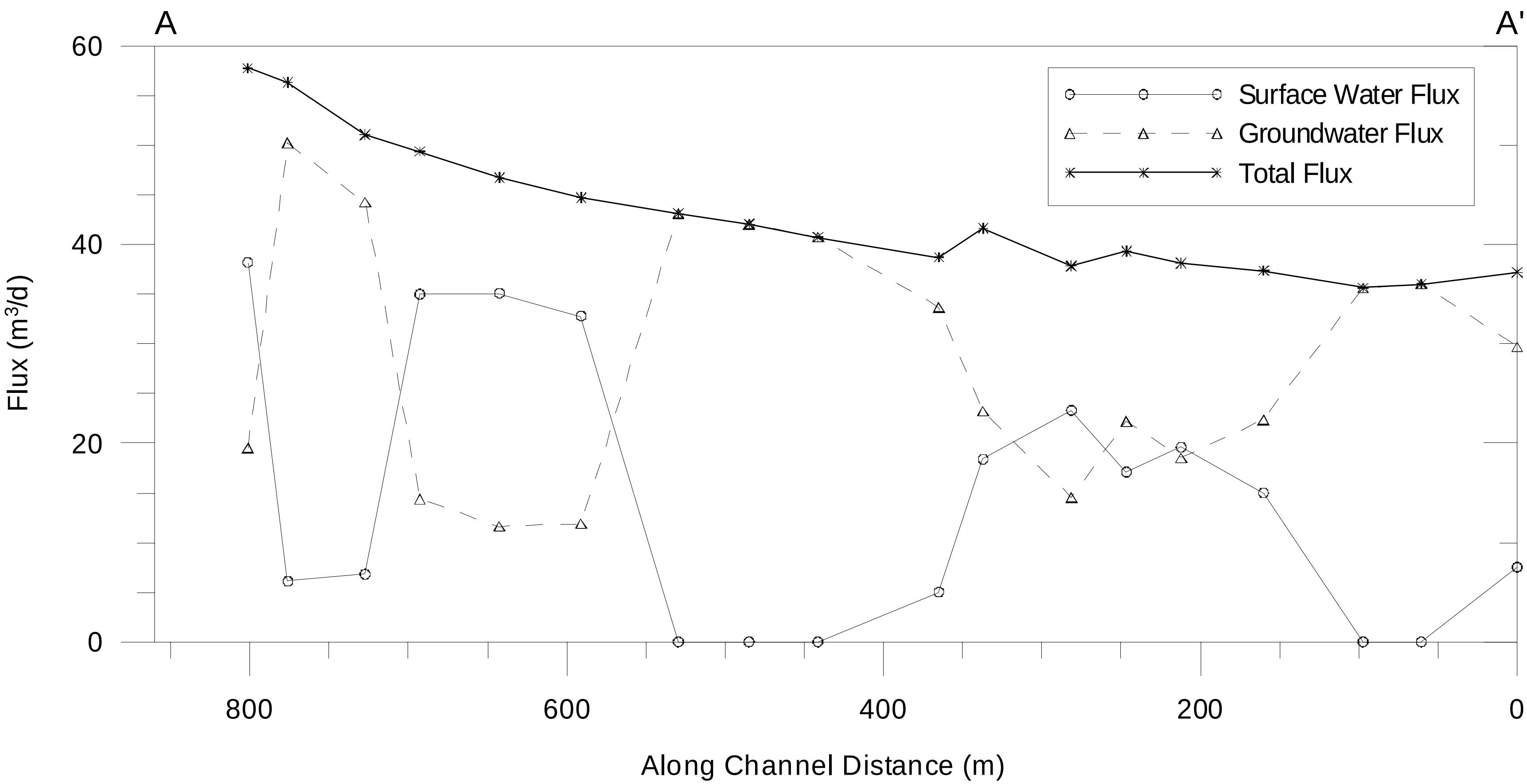

Figure 17: Simulated longitudinal variation in surface-water and groundwater flux in Cottonwood Springs transient model during stress period 3 (A-A’ on Fig. 5 and Plate 1a).

represent a vegetative response to the current period of below average precipitation in the Southwestern U.S., however the decreasing trends in low 3-day mean winter discharge observed at both springs likely represent decreases in recharge or storage in the aquifer which supplies the springs. Winter base flow at Cottonwood Springs decreased 19% between 1995 and 2001, while a 25% decrease was observed at Indian Gardens Springs between 1994 and 2001. If current trends in winter baseflow at Cottonwood Springs continue, winter baseflow may decrease to 8 m^3/day by the year 2020.

Regional groundwater modeling studies indicate the potential for groundwater pumping-induced decreases in spring discharge (e.g. Montgomery and Associates 1996; 1998; Springer and Kessler, personal communication), however limited data regarding rates of abstraction through time are available, making it difficult to draw a causal relationship between pumping and discharge. Alternatively, the trends may be the result of changes in climate, and such scenarios have not been simulated with existing regional groundwater models. Over short timescales (yrs), reduced precipitation input may influence discharge through a vegetative feedback, while over longer timescales (100s to 1000s of yrs) reduced precipitation may result in reduced discharge through variations in recharge to the regional aquifer. Either groundwater pumping or short- or long- term climate change may be responsible for the observed decreases in discharge, however more data is needed to distinguish between these various signals.

Surface water/groundwater interaction was simulated at an unprecedented scale (1-m grid scale spacing) with steady-state and transient surface water/groundwater flow models. The criterion for a good-fit was met at all discharge stations for the steady-state simulation and at most discharge stations and wells during most stress periods for the transient simulation. Additionally, the criterion for a good-fit with the flow/no flow data was met for the steady-state model and for stress periods 1 and 6 in the transient model. During stress periods 2 through 5, the transient model overestimated the extent of surface flow in the channel leading to low percentages of correctly-simulated cells. Although these percentages are below the criterion for a good-fit, many of the cells simulated incorrectly as flowing were almost dry (low discharge values). Overall, the calibration was successful and the transient model does a reasonably good job of simulating the seasonal variability of surface-water and groundwater flow in Cottonwood Springs riparian aquifer during the simulation period. During the peak of the growing season, high rates of ET result in downstream decreases in water availability and the total flux of water decreases from ~60 m^3/d in upstream areas to ~35 m^3/d in downstream areas.

Future work will relate these spatial variation in flux to spatial variations in vegetation characteristics to develop a vegetation water-use model. Simulations of the surface water/groundwater flow models under various future discharge scenarios will provide estimates of changes in flux. In conjunction with the vegetation water-use model, these changes in flux will be used to estimate the response of woody riparian vegetation to reductions in spring discharge.

Many of the other South Rim springs discharge at a similar stratigraphic level, have riparian areas composed of similar geologic materials, have similar steep topographic gradients, and support similar stands of riparian vegetation as Cottonwood Springs. The results are therefore likely applicable to other South Rim Springs, at least qualitatively. These results suggest that the potential for further decreases in spring discharge over relatively short timescales is great. Such decreases would result in reduced water availability in the spring-fed riparian aquifers, and possibly negative impacts to the associated riparian ecosystems.

As with any modeling effort, many assumptions and simplifications were made in the simulation of surface-water and groundwater flow in this system. Aquifer test data would provide more accurate measurements of the hydraulic properties of the aquifer material, and geophysical studies would help better constrain the thickness of the shallow alluvial aquifer and variations in substrate properties with depth. This study did not fully evaluate the effects of runoff events on water storage and availability, and further research in this area is warranted. The models adequately simulated conditions as observed in the filed, suggesting that the model codes properly simulated stream/aquifer exchanges in this system, however more rigorous testing of the codes is needed.

6. Conclusions

Characterization of the topography, geology, and geomorphology of the riparian aquifer associated with Cottonwood Springs provided the foundation for the construction of numerical surface-water and groundwater flow models. Repeated field observations of stream discharge at ten locations, repeated mapping of the extent of dry and flowing reaches, and water-level data collected at two wells allowed us to characterize the seasonal range of water availability at the site and to calibrate the models. A steady-state model was calibrated to simulate the maximum water availability condition observed on March 21, 2003. To simulate the seasonal variability of water availability at the site, a transient model with six stress periods was calibrated to simulate conditions observed between April 26, 2003 and January 16, 2004. The models were used to quantify temporal and spatial variations in surface-water and groundwater flux, and they reveal a pattern of progressively decreasing flux in the downstream direction during the growing season.

Stream gauge data at Cottonwood and Indian Gardens Springs show trends of decreasing spring discharge since at least 1994. These observed decreases coupled with the PDO evidence that precipitation in the region may be below average for the next 20-30 yrs suggests that the potential for alteration to these riparian ecosystems over relatively short timescales is great. Because of the hydrogeological and topographical similarity of Cottonwood Springs to many of the other South Rim Springs, the results are likely qualitatively applicable to many of the other springs.

The discharge trends may be the result of decreases in precipitation associated with current drought conditions in the Southwestern U.S. through a vegetative feedback. However, because trends were seen in winter base flow, and regional groundwater models predict the potential for groundwater pumping to influence spring discharge, groundwater abstraction may be the cause of these decreases. Thus, careful monitoring of spring discharges, precipitation rates, and groundwater abstraction rates, is critical to properly manage this spring-aquifer system. Careful consideration of the potential risks of water development must be made to ensure that the hydrologic and ecological integrity of the South Rim springs is preserved.

Acknowledgements

Major funding for this project was provided by a grant from Grand Canyon National Park passed through the Colorado Plateau Cooperative Ecosystem Studies Unit. Additional funding was provided by a research grant from the Geological Society of America, and scholarships from the Friday Lunch Clubbe, Montgomery and Associates, and the L.B.C. McCullough Foundation. Significant contributions to the study were provided by John Rihs who served as the National Park Service Technical Representative, as well as Diana Anderson, Ronald Blakey, Steve Monroe, John Rihs, Sean Welch, James Rumbaugh, and numerous student assistants.

References

Adams, E.E., and Gelhar, L.W., 1992. Field study of dispersion in a heterogeneous aquifer. Water Resources Research, v. 28, no. 12, pp. 3293-3307.

Auble, G.T., Friedman, J.M., and Scott, M.L., 1994. Relating riparian vegetation to present and future streamflows. Ecological Applications, v. 4, pp. 544-554.

Ball, J.T., Brummer, J., Burnett, E., and Busch, D., 1995. Vegetation management study Lower Colorado River, Phase II. Final Report to the Bureau of Reclamation, Lower Colorado Region, Boulder City, NV, 72 pp.

Billingsley, G.H., and Huntoon, P.W., 1983. Geologic map of the western Grand Canyon Formation, Arizona. Grand Canyon Natural History Association, Grand Canyon, AZ.

Bissett, L., 1994. Field assessment of stream/aquifer interaction under semi-arid conditions and problems with computer representation. Unpublished M.E. Thesis, Colorado School of Mines, Golden, CO, 95 p.

Busch, D.E., and Smith, S.D., 1995. Mechanisms associated with the decline of woody species in riparian ecosystems of the southwestern U.S. Ecological Monograph 65, pp. 347-370.

Dahm, C.N., Cleverly, J.R, and Coonrod, J.E.A., 2002. Evapotranspiration at the land/water interface in a semi-arid drainage basin. Freshwater Biology v. 47, pp. 831-843.

Davis, S.N., 1969. Porosity and permeability of natural materials, In: De Wiest, R.J.M. (editor), Flow through porous media. Academic Press, New York, pp. 54-89.

Environmental Simulations Inc., 2000. Groundwater Vistas v. 3.45, pre- and post-processor for MODFLOW 2000, Reinhold, PA.

Environmental Systems Research Institute Inc. (ESRI), 1999-2001. ArcView v. 8.2. Geographic Information System software, Redlands, CA.

Franz, E.H., and Bazzaz, F.A., 1977. Simulation of vegetation response to modified hydrologic regimes: a probabilistic model based on niche differentiation in a floodplain forest. Ecology, v. 58, pp. 176-183.

Harbaugh, A.W., Banta, E.R., Hill, M.C., and McDonald, M.G., 2000. MODFLOW-2000, The U.S. Geological Survey modular ground-water model, User guide to modularization concepts and the ground-water flow process. U.S. Geological Survey Open File Report 00-92, 121 p.

Harshbarger and Associates, Inc., 1973. Groundwater conditions and potential development on Babbit Ranch area, Coconino County, Arizona. Unpublished.

Hereford, R., Webb, R.H., and Graham, S., 2002. Precipitation history of the Colorado Plateau region, 1900-2000. U.S. Geological Survey Fact Sheet 119-02, 4 p.

Huntoon, P.W., and Billingsley, G.H., 1996. Geologic map of the eastern part of the Grand Canyon National Park, Arizona. Grand Canyon Association, 1:62,500 scale.

Kessler, J.A., 2002. Grand Canyon springs and the Redwall-Muav aquifer: Comparison of geologic framework and groundwater flow models. Unpublished M.S. Thesis, Northern Arizona University, Flagstaff, AZ, 122 p.

Masch, F.E., and Denny, K.J., 1966. Grain size distribution and its effect on the permeability of unconsolidated sands. Water Resources Research v. 2, pp. 665-677.

McCabe, J.G., and Dettinger, M.D., 1999. Decadal variations in the strength of ENSO teleconnections with precipitation in the western United States. International Journal of Climatology, v. 19, pp. 1399-1410.

McDonald, M.G., and Harbaugh, A., 1984. A modular three-dimensional finite-difference ground-water flow model. U.S. Geological Survey Open File Report 83-875, 528 p.

Mehl, S.W., and Hill, M.C., 2001. MODFLOW-2000, the U.S. Geological Survey modular ground-water model - user guide to the Link-Amg (LMG) package for solving matrix equations using an algebraic multigrid solver. U.S. Geological Survey Open File Report 01-177, 33 p.

Metzger, D.G., 1961. Geology in relation to availability of water along the South Rim, Grand Canyon National Park, Arizona. U.S. Geological Survey Water Supply Paper 1475-C, 138 p.

Montgomery and Associates, Inc. 1998. Supplemental assessment of the hydrologic conditions and potential effects of proposed ground water withdrawal, Coconino Plateau groundwater sub-basin, Coconino County, Arizona. In: Appendix of the Final Environmental Impact Statement for Tusayan growth. Kaibab National Forest, 85 p.

Montgomery and Associates, Inc. 1996. Assessment of the hydrologic conditions and potential effects of proposed ground water withdrawal for Canyon Forest Village, Coconino County, Arizona, In: Appendix of the Final Environmental Impact Statement for Tusayan growth. Kaibab National Forest, 64 p.

National Oceanic and Atmospheric Administration (NOAA), 2004a. United States hourly/daily precipitation data (http://precip.fsl.noaa.gov/hourly_precip.html).

National Oceanic and Atmospheric Administration (NOAA), 2004b. United States monthly precipitation data (http://lwf.ncdc.noaa.gov/oa/climate/online/coop-precip.html).

Pang, L., Close, M., and Nooram, M., 1998. Rhodamine WT and Bacillus subtilis transport through an alluvial gravel aquifer. Ground Water, v. 36 no. 1, pp. 112-122.

Primack, A.G.B., 2000. Simulation of climate-change effects on riparian vegetation in the Pere Marquette River, Michigan. Wetlands, v. 20, pp. 538-547.

Prudic, D.E., 1989. Documentation of a computer program to simulate stream-aquifer relations using a modular, finite-difference, ground-water flow model. U.S. Geological Survey Open File Report 88-729, 113 p.

Rains, M.C., Mount, J.F., and Larsen, E.W., 2004. Simulated changes in shallow groundwater and vegetation distributions under different reservoir operations scenarios. Ecological Application, v. 14, no. 1, pp. 192-207.

Robinson, T.W., 1970. Evapotranspiration by woody phreatophytes in the Humboldt River valley near Winnemucca, Nevada. U.S. Geological Survey Professional Paper 491-D, 41 p.

Rood, S.B., Mahoney, J.M., Reid, D.E., and Zilm, L., 1995. Instream flows and the decline of riparian cottonwoods along the St. Mary River, Alberta. Canadian Journal of Botany, v. 73, pp. 1250-1260.

Sammis, T.W., 1972. Water disposition in ephemeral stream channels, In: Hydrology and water resources in Arizona and the Southwest, v. 2, Proceedings of the 1972 meetings of the Arizona Section, American Water Resources Association, and the Hydrology Section, Arizona Academy of Science, Prescott, AZ, pp. 473-491.

Scott, M.L., Auble, G.T., and Friedman, J.M., 1997. Flood dependency of cottonwood establishment along the Missouri River, Montana, USA. Ecological Applications, v. 7, pp. 677-690.

Scott, M.L., Shafroth, P.B., and Auble, G.T., 1999. Responses of riparian cottonwoods to alluvial water table declines. Environmental Management, v. 23, pp. 347-358.

Shafroth, P.B., Auble, G.T., Stromberg, J.C., and Patten, D.T., 1998. Establishment of woody riparian vegetation in relation to annual patterns of streamflow, Bill Williams River, Arizona. Wetlands, v. 18., no. 4, pp. 577–590.

Shafroth, P.B., Stromberg, J.C., and Patten, D.T., 2000. Woody Riparian Vegetation Response to Different Alluvial Water Table Regimes. Western North American Naturalist, v. 60, pp. 66-76.

Shepherd, RG., 1989. Correlations of permeability and grain size. Ground Water, v. 27, no. 5, pp. 633-638.

Shibing, P., Zhongjing, W., and Weiguo, X., 2002. Discussion on numerical simulation for stream-aquifer system. Shuiwen-Hydrology, v. 22, no. 4, pp. 19-21.

Stevens, L.E., and Ayers, T.J., 2002. The biodiversity and distribution of alien vascular plant and animals in the Grand Canyon region, In: B. Tellman (editor), Invasive exotic species in the Sonoran Region. University of Arizona Press, Tucson pp. 241-265.

Springer, A.E., Petroutson, W.D., and Semmens, B.A., 1999a. Spatial and temporal variability of hydraulic conductivity in active reattachment bars of the Colorado River, Grand Canyon. Ground Water, v. 37, no. 3, pp. 338-344.

Springer, A.E., Wright, J.M., Shafroth, P.B., Stromberg, J.C., and Patten, D.T., 1999b. Coupling groundwater and riparian vegetation models to asses effects of reservoir releases. Water Resources Research, v. 35, no. 12, pp. 3621-3630.

Stromberg, J.C., Tiller, R., and Richter, B.D., 1996. Effects of groundwater decline on riparian vegetation of semi-arid regions, the San Pedro, Arizona. Ecological Applications, v. 6, pp. 113-131.

Swain, E.D., and Wexler, E.J., 1996. A coupled surface-water and ground-water flow model (MODBRNCH) for simulation of stream-aquifer interaction. U.S. Geological Survey Techniques of Water-Resources Investigations, book 6, chap. A6, 125 p.

Sykes, J.F., Pahwa, S.B., Lantz, R.B., and Ward, D.S., 1982. Numerical simulation of flow and contaminant migration at an extensively monitored landfill. Water Resources Research, v. 18, no. 6, pp. 1687-1704.

Tellman B., Yarde, R., and Wallace, M.G., 1997. Arizona's changing rivers: How people have affected the rivers. Issue Paper 19, Water Resources Research Center, University of Arizona, Tucson, Arizona, 198 p.

United States Geological Survey (USGS), 2002. United States daily streamflow data (http://nwis.waterdata.usgs.gov/usa/nwis/discharge).

United States Geological Survey (USGS), 2004a. Unpublished 15-minute streamflow data. Steve Monroe, Water Resources Division, Flagstaff, AZ.

United States Geological Survey (USGS), 2004b. Unpublished bedrock source discharge data collected by Steve Monroe between 2000 and 2001. Water Resources Division, Flagstaff, AZ.

Western Regional Climate Center (WRCC), 2001. United States average monthly pan evaporation data (www.wrcc.dri.edu/htmlfiles/westevap.final.html).

Wilson, E., 2000. Geologic framework and numerical groundwater models of the South Rim of the Grand Canyon, Arizona. Unpublished M.S. Thesis, Northern Arizona University, Flagstaff, AZ, 72 p.

Woessner, W.W., Ball, P.N., DeBorde D.C., and Troy, T.L., 2001. Viral transport in a sand and gravel aquifer under field pumping conditions. Ground Water, v. 39, no. 6, pp. 886-894.

Zhang, Y., Wallace, J.M., and Battisti, D.S., 1997. ENSO-like interdecadal variability 1903-93. Journal of Climate, v. 10, pp. 1004-1020.

CHAPTER 3

SITE CHARACTERIZATION

Extensive field data were collected to characterize the riparian area associated with Cottonwood Springs, and provide the framework for the construction and calibration of local, coupled, surface-water and groundwater flow models. These data included a physical characterization of the topography, geomorphology, geology, and hydrostratigraphy of the site, in addition to a hydrologic characterization of groundwater and surface-water availability.

Topography

A detailed topographic survey was conducted using an electronic Total Station (Topcon Positioning Systems Inc., Pleasanton, CA) to characterize the topography of the riparian area and provide topographic data for measuring channel morphologic parameters. Points were shot at major vertical and horizontal inflection points along the thalweg of the channel, as well as along 31 cross sections oriented perpendicular to the thalweg. The horizontal point closure ratio of the survey was 1:12,000 classifying it as a third-order class I survey (closure standard = 1:10,000) based on the U.S. Army Corps of Engineers (USACE) classification scheme (ASCE, 2000). The elevation misclosure was 0.028 ft classifying it as a third-order survey (closure standard = 0.035 ft) based on USACE standards. The point data were imported into a Geographic Information System (GIS) using ArcView v.8.2 (ESRI, Redlands, CA). Additional elevation points were generated using hand-leveling techniques during a subsequent vegetation survey (Scott and Shafroth, unpublished data). These points were incorporated into the GIS and contoured using an inverse-distance-weighted interpolation scheme to produce a 1-meter contour interval topographic base map (Fig. 6; Plate 1a). Figure 18 shows the resulting longitudinal profile of the study reach. 31 channel cross-sections were plotted and bank-full channel widths and depths were estimated by assuming that the lowest major break in slope above the thalweg was representative of bank-full conditions (Appendix B, Figs. 24-30).

Hydrogeology and Geomorphology

To characterize the hydrogeology and geomorphology of the riparian area, geomorphic surfaces and fluvial and colluvial deposits were identified on the basis of grain-size characteristics, topographic relationships, and vegetation differences. The fluvial deposits in the riparian area were divided into three major mappable units, the active channel deposits, older fluvial terrace deposits, and adjacent colluvial deposits. The active channel deposits were then subdivided into three units based on grain-size characteristics observable in the field. The terrace deposits were also subdivided into three sets of terraces each corresponding to the grain-size characteristics of the adjacent active channel deposits. The lateral boundaries of the map area represent the major break in topographic slope associated with the hillslope/valley transition. This break in slope is generally associated with the contact between fluvial deposits and adjacent colluvial deposits. In portions of the study area the major break in topographic slope occurs part way into the colluvial deposits, and in these locations some colluvial material was included in the mapped area (Fig. 6; Plate 1a). In these areas, the colluvial deposits have

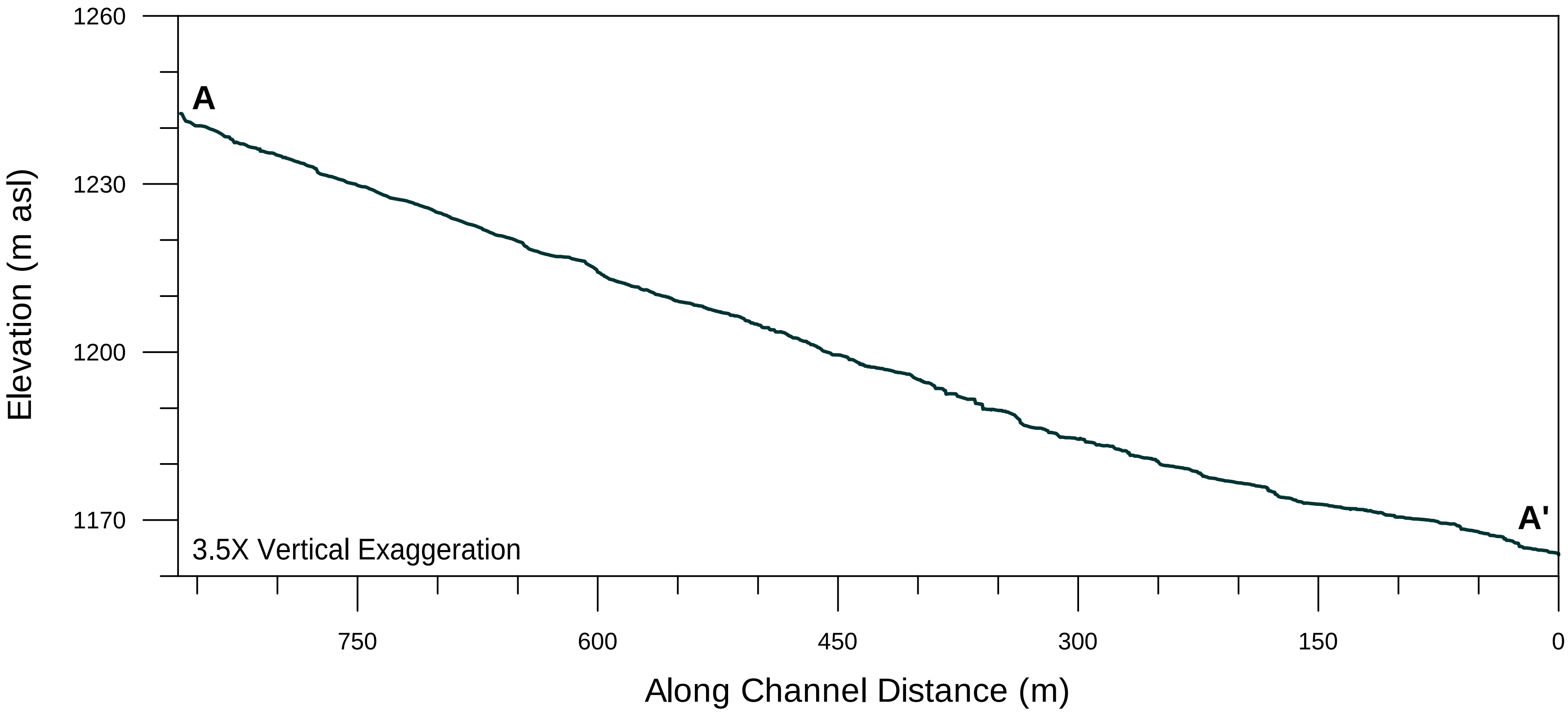

Figure 18: Longitudinal profile of the study reach at Cottonwood Creek, vertical exaggeration is 3.5X (A-A' on Fig. 2 and Plate 1a).

been eroded by surface runoff associated with steep, low-order tributaries, and in some locations form strath terraces. In a few locations, the lateral limit of xeroriparian vegetation (Scott and Shafroth, unpublished data) was used to define the lateral extent of the colluvial material included in the mapped area. Distances from the thalweg to the various contacts described above were measured and plotted in the field on the topographic base map. Contacts were then mapped and the results were incorporated with the topographic data in the GIS (Fig. 6; Plate 1a).

For logistical reasons and to minimize the environmental impacts of the study, no major trenching or geophysical techniques were employed to ascertain the thickness of the fluvial or colluvial units, or describe changes in sediment characteristics with depth; however, some constraints were possible. Small pits were dug at several locations in the channel and bedrock was reached at one location. Alluvium thickness was measured at this location, and minimum alluvium thickness was recorded at the other locations. Changes in grain-size, sorting, and degree of consolidation with depth were also noted at these locations. Additional constraints on the location of the underlying Bright Angle Shale were also possible, as bedrock outcrops in the channel near the center of the study reach and again at the base of the study reach (Fig. 6; Plate 1a).

Unit Descriptions

<u>Qs1 and Qt1</u>

Unit Qs1 is a fine sand, Holocene stream-channel alluvium and floodplain deposit. It ranges in thickness from 1-5 m and consists of unconsolidated, well-sorted, subrounded, fine sand with lesser amounts of silt and clay. Additionally, the deposit contains high amounts of organic material. The mean grain size is ~0.1 mm (Table 2; Appendix C, Fig. 31a). No vertical variation in the degree of consolidation was observed. Dense stands of willow trees likely contribute to the accumulation and attenuation of this fine sand and silt which is up to several meters in thick. Unit Qt1 is a fine sand alluvial terrace deposit composed of the same materials as Qs1 (Table 2; Appendix C, Fig. 31b). The terraces represent incision into a former floodplain and are most likely Holocene in age.

Qs2 and Qt2

Unit Qs2 is a fine gravel, Holocene stream-channel alluvium and floodplain deposit. It ranges in thickness from 0-1 m and is almost exclusively composed of unconsolidated, moderately well-sorted, subangular, fine gravel clasts of Bright Angel Shale. A few outsized subrounded, cobble clasts of Muav Limestone and Redwall Limestone are present, and a moderate degree of clast imbrication in the direction of the modern gradient was observed. The mean grain size is ~2.6 mm (Table 2; Appendix C, Fig. 32a). A slight increase in the degree of consolidation was observed below 10 cm. The subangular clasts and dominance of Bright Angel Shale indicate limited transport distance consistent with a source area from the spring-fed tributary entering WFCC near the USGS stream gauge (Figs. 6 and 9, Plate 1a) which has a small drainage with Bright Angel Shale bedrock throughout. Unit Qt2 is a fine gravel alluvial terrace deposit composed of the same materials as Qs2, except for at land surface where the terraces are partially mantled with coarse gravel and cobbles (Table 2; Appendix C, Fig. 32b). The terraces are incisional features and the gravel mantle represents recent overbank deposition during runoff events.

Qs3 and Qt3

Unit Qs3 is a gravel, Holocene stream-channel alluvium and floodplain deposit. It ranges in thickness from 0-3 m and consists predominately of unconsolidated, poorly-sorted, subangular to subrounded, gravel, cobble, and boulder clasts of Muav Limestone and Redwall Limestone. Additionally, this unit includes lesser amounts of angular to subangular, sand and silt clasts of Bright Angel Shale. The mean grain size is ~30 mm (Table 2). Boulders, where present, form knickpoints in the channel with cobbles concentrated upstream and downstream. A slight increase in the degree of consolidation below 10 cm was observed as was a moderate degree of clast imbrication in the direction of the modern gradient. Weakly-consolidated, clast-supported gravel bars occur in places. The subrounded and dominantly limestone clasts indicate a longer transport distance consistent with a source area from the main stem of Cottonwood Creek and from the ephemeral tributary just upstream of this confluence (Figs. 6 and 9, Plate 1a). These two tributaries have much larger drainage areas than WFCC and are underlain by bedrock of the Redwall Limestone and Muav Limestone in addition to the Bright Angel Shale. Unit Qt2 is a gravel alluvial terrace deposit composed of the same materials as Qs3, except for in the upper 10 cm where recent runoff events have deposited excess fines as overbank deposits.

Qd

Unit Qd is a Holocene to Pleistocene undifferentiated colluvial deposit. This unit ranges in thickness from 1-8 m and consists of weakly to moderately well-consolidated, poorly-sorted, subangular, clasts of Muav Limestone and Redwall Limestone with lesser amounts of Bright Angel Shale, and Coconino Sandstone. Clast sizes range from silt to boulders but are predominantly gravel-sized. The mean grain size is ~37 mm (Table 2). The unit is dominantly matrix-supported, however discrete clast-supported lenses occur in places. The colluvial materials are chiefly debris-flow deposits that have been subsequently eroded into strath terraces by runoff events in the main stem of the channel. In places tributary runoff has also contributed to the erosion, as many of the terraces occur at the junction of steep, low-order tributaries.

Cba

A measured section from Cottonwood Canyon indicates that the Middle Cambrian Bright Angel Shale (Cba) is ~100 m thick in the study area and consists predominantly of a lenticular heterolithic facies composed of fissile mudshale and clayshale with lenses of fine-grained sandstone (Martin, 1985). The formation overlies the Tapeats Sandstone and forms slopes. The lower portion of the formation consists of a series of upward-fining sequences and additional facies include cross-stratified sandstone, conglomeratic sandstone, and sandstone interbedded with sheet siltstone, mudshale, and clayshale. The middle portion of the formation consists of a series of upward-coarsening sequences and additional facies include mottled siltstone and cross-stratified sandstone. The upper portion of the section also consists of a series of upward-coarsening sequences and additional facies include massive bioturbated sandstone and cross-stratified sandstone (Martin, 1985). The contact with the overlying Muav Limestone is gradational and some intertonguing of the two formations occurs in the upper ~ 20 m of the section (Martin, 1985).

Hydraulic Conductivity

To obtain initial estimates of the hydraulic conductivity values (K) of the various units described above, representative samples were collected at various depths. For dominantly sand-size samples, a grain-size analysis was performed using standard dry sieve techniques, and cumulative curves were constructed (Appendix C, Figs. 31 and 32). Estimates of K were then made using the grain-size distribution data, and physical descriptions of rounding and sorting. The empirical relationship developed by Shepherd (1989) was used to calculate K (Eq. 3):

$$K = Cd^{j}_{50} \qquad (3)$$

where C is a shape factor, d_{50} is the mean grain size (mm), and j is an exponent based on rounding and sorting. For samples that were not dominantly sand, a pebble count was performed in the field to determine the d_{50} grain size, and the material was described in terms of rounding and sorting; published estimates of K for sediments with similar characteristics were used (Table 2).

Streambed Roughness

To route streamflows using numerical models, estimates of Manning's Roughness Coefficient (n) are needed; Manning's n was estimated in the field for three distinct reaches using the method described by Arcement and Schneider, 1989:

$$n = (n_b + n_1 + n_2 + n_3 + n_4)m \qquad (4)$$

where n_b is base value for straight, uniform, smooth channels in natural materials, n_1 is a correction factor for the effect of surface irregularities, n_2 is a value for variation in the shape and size of the channel cross section, n_3 is a value for obstructions, n_4 is a value for vegetation and flow conditions, and m is a correction factor for meandering of the channel (Table 10).

Table 10: Summary of parameters in Eq. 3 and calculated Manning's Roughness Coefficient values for an upstream, middle, and downstream reaches at Cottonwood Creek.

	upstream	middle	downstream
n	0.0450	0.0400	0.0350
n_b	0.0270	0.0280	0.0270
n_1	0.0040	0.0040	0.0030
n_2	0.0020	0.0020	0.0010
n_3	0.0040	0.0040	0.0030
n_4	0.0080	0.0020	0.0010
m	1.0000	1.0000	1.0000

Water-Table Fluctuations

Two 1.5-in diameter, shallow, observation wells constructed of slotted PVC piping were installed 0.6-1.1 m deep in the channel bed (see Fig. 6 and Plate 1a for locations) to monitor water-table elevations. LT Levelogger pressure transducers (Solinist, Waterloo, Ontario) were installed in each well at a known depth below land surface. They were set to correct for elevation, and total pressure measurements were recorded at 15-minute intervals from July 20, 2003 – April 18, 2004. A baralogger (Solinist, Waterloo, Ontario) was also installed adjacent to the stream channel and at an elevation intermediate to the two wells. Barometric pressure measurements were also recorded at 15-minute intervals over the same period. The pressure measurements of both instruments automatically convert the data to equivalent columns of water in cm, however to obtain water-level measurements it is necessary to correct for barometric pressure using eq. 5:

$$P_w = P_t - P_b \quad (5)$$

where P_w is water-level pressure, P_t is total pressure, and P_b is barometric pressure. Both the LT Levelogger and the Baralogger transducers have an accuracy of 0.1% FS, a range of 9 m at sea level, and a resolution of 0.3 cm.

Water levels in both wells were measured using a chalked steel meter stick at the time of well installation and each time the pressure data were downloaded. Any discrepancies between the field measurements and the transducer measurements were evaluated for their significance and corrected if necessary. In general, the numbers agreed to within 2 cm except following one high flow event, where the downstream well (DW) shifted several cm. Water-level data in well DW were corrected for the movement

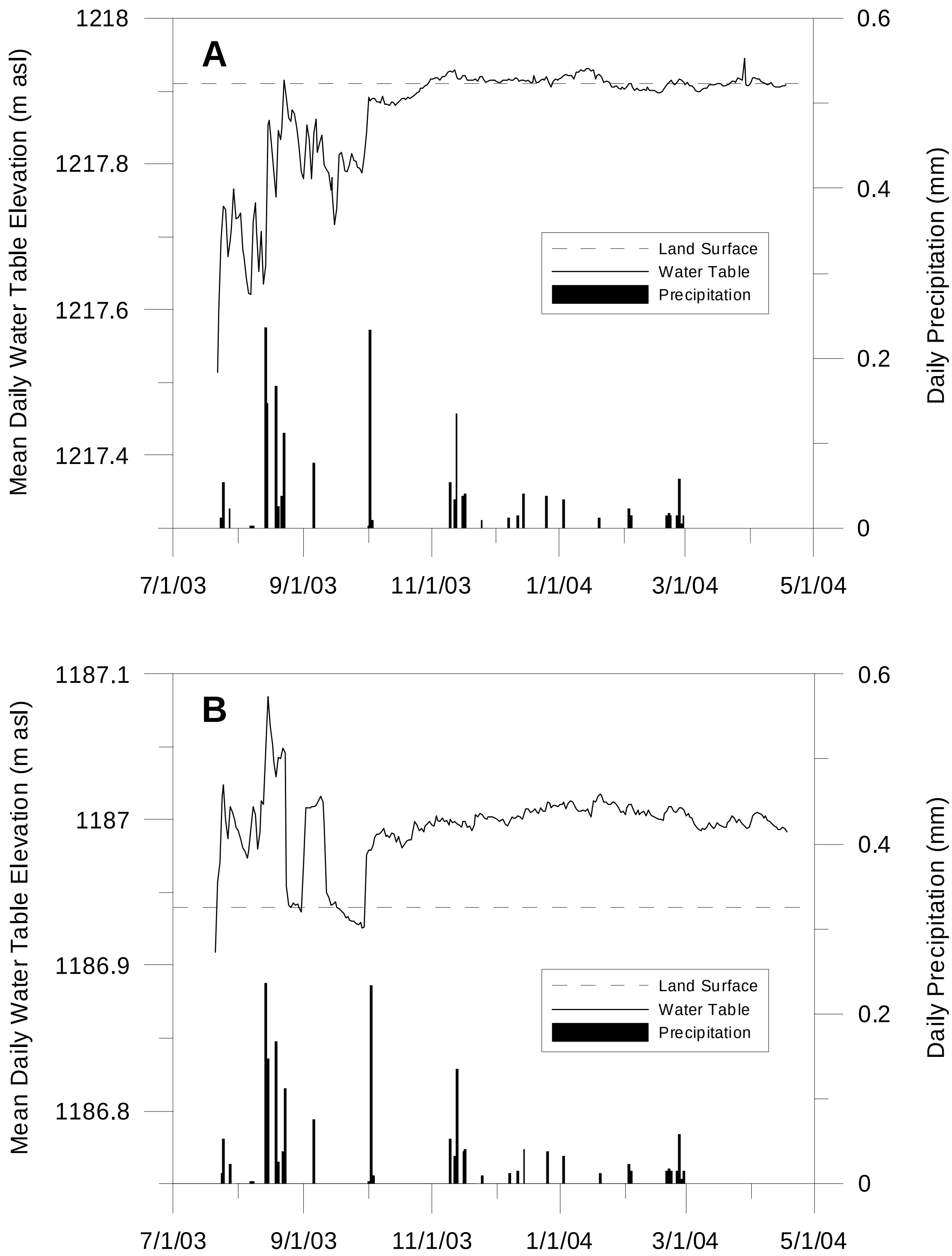

Figure 19: Mean daily water table elevations at (A) upstream well (UW) and (B) downstream well (DW) at Cottonwood Springs, and daily precipitation totals from Phantom Ranch (NOAA, 2004b). See Fig. 6 and Plate 1a for well locations.

with a linear correction. Average daily water-level data for each well over the entire period of record are shown in Fig. 19. The data are plotted with daily precipitation data from Phantom Ranch, and the water level data show sharp peaks in elevation associated with some of the larger precipitation events. Water levels recover over relatively short periods after precipitation ceases (Fig. 19).

Evapotranspiration

Estimates of evapotranspiration rates (ET) for various reaches were needed to simulate transpiration of vegetation. Woody riparian vegetation at Cottonwood Springs consists dominantly of cottonwood and willow trees, and a mix of xeroriparian species including mesquite, acacia, and rosebud. The woody riparian vegetation is confined to a relatively narrow zone adjacent to the stream channel. The relative abundances of the various riparian vegetation types vary longitudinally along the stream channel. Percent cover of the various riparian vegetation species was mapped in the field on a digital orthophoto quad, and three primary zones of ET were determined, an upstream reach dominated by willow, a central reach dominated by cottonwood, and a downstream reach dominated by an open canopy of cottonwood and a mix of xeroriparian species including mesquite, acacia, and rosebud (Scott and Shafroth, unpublished data). The mapped area corresponding to these three zones was measured as 2,740, 1,280, and 1,690 m^2 respectively.

Using the percent cover values in conjunction with published estimates of ET from similar vegetation assemblages, an average growing season daily ET rate for each of

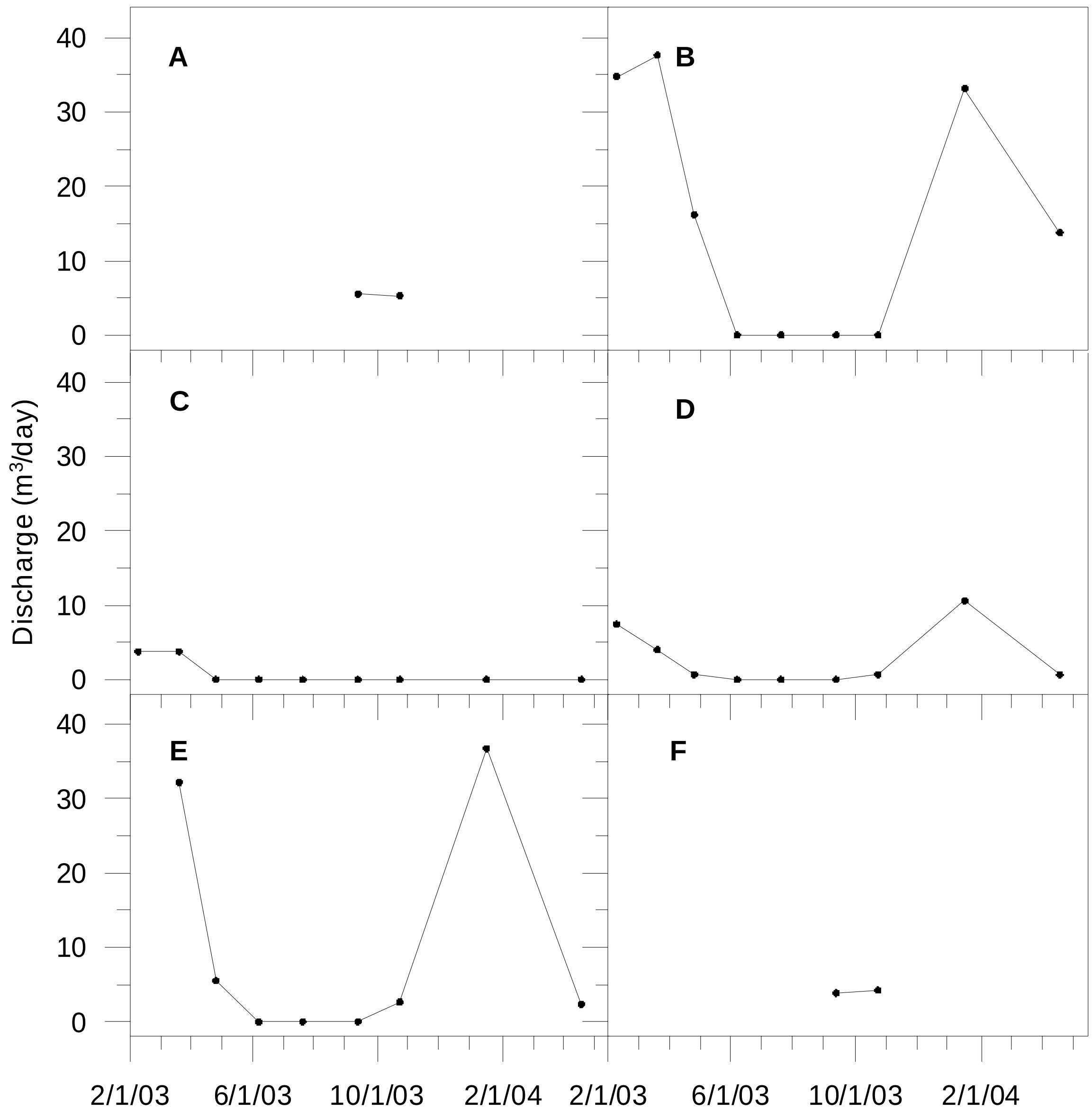

Figure 20: Stream discharge measurements at Cottonwood Springs discharge stations; (A) station 1, (B) station 2, (C) station 3, (D) station 4, (E) station 5, and (F) station 6 (see Fig. 6 and Plate 1a for locations).

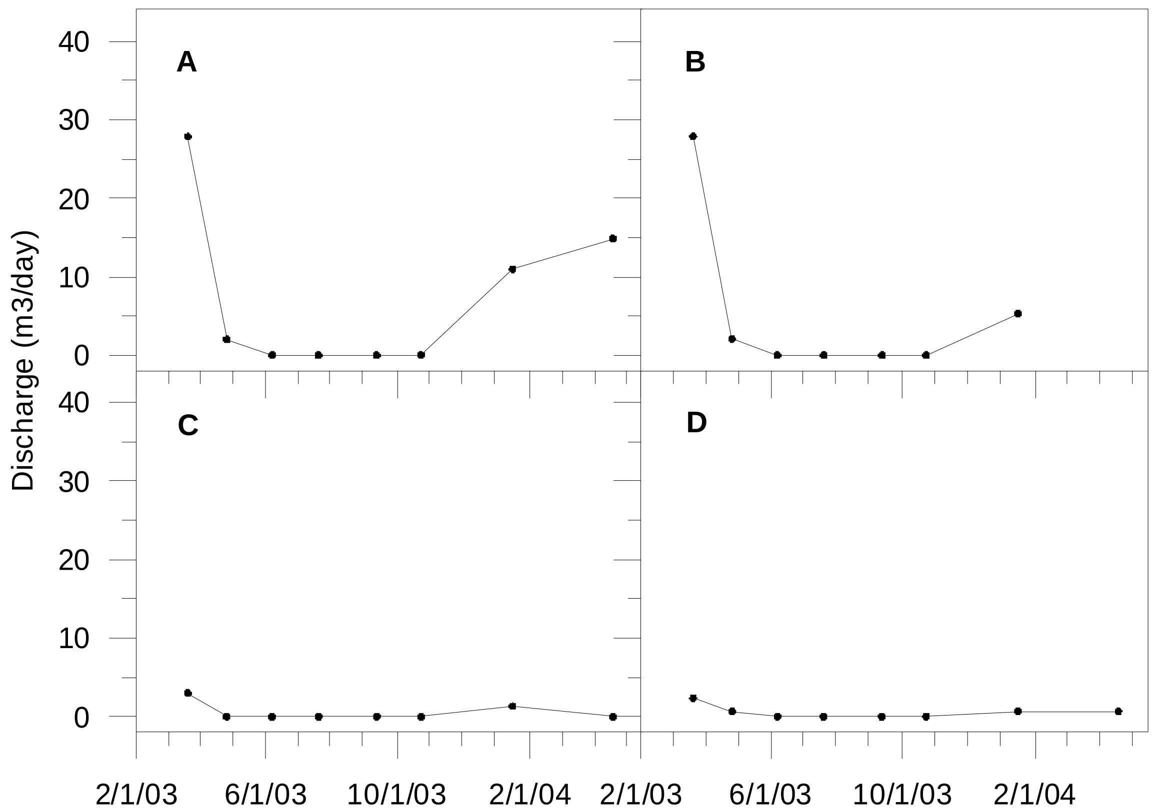

Figure 21: Stream discharge measurements at Cottonwood Springs discharge stations; (A) station 7, (B) station 8, (C) station 9, (D) station 10 (see Fig. 6 and Plate 1a for locations).

the three ET zones was calculated (Table 3). This approach assumed a 7-month growing season. Daily rates are likely higher than these during the peak of the growing season and are expected to be lower during the beginning and end of the growing season.

Flow Observations

To characterize the spatial and temporal variability of surface flows, stream discharge was measured every ~6 weeks for a period of 1 year at 8 locations in the channel using a v-notch weir; additional measurements were taken sporadically at two other stations (Figs. 20 and 21; Appendix D, Table 39) (see Fig. 6 and Plate 1a for station

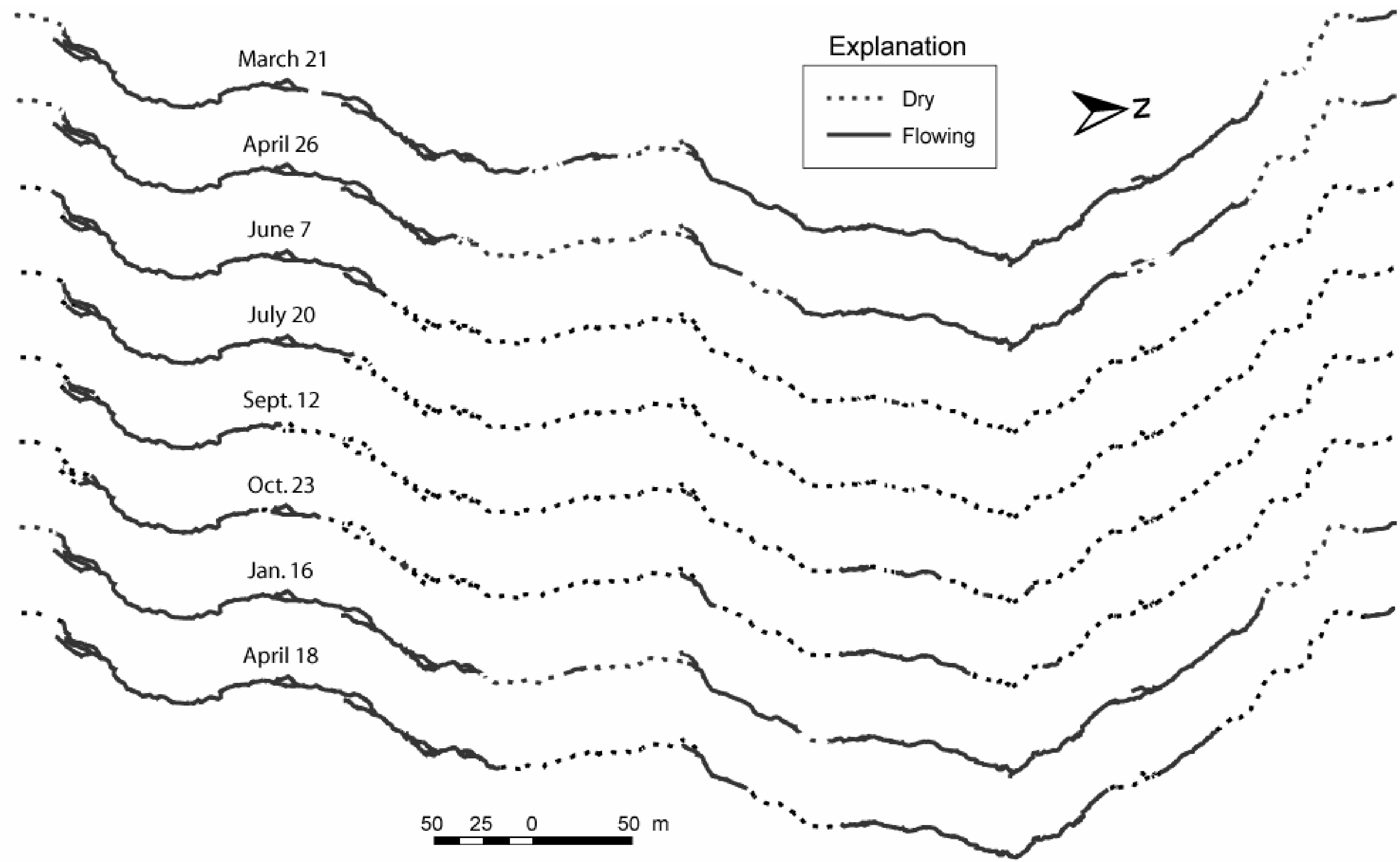

Figure 22: Dry and flowing reaches of surface-water flow at Cottonwood Springs between March 2003 and April 2004.

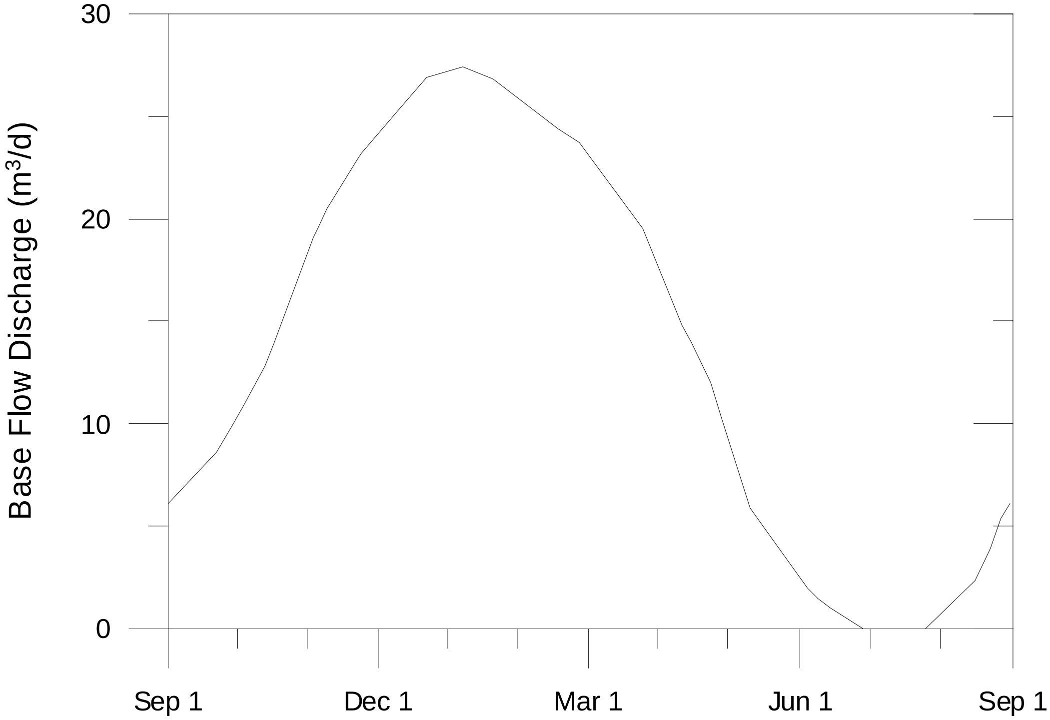

Figure 23: Generalized base flow hydrograph for Cottonwood Springs USGS gauge. Data from 1994 – 2002 (USGS, 2002; 2004a).

locations). The extent of dry, damp, and flowing reaches were also mapped every ~6 weeks, and incorporated into the GIS (Fig. 22). Existing U.S. Geological Survey (USGS) gauge data (1994-present) at one location in the channel (see Fig. 6 and Plate 1a) were compiled, and the base flow component of the discharge was isolated using graphical techniques involving the removal of peaks associated with precipitation events. A generalized base flow hydrograph representing average flow conditions for the period of record was then constructed (Figure 23).

CHAPTER 4

CONCLUSIONS

Topographic, geologic, and geomorphic data were used as the framework for numerical surface-water and groundwater flow models for Cottonwood Springs riparian aquifer. Repeated field observations of stream discharge, mapping of the extent of dry and flowing reaches, and water-level data collected at two wells allowed us to characterize the seasonal range of water availability at the site and provided data with which to calibrate the models. A steady-state model was calibrated to conditions on March 21, 2003, and a transient model with six stress periods was calibrated to field data collected between April 26, 2003 and January 16, 2004. Both models were calibrated to discharge data at five locations. In the steady-state model, all residual values were less than 15% of the range of observed values; this criterion was also met in the transient model except at a few stations during stress period 6. The models were also calibrated to the extent of surface-flow data and more than 80% of the stream cells were simulated correctly in the steady-state model and in the transient model during stress periods 1 and 6. The percentages were lower in stress periods 2 through 5. The transient model was also calibrated to water-level data at two wells such that all head residuals were less than 5 cm, except at well UW during stress period 1.

This study simulated the transient effects of transpiration and surface water/groundwater interaction at an unprecedented scale (1-m grid scale spacing). Model estimates of spatial and temporal variations in surface-water and groundwater flux were made for use in future vegetation modeling. During the winter and early spring, the total flux of water was relatively constant throughout the model area and was ~60 m^3/d. During the peak of the growing season, the total flux of water in the upstream portion of the transient model was ~60 m^3/d and decreased progressively down to ~35 m^3/d in the downstream portion of the model.

Stream gauge data at Cottonwood Springs and Indian Gardens Springs show trends of decreasing discharge since at least 1994. These observed decreases coupled with continuing groundwater pumping and the predicted continuation of below average precipitation suggests that the potential for alteration to these riparian ecosystems over relatively short timescales is great. Because of the hydrogeological and topographical similarity of Cottonwood Springs to many of the other South Rim Springs, the results of this study are likely qualitatively applicable to many of the other springs. The discharge trends may be the result of decreases in precipitation associated with current drought conditions in the Southwestern U.S. through a vegetative feedback. However, because trends were seen in winter base flow, and regional groundwater models predict the potential for groundwater pumping to influence spring discharge, groundwater abstraction may be the cause of these decreases. Long-term climate change may also have influenced the discharge trends through changes in recharge to the regional aquifer. Careful monitoring of spring discharges, precipitation rates, and groundwater abstraction rates, is critical to properly manage this spring-aquifer system, and develop any casual links between groundwater pumping or climate change and discharge at the springs. Careful consideration of the potential risks of water development must be made to ensure that the hydrologic and ecological integrity of the South Rim springs is preserved.

REFERENCES

Adams, E.E., and Gelhar, L.W., 1992. Field study of dispersion in a heterogeneous aquifer. Water Resources Research, v. 28, no. 12, pp. 3293-3307.

Arcement, G.J., and Schneider, V.R., 1989. Guide for selecting Manning's roughness coefficients for natural channels and floodplains. U.S. Geological Survey Water Supply Paper 2336, 38 p.

American Society of Civil Engineers (ASCE), 2000. Topographic Surveying. American Society of Civil Engineers Press, Reston, VA, 96 p.

Auble, G.T., Friedman, J.M., and Scott, M.L., 1994. Relating riparian vegetation to present and future streamflows. Ecological Applications, v. 4, pp. 544-554.

Ball, J.T., Brummer, J., Burnett, E., and Busch, D., 1995. Vegetation management study Lower Colorado River, Phase II. Final Report to the Bureau of Reclamation, Lower Colorado Region, Boulder City, NV, 72 pp.

Beus, S.S., 2003. Redwall Limestone and Surprise Canyon Formation, In: Beus, S.S., and Morales, M. (editors), Grand Canyon geology. Oxford University Press, New York, pp. 115-135.

Beus, S.S., and Morales, M., 2003. Grand Canyon geology. Oxford University Press, New York, 432 p.

Billingsley, G.H., and Huntoon, P.W., 1983. Geologic map of the western Grand Canyon Formation, Arizona. Grand Canyon Natural History Association, Grand Canyon, AZ.

Billingsley, G.H., and Hendricks, J.D., 1989. Physiographic features of Northwestern Arizona, In: Elston, D.P., Billingsly, G.H., and Young, R.A. (editors), Geology of Grand Canyon, Northern Arizona (with Colorado River guide). American Geophysical Union, Washington, D.C., pp. 67-71.

Bills, D.J., and Flynn, M.E., 2002. Hydrogeologic Data for the Coconino Plateau and Adjacent Areas, Coconino and Yavapai Counties, Arizona. U.S. Geological Survey Open-File Report 02-265, 29 p.

Bissett, L., 1994. Field assessment of stream/aquifer interaction under semi-arid conditions and problems with computer representation. Unpublished M.E. Thesis, Colorado School of Mines, Golden, CO, 95 p.

Blakey, R.C., 2004. Unpublished stratigraphic section along the South Kaibab Trail, modified from Beus and Morales (2003).

Busch, D.E., and Smith, S.D., 1995. Mechanisms associated with the decline of woody species in riparian ecosystems of the southwestern U.S. Ecological Monograph 65, pp. 347-370.

Dahm, C.N., Cleverly, J.R, and Coonrod, J.E.A., 2002. Evapotranspiration at the land/water interface in a semi-arid drainage basin. Freshwater Biology v. 47, pp. 831-843.

Davis, S.N., 1969. Porosity and permeability of natural materials, In: De Wiest, R.J.M. (editor), Flow through porous media. Academic Press, New York, pp. 54-89.

Environmental Simulations Inc., 2000. Groundwater Vistas v. 3.45, pre- and post-processor for MODFLOW 2000, Reinhold, PA.

Environmental Systems Research Institute Inc. (ESRI), 1999-2001. ArcView v. 8.2. Geographic Information System software, Redlands, CA.

Franz, E.H., and Bazzaz, F.A., 1977. Simulation of vegetation response to modified hydrologic regimes: a probabilistic model based on niche differentiation in a floodplain forest. Ecology, v. 58, pp. 176-183.

Harbaugh, A.W., Banta, E.R., Hill, M.C., and McDonald, M.G., 2000. MODFLOW-2000, The U.S. Geological Survey modular ground-water model, User guide to modularization concepts and the ground-water flow process. U.S. Geological Survey Open File Report 00-92, 121 p.

Harshbarger and Associates, Inc., 1973. Groundwater conditions and potential development on Babbit Ranch area, Coconino County, Arizona. Unpublished.

Hereford, R., Webb, R.H., and Graham, S., 2002. Precipitation history of the Colorado Plateau region, 1900-2000. U.S. Geological Survey Fact Sheet 119-02, 4 p.

Huntoon, P.W., and Billingsley, G.H., 1996. Geologic map of the eastern part of the Grand Canyon National Park, Arizona. Grand Canyon Association, 1:62,500 scale.

Kessler, J.A., 2002. Grand Canyon springs and the Redwall-Muav aquifer: Comparison of geologic framework and groundwater flow models. Unpublished M.S. Thesis, Northern Arizona University, Flagstaff, AZ, 122 p.

Martin, D.L., 1985. Depositional systems and ichnology of the Bright Angel Shale (Cambrian), eastern Grand Canyon, Arizona. Unpublished M.S. Thesis, Northern Arizona University, Flagstaff, AZ, 365 p.

Masch, F.E., and Denny, K.J., 1966. Grain size distribution and its effect on the permeability of unconsolidated sands. Water Resources Research v. 2, pp. 665-677.

McCabe, J.G., and Dettinger, M.D., 1999. Decadal variations in the strength of ENSO teleconnections with precipitation in the western United States. International Journal of Climatology, v. 19, pp. 1399-1410.

McDonald, M.G., and Harbaugh, A., 1984. A modular three-dimensional finite-difference ground-water flow model. U.S. Geological Survey Open File Report 83-875, 528 p.

Mehl, S.W., and Hill, M.C., 2001. MODFLOW-2000, the U.S. Geological Survey modular ground-water model - user guide to the Link-Amg (LMG) package for solving matrix equations using an algebraic multigrid solver. U.S. Geological Survey Open File Report 01-177, 33 p.

Metzger, D.G., 1961. Geology in relation to availability of water along the South Rim, Grand Canyon National Park, Arizona. U.S. Geological Survey Water Supply Paper 1475-C, 138 p.

Middleton, L.T., and Elliot, D.K., 2003. Tonto Group, In: Beus, S.S., and Morales, M. (editors), Grand Canyon geology. Oxford University Press, New York, pp. 90-106.

Montgomery and Associates, Inc. 1996. Assessment of the hydrologic conditions and potential effects of proposed ground water withdrawal for Canyon Forest Village, Coconino County, Arizona, In: Appendix of the Final Environmental Impact Statement for Tusayan growth. Kaibab National Forest, 64 p.

Montgomery and Associates, Inc. 1998. Supplemental assessment of the hydrologic conditions and potential effects of proposed ground water withdrawal, Coconino Plateau groundwater sub-basin, Coconino County, Arizona. In: Appendix of the Final Environmental Impact Statement for Tusayan growth. Kaibab National Forest, 85 p.

National Oceanic and Atmospheric Administration (NOAA), 2004a. United States hourly/daily precipitation data (http://precip.fsl.noaa.gov/hourly_precip.html).

National Oceanic and Atmospheric Administration (NOAA), 2004b. United States monthly precipitation data (http://lwf.ncdc.noaa.gov/oa/climate/online/coop-precip.html).

Pang, L., Close, M., and Nooram, M., 1998. Rhodamine WT and Bacillus subtilis transport through an alluvial gravel aquifer. Ground Water, v. 36 no. 1, pp. 112-122.

Primack, A.G.B., 2000. Simulation of climate-change effects on riparian vegetation in the Pere Marquette River, Michigan. Wetlands, v. 20, pp. 538-547.

Prudic, D.E., 1989. Documentation of a computer program to simulate stream-aquifer relations using a modular, finite-difference, ground-water flow model. U.S. Geological Survey Open File Report 88-729, 113 p.

Rains, M.C., Mount, J.F., and Larsen, E.W., 2004. Simulated changes in shallow groundwater and vegetation distributions under different reservoir operations scenarios. Ecological Application, v. 14, no. 1, pp. 192-207.

Robinson, T.W., 1970. Evapotranspiration by woody phreatophytes in the Humboldt River valley near Winnemucca, Nevada. U.S. Geological Survey Professional Paper 491-D, 41 p.

Rood, S.B., Mahoney, J.M., Reid, D.E., and Zilm, L., 1995. Instream flows and the decline of riparian cottonwoods along the St. Mary River, Alberta. Canadian Journal of Botany, v. 73, pp. 1250-1260.

Rose, E.C., 2003. Depositional environment and history of the Cambrian Tonto Group, Grand Canyon, Arizona. Unpublished M.S. Thesis, Northern Arizona University, Flagstaff, AZ, 349 p.

Sammis, T.W., 1972. Water disposition in ephemeral stream channels, In: Hydrology and water resources in Arizona and the Southwest, v. 2, Proceedings of the 1972 meetings of the Arizona Section, American Water Resources Association, and the Hydrology Section, Arizona Academy of Science, Prescott, AZ, pp. 473-491.

Scott, M.L., Auble, G.T., and Friedman, J.M., 1997. Flood dependency of cottonwood establishment along the Missouri River, Montana, USA. Ecological Applications, v. 7, pp. 677-690.

Scott, M.L., Shafroth, P.B., and Auble, G.T., 1999. Responses of riparian cottonwoods to alluvial water table declines. Environmental Management, v. 23, pp. 347-358.

Shafroth, P.B., Auble, G.T., Stromberg, J.C., and Patten, D.T., 1998. Establishment of woody riparian vegetation in relation to annual patterns of streamflow, Bill Williams River, Arizona. Wetlands, v. 18., no. 4, pp. 577–590.

Shafroth, P.B., Stromberg, J.C., and Patten, D.T., 2000. Woody Riparian Vegetation Response to Different Alluvial Water Table Regimes. Western North American Naturalist, v. 60, pp. 66-76.

Shepherd, RG., 1989. Correlations of permeability and grain size. Ground Water, v. 27, no. 5, pp. 633-638.

Shibing, P., Zhongjing, W., and Weiguo, X., 2002. Discussion on numerical simulation for stream-aquifer system. Shuiwen-Hydrology, v. 22, no. 4, pp. 19-21.

Springer, A.E., Petroutson, W.D., and Semmens, B.A., 1999a. Spatial and temporal variability of hydraulic conductivity in active reattachment bars of the Colorado River, Grand Canyon. Ground Water, v. 37, no. 3, pp. 338-344.

Springer, A.E., Wright, J.M., Shafroth, P.B., Stromberg, J.C., and Patten, D.T., 1999b. Coupling groundwater and riparian vegetation models to asses effects of reservoir releases. Water Resources Research, v. 35, no. 12, pp. 3621-3630.

Stevens, L.E., and Ayers, T.J., 2002. The biodiversity and distribution of alien vascular plant and animals in the Grand Canyon region, In: B. Tellman (editor), Invasive exotic species in the Sonoran Region. University of Arizona Press, Tucson pp. 241-265.

Stromberg, J.C., Tiller, R., and Richter, B.D., 1996. Effects of groundwater decline on riparian vegetation of semi-arid regions, the San Pedro, Arizona. Ecological Applications, v. 6, pp. 113-131.

Swain, E.D., and Wexler, E.J., 1996. A coupled surface-water and ground-water flow model (MODBRNCH) for simulation of stream-aquifer interaction. U.S. Geological Survey Techniques of Water-Resources Investigations, book 6, chap. A6, 125 p.

Sykes, J.F., Pahwa, S.B., Lantz, R.B., and Ward, D.S., 1982. Numerical simulation of flow and contaminant migration at an extensively monitored landfill. Water Resources Research, v. 18, no. 6, pp. 1687-1704.

Tellman B., Yarde, R., and Wallace, M.G., 1997. Arizona’s changing rivers: How people have affected the rivers. Issue Paper 19, Water Resources Research Center, University of Arizona, Tucson, Arizona, 198 p.

United States Geological Survey (USGS), 2002. United States daily streamflow data (http://nwis.waterdata.usgs.gov/usa/nwis/discharge).

United States Geological Survey (USGS), 2004a. Unpublished 15-minute streamflow data. Steve Monroe, Water Resources Division, Flagstaff, AZ.

United States Geological Survey (USGS), 2004b. Unpublished bedrock source discharge data collected by Steve Monroe between 2000 and 2001. Water Resources Division, Flagstaff, AZ.

Western Regional Climate Center (WRCC), 2001. United States average monthly pan evaporation data (www.wrcc.dri.edu/htmlfiles/westevap.final.html).

Wilson, E., 2000. Geologic framework and numerical groundwater models of the South Rim of the Grand Canyon, Arizona. Unpublished M.S. Thesis, Northern Arizona University, Flagstaff, AZ, 72 p.

Woessner, W.W., Ball, P.N., DeBorde D.C., and Troy, T.L., 2001. Viral transport in a sand and gravel aquifer under field pumping conditions. Ground Water, v. 39, no. 6, pp. 886-894.

Zhang, Y., Wallace, J.M., and Battisti, D.S., 1997. ENSO-like interdecadal variability 1903-93. Journal of Climate, v. 10, pp. 1004-1020.

APPENDIX A

Parameters used for the stream boundary conditions in the steady-state and transient models of Cottonwood Springs riparian aquifer.

Table 11: Parameters used for the stream boundary conditions in the Cottonwood Springs models for reaches 1-34.

Reach	Bottom Elevation (m asl)	Top Elevation (m asl)	Width (m)	Slope (m/m)	Rougness Coefficient	Streambed Conductance
1	1242.44	1242.49	1.14	0.13	0.045	106.00
2	1242.10	1242.15	1.14	0.29	0.045	106.00
3	1241.56	1241.61	1.14	0.29	0.045	106.00
4	1241.20	1241.25	1.14	0.29	0.045	106.00
5	1241.13	1241.18	1.14	0.29	0.045	106.00
6	1241.05	1241.10	1.14	0.29	0.045	106.00
7	1240.69	1240.74	1.14	0.19	0.045	106.00
8	1240.49	1240.54	1.14	0.19	0.045	106.00
9	1240.29	1240.34	1.14	0.19	0.045	106.00
10	1240.28	1240.33	1.14	0.03	0.045	106.00
11	1240.27	1240.32	1.14	0.03	0.045	106.00
12	1240.26	1240.31	1.14	0.03	0.045	106.00
13	1240.25	1240.30	1.14	0.03	0.045	106.00
14	1240.23	1240.28	1.14	0.03	0.045	106.00
15	1240.11	1240.16	1.14	0.03	0.045	106.00
16	1239.97	1240.02	1.14	0.13	0.045	106.00
17	1239.84	1239.89	1.14	0.13	0.045	106.00
18	1239.70	1239.75	1.14	0.13	0.045	106.00
19	1239.63	1239.68	1.14	0.13	0.045	106.00
20	1239.56	1239.61	1.14	0.13	0.045	106.00
21	1239.45	1239.50	1.14	0.14	0.045	106.00
22	1239.33	1239.38	1.14	0.14	0.045	106.00
23	1239.22	1239.27	1.14	0.14	0.045	106.00
24	1239.09	1239.14	1.14	0.14	0.045	106.00
25	1238.95	1239.00	1.14	0.14	0.045	106.00
26	1238.82	1238.87	1.14	0.14	0.045	106.00
27	1238.66	1238.71	1.14	0.10	0.045	106.00
28	1238.51	1238.56	1.14	0.10	0.045	106.00
29	1238.39	1238.44	1.14	0.10	0.045	106.00
30	1238.31	1238.36	1.14	0.10	0.045	106.00
31	1238.31	1238.36	1.14	0.10	0.045	106.00
32	1237.98	1238.03	1.14	0.21	0.045	106.00
33	1237.80	1237.85	1.14	0.21	0.045	106.00
34	1237.57	1237.62	1.14	0.21	0.045	106.00

Table 12: Parameters used for the stream boundary conditions in the Cottonwood Springs models for reaches 35-68.

Reach	Bottom Elevation (m asl)	Top Elevation (m asl)	Width (m)	Slope (m/m)	Rougness Coefficient	Streambed Conductance
35	1237.34	1237.39	1.14	0.21	0.045	106.00
36	1237.31	1237.36	1.14	0.21	0.045	106.00
37	1237.28	1237.33	1.14	0.07	0.045	106.00
38	1237.21	1237.26	1.14	0.07	0.045	106.00
39	1237.14	1237.19	1.14	0.07	0.045	106.00
40	1237.06	1237.11	1.14	0.07	0.045	106.00
41	1237.06	1237.11	1.14	0.07	0.045	106.00
42	1237.05	1237.10	1.14	0.07	0.045	106.00
43	1236.98	1237.03	1.14	0.14	0.045	106.00
44	1236.91	1236.96	1.14	0.14	0.045	106.00
45	1236.71	1236.76	1.14	0.14	0.045	106.00
46	1236.59	1236.64	1.14	0.06	0.045	106.00
47	1236.52	1236.57	1.14	0.06	0.045	106.00
48	1236.45	1236.50	1.14	0.06	0.045	106.00
49	1236.38	1236.43	1.14	0.06	0.045	106.00
50	1236.31	1236.36	1.14	0.06	0.045	106.00
51	1236.10	1236.15	1.14	0.11	0.045	106.00
52	1235.77	1235.82	1.14	0.11	0.045	106.00
53	1235.76	1235.81	1.14	0.11	0.045	106.00
54	1235.70	1235.75	1.14	0.11	0.045	106.00
55	1235.62	1235.67	1.14	0.11	0.045	106.00
56	1235.57	1235.62	1.14	0.02	0.045	106.00
57	1235.52	1235.57	1.14	0.02	0.045	106.00
58	1235.47	1235.52	1.14	0.02	0.045	106.00
59	1235.42	1235.47	1.14	0.02	0.045	106.00
60	1235.46	1235.51	1.14	0.02	0.045	106.00
61	1235.35	1235.40	1.14	0.10	0.045	106.00
62	1235.19	1235.24	1.14	0.10	0.045	106.00
63	1235.10	1235.15	1.14	0.10	0.045	106.00
64	1235.00	1235.05	1.14	0.10	0.045	106.00
65	1234.91	1234.96	1.14	0.10	0.045	106.00
66	1234.62	1234.67	1.14	0.11	0.045	106.00
67	1234.62	1234.67	1.14	0.11	0.045	106.00
68	1234.63	1234.68	1.14	0.11	0.045	106.00

Table 13: Parameters used for the stream boundary conditions in the Cottonwood Springs models for reaches 69-102.

Reach	Bottom Elevation (m asl)	Top Elevation (m asl)	Width (m)	Slope (m/m)	Rougness Coefficient	Streambed Conductance
69	1234.44	1234.49	1.14	0.11	0.045	106.00
70	1234.39	1234.44	1.14	0.11	0.045	106.00
71	1234.33	1234.38	1.14	0.11	0.045	106.00
72	1234.19	1234.24	1.14	0.11	0.045	106.00
73	1234.05	1234.10	1.14	0.11	0.045	106.00
74	1233.97	1234.02	1.14	0.11	0.045	106.00
75	1233.90	1233.95	1.14	0.11	0.045	106.00
76	1233.43	1233.48	1.14	0.07	0.045	106.00
77	1233.73	1233.78	1.14	0.07	0.045	106.00
78	1233.67	1233.72	1.14	0.07	0.045	106.00
79	1233.60	1233.65	1.14	0.07	0.045	106.00
80	1233.55	1233.60	1.14	0.07	0.045	106.00
81	1233.43	1233.48	1.14	0.13	0.045	106.00
82	1233.25	1233.30	1.14	0.13	0.045	106.00
83	1233.19	1233.24	1.14	0.13	0.045	106.00
84	1233.13	1233.18	1.14	0.13	0.045	106.00
85	1233.07	1233.12	1.14	0.10	0.045	106.00
86	1233.03	1233.08	1.14	0.10	0.045	106.00
87	1232.99	1233.04	1.14	0.10	0.045	106.00
88	1232.91	1232.96	1.14	0.10	0.045	106.00
89	1232.69	1232.74	1.14	0.10	0.045	106.00
90	1232.29	1232.34	1.14	0.23	0.045	106.00
91	1231.83	1231.88	1.14	0.23	0.045	106.00
92	1231.73	1231.78	1.14	0.23	0.045	106.00
93	1231.62	1231.67	1.14	0.23	0.045	106.00
94	1231.52	1231.57	1.14	0.07	0.045	106.00
95	1231.46	1231.51	1.14	0.07	0.045	106.00
96	1231.39	1231.44	1.14	0.07	0.045	106.00
97	1231.31	1231.36	1.14	0.07	0.045	106.00
98	1231.23	1231.28	1.14	0.07	0.045	106.00
99	1231.20	1231.25	1.14	0.07	0.045	106.00
100	1231.09	1231.14	1.14	0.07	0.045	106.00
101	1231.03	1231.08	1.14	0.11	0.045	106.00
102	1230.97	1231.02	1.14	0.11	0.045	106.00

Table 14: Parameters used for the stream boundary conditions in the Cottonwood Springs models for reaches 103-136.

Reach	Bottom Elevation (m asl)	Top Elevation (m asl)	Width (m)	Slope (m/m)	Rougness Coefficient	Streambed Conductance
103	1230.85	1230.90	1.14	0.11	0.045	106.00
104	1230.78	1230.83	1.14	0.07	0.045	106.00
105	1230.73	1230.78	1.14	0.07	0.045	106.00
106	1230.67	1230.72	1.14	0.07	0.045	106.00
107	1230.62	1230.67	1.14	0.12	0.045	106.00
108	1230.57	1230.62	1.14	0.12	0.045	106.00
109	1230.51	1230.56	1.14	0.12	0.045	106.00
110	1230.38	1230.43	1.14	0.12	0.045	106.00
111	1230.24	1230.29	1.14	0.12	0.045	106.00
112	1230.12	1230.17	1.14	0.06	0.045	106.00
113	1230.07	1230.12	1.14	0.06	0.045	106.00
114	1230.01	1230.06	1.14	0.06	0.045	106.00
115	1229.96	1230.01	1.14	0.06	0.045	106.00
116	1229.90	1229.95	1.14	0.06	0.045	106.00
117	1229.85	1229.90	1.14	0.06	0.045	106.00
118	1229.61	1229.66	1.09	0.05	0.045	106.00
119	1229.54	1229.59	1.09	0.05	0.045	106.00
120	1229.47	1229.52	1.09	0.05	0.045	106.00
121	1229.40	1229.45	1.09	0.05	0.045	106.00
122	1229.38	1229.43	1.09	0.05	0.045	106.00
123	1229.26	1229.31	1.09	0.11	0.045	106.00
124	1229.15	1229.20	1.09	0.11	0.045	106.00
125	1229.03	1229.08	1.09	0.11	0.045	106.00
126	1228.96	1229.01	1.09	0.11	0.045	106.00
127	1228.88	1228.93	1.09	0.15	0.045	106.00
128	1228.70	1228.75	1.04	0.15	0.045	106.00
129	1228.59	1228.64	1.04	0.15	0.045	106.00
130	1228.48	1228.53	1.04	0.15	0.045	106.00
131	1228.43	1228.48	1.04	0.12	0.045	106.00
132	1228.31	1228.36	1.04	0.12	0.045	106.00
133	1228.24	1228.29	1.04	0.12	0.045	106.00
134	1228.17	1228.22	1.04	0.12	0.045	106.00
135	1228.03	1228.08	1.04	0.12	0.045	106.00
136	1227.87	1227.92	1.00	0.03	0.045	106.00

Table 15: Parameters used for the stream boundary conditions in the Cottonwood Springs models for reaches 137-170.

Reach	Bottom Elevation (m asl)	Top Elevation (m asl)	Width (m)	Slope (m/m)	Rougness Coefficient	Streambed Conductance
137	1227.79	1227.84	1.00	0.03	0.045	106.00
138	1227.67	1227.72	1.00	0.03	0.045	106.00
139	1227.42	1227.47	1.00	0.03	0.045	106.00
140	1227.51	1227.56	1.00	0.03	0.045	106.00
141	1227.59	1227.64	1.00	0.03	0.045	106.00
142	1227.68	1227.73	1.00	0.03	0.045	106.00
143	1227.55	1227.60	1.00	0.13	0.045	106.00
144	1227.45	1227.50	1.00	0.13	0.045	106.00
145	1227.35	1227.40	1.00	0.13	0.045	106.00
146	1227.26	1227.31	1.00	0.13	0.045	106.00
147	1227.16	1227.21	1.00	0.13	0.045	106.00
148	1227.06	1227.11	1.00	0.05	0.045	106.00
149	1227.03	1227.08	0.95	0.05	0.045	106.00
150	1227.00	1227.05	0.95	0.05	0.045	106.00
151	1226.94	1226.99	0.95	0.08	0.045	106.00
152	1226.90	1226.95	0.95	0.08	0.045	106.00
153	1226.83	1226.88	0.95	0.08	0.045	106.00
154	1226.71	1226.76	0.95	0.08	0.045	106.00
155	1226.58	1226.63	0.95	0.08	0.045	106.00
156	1226.53	1226.58	0.95	0.10	0.045	106.00
157	1226.34	1226.39	0.95	0.10	0.045	106.00
158	1226.29	1226.34	0.95	0.10	0.045	106.00
159	1226.22	1226.27	0.90	0.10	0.045	106.00
160	1226.08	1226.13	0.90	0.10	0.045	106.00
161	1225.96	1226.01	0.90	0.08	0.045	106.00
162	1225.85	1225.90	0.90	0.08	0.045	106.00
163	1225.75	1225.80	0.90	0.08	0.045	106.00
164	1225.69	1225.74	0.90	0.08	0.045	106.00
165	1225.63	1225.68	0.90	0.08	0.045	106.00
166	1225.54	1225.59	0.90	0.13	0.045	106.00
167	1225.44	1225.49	0.90	0.13	0.045	106.00
168	1225.40	1225.45	0.90	0.13	0.045	106.00
169	1225.36	1225.41	0.90	0.13	0.045	106.00
170	1225.17	1225.22	0.90	0.13	0.045	106.00

Table 16: Parameters used for the stream boundary conditions in the Cottonwood Springs models for reaches 171-204.

Reach	Bottom Elevation (m asl)	Top Elevation (m asl)	Width (m)	Slope (m/m)	Rougness Coefficient	Streambed Conductance
171	1225.00	1225.05	0.85	0.13	0.045	106.00
172	1224.85	1224.90	0.85	0.13	0.045	106.00
173	1224.73	1224.78	0.85	0.13	0.045	106.00
174	1224.62	1224.67	0.85	0.14	0.045	106.00
175	1224.50	1224.55	0.85	0.14	0.045	106.00
176	1224.39	1224.44	0.85	0.14	0.045	106.00
177	1224.27	1224.32	0.85	0.14	0.045	106.00
178	1224.14	1224.19	0.80	0.14	0.045	106.00
179	1223.85	1223.90	0.80	0.14	0.045	106.00
180	1223.57	1223.62	0.80	0.09	0.045	106.00
181	1223.48	1223.53	0.80	0.09	0.045	106.00
182	1223.39	1223.44	0.80	0.09	0.045	106.00
183	1223.30	1223.35	0.80	0.09	0.045	106.00
184	1223.22	1223.27	0.80	0.09	0.045	106.00
185	1223.13	1223.18	0.76	0.09	0.045	106.00
186	1223.04	1223.09	0.76	0.09	0.045	106.00
187	1222.94	1222.99	0.76	0.11	0.045	106.00
188	1222.83	1222.88	0.76	0.11	0.045	106.00
189	1222.73	1222.78	0.76	0.06	0.045	106.00
190	1222.69	1222.74	0.76	0.06	0.045	106.00
191	1222.64	1222.69	0.76	0.06	0.045	106.00
192	1222.58	1222.63	0.76	0.06	0.045	106.00
193	1222.52	1222.57	0.76	0.06	0.045	106.00
194	1222.38	1222.43	0.76	0.15	0.045	106.00
195	1222.29	1222.34	0.76	0.15	0.045	106.00
196	1222.20	1222.25	0.76	0.15	0.045	106.00
197	1222.00	1222.05	0.76	0.15	0.045	106.00
198	1221.90	1221.95	0.76	0.15	0.045	106.00
199	1221.79	1221.84	0.76	0.15	0.045	106.00
200	1221.72	1221.77	0.76	0.12	0.045	106.00
201	1221.65	1221.70	0.76	0.12	0.045	106.00
202	1221.58	1221.63	0.76	0.12	0.045	106.00
203	1221.46	1221.51	0.76	0.12	0.045	106.00
204	1221.35	1221.40	0.76	0.12	0.045	106.00

Table 17: Parameters used for the stream boundary conditions in the Cottonwood Springs models for reaches 205-238.

Reach	Bottom Elevation (m asl)	Top Elevation (m asl)	Width (m)	Slope (m/m)	Rougness Coefficient	Streambed Conductance
205	1221.23	1221.28	0.76	0.08	0.045	106.00
206	1221.16	1221.21	0.76	0.08	0.045	106.00
207	1221.09	1221.14	0.76	0.08	0.045	106.00
208	1220.85	1220.90	0.76	0.05	0.045	106.00
209	1220.74	1220.79	0.76	0.05	0.045	106.00
210	1220.71	1220.76	0.76	0.05	0.045	106.00
211	1220.67	1220.72	0.76	0.05	0.045	106.00
212	1220.61	1220.66	0.76	0.09	0.045	106.00
213	1220.56	1220.61	0.76	0.09	0.045	106.00
214	1220.51	1220.56	0.76	0.09	0.045	106.00
215	1220.45	1220.50	0.76	0.09	0.045	106.00
216	1220.39	1220.44	0.76	0.09	0.045	106.00
217	1220.33	1220.38	0.76	0.09	0.045	106.00
218	1220.28	1220.33	0.76	0.09	0.045	106.00
219	1220.21	1220.26	0.76	0.09	0.045	106.00
220	1220.13	1220.18	0.76	0.09	0.045	106.00
221	1220.03	1220.08	0.76	0.09	0.045	106.00
222	1219.92	1219.97	0.76	0.09	0.045	106.00
223	1219.82	1219.87	0.76	0.09	0.045	106.00
224	1219.66	1219.71	0.76	0.17	0.045	106.00
225	1219.51	1219.56	0.76	0.17	0.045	106.00
226	1219.35	1219.40	0.76	0.17	0.045	106.00
227	1219.19	1219.24	0.76	0.17	0.045	106.00
228	1218.83	1218.88	0.76	0.17	0.045	106.00
229	1218.70	1218.75	0.76	0.17	0.045	106.00
230	1218.28	1218.33	0.76	0.08	0.045	106.00
231	1218.21	1218.26	0.76	0.08	0.045	106.00
232	1218.13	1218.18	0.76	0.08	0.045	106.00
233	1218.07	1218.12	0.76	0.08	0.045	106.00
234	1218.00	1218.05	0.76	0.08	0.045	106.00
235	1217.97	1218.02	0.76	0.08	0.045	106.00
236	1217.94	1217.99	0.76	0.09	0.045	106.00
237	1217.82	1217.87	0.76	0.09	0.045	106.00
238	1217.76	1217.81	0.76	0.09	0.045	106.00

Table 18: Parameters used for the stream boundary conditions in the Cottonwood Springs models for reaches 239-272.

Reach	Bottom Elevation (m asl)	Top Elevation (m asl)	Width (m)	Slope (m/m)	Rougness Coefficient	Streambed Conductance
239	1217.70	1217.75	0.76	0.09	0.045	106.00
240	1217.54	1217.59	0.76	0.05	0.045	106.00
241	1217.48	1217.53	0.76	0.05	0.045	106.00
242	1217.41	1217.46	0.76	0.05	0.045	106.00
243	1217.35	1217.40	0.76	0.05	0.045	106.00
244	1217.32	1217.37	0.76	0.07	0.045	106.00
245	1217.29	1217.34	0.76	0.07	0.045	106.00
246	1217.15	1217.20	0.76	0.07	0.045	106.00
247	1217.10	1217.15	0.76	0.07	0.045	106.00
248	1217.05	1217.10	0.76	0.07	0.045	106.00
249	1217.00	1217.05	0.76	0.07	0.045	106.00
250	1217.05	1217.10	0.76	0.02	0.045	106.00
251	1216.95	1217.00	0.76	0.02	0.045	106.00
252	1216.96	1217.01	0.76	0.02	0.045	106.00
253	1216.93	1216.98	0.76	0.02	0.045	106.00
254	1216.90	1216.95	0.76	0.02	0.045	106.00
255	1216.87	1216.92	0.76	0.02	0.045	106.00
256	1216.84	1216.89	0.76	0.03	0.045	106.00
257	1216.80	1216.85	0.76	0.03	0.045	106.00
258	1216.77	1216.82	0.76	0.03	0.045	106.00
259	1216.71	1216.76	0.76	0.05	0.045	106.00
260	1216.65	1216.70	0.76	0.05	0.045	106.00
261	1216.58	1216.63	0.76	0.05	0.045	106.00
262	1216.52	1216.57	0.76	0.05	0.045	106.00
263	1216.49	1216.54	0.76	0.05	0.045	106.00
264	1216.46	1216.51	0.76	0.05	0.045	106.00
265	1216.43	1216.48	0.76	0.06	0.045	106.00
266	1216.40	1216.45	0.76	0.06	0.045	106.00
267	1216.39	1216.44	0.76	0.06	0.045	106.00
268	1216.39	1216.44	0.76	0.06	0.045	106.00
269	1216.38	1216.43	0.76	0.06	0.045	106.00
270	1216.23	1216.28	0.76	0.06	0.045	106.00
271	1215.89	1215.94	0.76	0.06	0.045	106.00
272	1215.55	1215.60	0.76	0.13	0.045	106.00

Table 19: Parameters used for the stream boundary conditions in the Cottonwood Springs models for reaches 273-306.

Reach	Bottom Elevation (m asl)	Top Elevation (m asl)	Width (m)	Slope (m/m)	Rougness Coefficient	Streambed Conductance
273	1215.47	1215.52	0.76	0.13	0.045	106.00
274	1215.39	1215.44	0.76	0.13	0.045	106.00
275	1215.25	1215.30	0.76	0.13	0.045	106.00
276	1215.12	1215.17	0.76	0.13	0.045	106.00
277	1214.98	1215.03	0.76	0.16	0.045	106.00
278	1214.78	1214.83	0.76	0.16	0.045	106.00
279	1214.63	1214.68	0.76	0.16	0.045	106.00
280	1214.47	1214.52	0.76	0.16	0.045	106.00
281	1214.36	1214.41	0.70	0.21	0.045	106.00
282	1214.19	1214.24	0.70	0.21	0.045	106.00
283	1214.03	1214.08	0.70	0.21	0.045	106.00
284	1213.87	1213.92	0.70	0.21	0.045	106.00
285	1213.66	1213.71	0.70	0.21	0.045	106.00
286	1213.44	1213.49	0.70	0.13	0.045	106.00
287	1213.19	1213.24	0.70	0.13	0.045	106.00
288	1213.04	1213.09	0.70	0.13	0.045	106.00
289	1212.91	1212.96	0.65	0.13	0.045	106.00
290	1212.85	1212.90	0.65	0.13	0.045	106.00
291	1212.81	1212.86	0.65	0.09	0.045	106.00
292	1212.76	1212.81	0.65	0.09	0.045	106.00
293	1212.65	1212.70	0.65	0.09	0.045	106.00
294	1212.51	1212.56	0.65	0.09	0.045	106.00
295	1212.45	1212.50	0.60	0.09	0.045	106.00
296	1212.44	1212.49	0.60	0.07	0.045	106.00
297	1212.30	1212.35	0.60	0.07	0.045	106.00
298	1212.17	1212.22	0.60	0.07	0.045	106.00
299	1212.07	1212.12	0.55	0.07	0.045	106.00
300	1212.05	1212.10	0.55	0.07	0.045	106.00
301	1211.89	1211.94	0.55	0.10	0.045	106.00
302	1211.81	1211.86	0.55	0.10	0.045	106.00
303	1211.74	1211.79	0.50	0.10	0.045	106.00
304	1211.67	1211.72	0.50	0.10	0.045	106.00
305	1211.66	1211.71	0.50	0.08	0.045	106.00
306	1211.59	1211.64	0.50	0.08	0.045	106.00

Table 20: Parameters used for the stream boundary conditions in the Cottonwood Springs models for reaches 307-340.

Reach	Bottom Elevation (m asl)	Top Elevation (m asl)	Width (m)	Slope (m/m)	Rougness Coefficient	Streambed Conductance
307	1211.55	1211.60	0.45	0.08	0.045	106.00
308	1211.52	1211.57	0.45	0.08	0.045	106.00
309	1211.40	1211.45	0.45	0.08	0.045	106.00
310	1211.25	1211.30	0.45	0.06	0.045	106.00
311	1211.10	1211.15	0.40	0.06	0.045	106.00
312	1211.04	1211.09	0.40	0.06	0.045	106.00
313	1210.99	1211.04	0.40	0.06	0.045	106.00
314	1210.99	1211.04	0.40	0.06	0.045	106.00
315	1210.99	1211.04	0.35	0.13	0.045	106.00
316	1210.93	1210.98	0.35	0.13	0.040	106.00
317	1210.73	1210.78	0.35	0.13	0.040	106.00
318	1210.69	1210.74	0.35	0.11	0.040	106.00
319	1210.45	1210.50	0.30	0.11	0.040	106.00
320	1210.21	1210.26	0.30	0.11	0.040	106.00
321	1210.16	1210.21	0.30	0.11	0.040	106.00
322	1210.14	1210.19	0.30	0.11	0.040	106.00
323	1210.10	1210.15	0.30	0.11	0.040	106.00
324	1210.02	1210.07	0.30	0.07	0.040	106.00
325	1209.94	1209.99	0.30	0.07	0.040	106.00
326	1209.86	1209.91	0.30	0.07	0.040	106.00
327	1209.82	1209.87	0.30	0.07	0.040	106.00
328	1209.77	1209.82	0.30	0.07	0.040	106.00
329	1209.71	1209.76	0.30	0.13	0.040	106.00
330	1209.60	1209.65	0.30	0.13	0.040	106.00
331	1209.46	1209.51	0.30	0.13	0.040	106.00
332	1209.29	1209.34	0.30	0.13	0.040	106.00
333	1209.18	1209.23	0.30	0.13	0.040	106.00
334	1209.11	1209.16	0.30	0.06	0.040	106.00
335	1209.04	1209.09	0.30	0.06	0.040	106.00
336	1208.98	1209.03	0.30	0.06	0.040	106.00
337	1208.91	1208.96	0.30	0.06	0.040	106.00
338	1208.83	1208.88	0.30	0.06	0.040	106.00
339	1208.76	1208.81	0.30	0.06	0.040	106.00
340	1208.72	1208.77	0.30	0.06	0.040	106.00

Table 21: Parameters used for the stream boundary conditions in the Cottonwood Springs models for reaches 341-374.

Reach	Bottom Elevation (m asl)	Top Elevation (m asl)	Width (m)	Slope (m/m)	Rougness Coefficient	Streambed Conductance
341	1208.69	1208.74	0.30	0.06	0.040	106.00
342	1208.67	1208.72	0.30	0.06	0.040	106.00
343	1208.64	1208.69	0.30	0.06	0.040	106.00
344	1208.61	1208.66	0.30	0.06	0.040	106.00
345	1208.46	1208.51	0.30	0.06	0.040	106.00
346	1208.31	1208.36	0.30	0.04	0.040	106.00
347	1208.28	1208.33	0.30	0.04	0.040	106.00
348	1208.26	1208.31	0.30	0.04	0.040	106.00
349	1208.24	1208.29	0.30	0.04	0.040	106.00
350	1208.19	1208.24	0.30	0.04	0.040	106.00
351	1208.14	1208.19	0.30	0.09	0.040	106.00
352	1208.10	1208.15	0.30	0.09	0.040	106.00
353	1208.06	1208.11	0.30	0.09	0.040	106.00
354	1207.83	1207.88	0.30	0.09	0.040	106.00
355	1207.71	1207.76	0.30	0.09	0.040	106.00
356	1207.66	1207.71	0.30	0.09	0.040	106.00
357	1207.53	1207.58	0.30	0.09	0.040	106.00
358	1207.46	1207.51	0.30	0.09	0.040	106.00
359	1207.36	1207.41	0.30	0.09	0.040	106.00
360	1207.30	1207.35	0.30	0.09	0.040	106.00
361	1207.19	1207.24	0.30	0.06	0.040	106.00
362	1207.12	1207.17	0.30	0.06	0.040	106.00
363	1207.06	1207.11	0.30	0.06	0.040	106.00
364	1206.97	1207.02	0.30	0.06	0.040	106.00
365	1206.93	1206.98	0.30	0.06	0.040	106.00
366	1206.88	1206.93	0.30	0.06	0.040	106.00
367	1206.85	1206.90	0.30	0.07	0.040	106.00
368	1206.82	1206.87	0.30	0.07	0.040	106.00
369	1206.75	1206.80	0.30	0.07	0.040	106.00
370	1206.49	1206.54	0.30	0.07	0.040	106.00
371	1206.47	1206.52	0.30	0.06	0.040	106.00
372	1206.45	1206.50	0.30	0.07	0.040	106.00
373	1206.37	1206.42	0.30	0.07	0.040	106.00
374	1206.35	1206.40	0.30	0.07	0.040	106.00

Table 22: Parameters used for the stream boundary conditions in the Cottonwood Springs models for reaches 375-408.

Reach	Bottom Elevation (m asl)	Top Elevation (m asl)	Width (m)	Slope (m/m)	Rougness Coefficient	Streambed Conductance
375	1206.29	1206.34	0.30	0.07	0.040	106.00
376	1206.19	1206.24	0.30	0.07	0.040	106.00
377	1206.14	1206.19	0.30	0.07	0.040	106.00
378	1205.91	1205.96	0.30	0.15	0.040	106.00
379	1205.56	1205.61	0.30	0.15	0.040	106.00
380	1205.49	1205.54	0.30	0.15	0.040	106.00
381	1205.43	1205.48	0.30	0.15	0.040	106.00
382	1205.37	1205.42	0.30	0.15	0.040	106.00
383	1205.11	1205.16	0.30	0.10	0.040	106.00
384	1205.02	1205.07	0.30	0.10	0.040	106.00
385	1204.92	1204.97	0.30	0.10	0.040	106.00
386	1204.86	1204.91	0.30	0.10	0.040	106.00
387	1204.80	1204.85	0.30	0.10	0.040	106.00
388	1204.74	1204.79	0.30	0.10	0.040	106.00
389	1204.67	1204.72	0.30	0.12	0.040	106.00
390	1204.33	1204.38	0.30	0.12	0.040	106.00
391	1204.23	1204.28	0.30	0.12	0.040	106.00
392	1204.23	1204.28	0.30	0.12	0.040	106.00
393	1204.22	1204.27	0.30	0.08	0.040	106.00
394	1204.22	1204.27	0.30	0.08	0.040	106.00
395	1203.87	1203.92	0.30	0.08	0.040	106.00
396	1203.88	1203.93	0.30	0.08	0.040	106.00
397	1203.88	1203.93	0.30	0.08	0.040	106.00
398	1203.49	1203.54	0.30	0.13	0.040	106.00
399	1203.48	1203.53	0.30	0.13	0.040	106.00
400	1203.48	1203.53	0.30	0.13	0.040	106.00
401	1203.41	1203.46	0.30	0.08	0.040	106.00
402	1203.40	1203.45	0.30	0.08	0.040	106.00
403	1203.39	1203.44	0.30	0.08	0.040	106.00
404	1203.31	1203.36	0.30	0.08	0.040	106.00
405	1203.26	1203.31	0.30	0.08	0.040	106.00
406	1203.08	1203.13	0.30	0.16	0.040	106.00
407	1202.89	1202.94	0.30	0.16	0.040	106.00
408	1202.72	1202.77	0.30	0.16	0.040	106.00

Table 23: Parameters used for the stream boundary conditions in the Cottonwood Springs models for reaches 409-442.

Reach	Bottom Elevation (m asl)	Top Elevation (m asl)	Width (m)	Slope (m/m)	Rougness Coefficient	Streambed Conductance
409	1202.70	1202.75	0.30	0.16	0.040	106.00
410	1202.48	1202.53	0.30	0.16	0.040	106.00
411	1202.42	1202.47	0.30	0.09	0.040	106.00
412	1202.36	1202.41	0.30	0.09	0.040	106.00
413	1202.30	1202.35	0.30	0.09	0.040	106.00
414	1202.10	1202.15	0.30	0.09	0.040	106.00
415	1201.98	1202.03	0.30	0.09	0.040	106.00
416	1201.89	1201.94	0.30	0.10	0.040	106.00
417	1201.82	1201.87	0.30	0.10	0.040	106.00
418	1201.80	1201.85	0.30	0.10	0.040	106.00
419	1201.75	1201.80	0.30	0.10	0.040	106.00
420	1201.57	1201.62	0.30	0.10	0.040	106.00
421	1201.39	1201.44	0.30	0.12	0.040	106.00
422	1201.32	1201.37	0.30	0.12	0.040	106.00
423	1201.26	1201.31	0.30	0.12	0.040	106.00
424	1201.19	1201.24	0.30	0.12	0.040	106.00
425	1200.95	1201.00	0.30	0.18	0.040	106.00
426	1200.68	1200.73	0.30	0.18	0.040	106.00
427	1200.54	1200.59	0.30	0.18	0.040	106.00
428	1200.39	1200.44	0.30	0.18	0.040	106.00
429	1200.16	1200.21	0.30	0.09	0.040	106.00
430	1200.11	1200.16	0.30	0.09	0.040	106.00
431	1200.06	1200.11	0.30	0.09	0.040	106.00
432	1199.95	1200.00	0.30	0.09	0.040	106.00
433	1199.84	1199.89	0.30	0.09	0.040	106.00
434	1199.69	1199.74	0.30	0.10	0.040	106.00
435	1199.63	1199.68	0.30	0.10	0.040	106.00
436	1199.56	1199.61	0.30	0.10	0.040	106.00
437	1199.49	1199.54	0.30	0.10	0.040	106.00
438	1199.41	1199.46	0.30	0.10	0.040	106.00
439	1199.40	1199.45	0.30	0.04	0.040	106.00
440	1999.38	1999.43	0.30	0.04	0.040	106.00
441	1199.32	1199.37	0.30	0.04	0.040	106.00
442	1199.27	1199.32	0.30	0.04	0.040	106.00

Table 24: Parameters used for the stream boundary conditions in the Cottonwood Springs models for reaches 443-476.

Reach	Bottom Elevation (m asl)	Top Elevation (m asl)	Width (m)	Slope (m/m)	Rougness Coefficient	Streambed Conductance
443	1199.21	1199.26	0.30	0.04	0.040	106.00
444	1199.20	1199.25	0.30	0.13	0.040	106.00
445	1199.18	1199.23	0.30	0.13	0.040	106.00
446	1199.14	1199.19	0.30	0.13	0.040	106.00
447	1198.84	1198.89	0.30	0.13	0.040	106.00
448	1198.54	1198.59	0.30	0.13	0.040	106.00
449	1198.54	1198.59	0.30	0.04	0.040	106.00
450	1198.51	1198.56	0.30	0.04	0.040	106.00
451	1198.35	1198.40	0.30	0.16	0.040	106.00
452	1198.18	1198.23	0.30	0.16	0.040	106.00
453	1198.02	1198.07	0.30	0.16	0.040	106.00
454	1197.71	1197.76	0.30	0.16	0.040	106.00
455	1197.65	1197.70	0.30	0.16	0.040	106.00
456	1197.57	1197.62	0.30	0.08	0.040	106.00
457	1197.50	1197.55	0.30	0.08	0.040	106.00
458	1197.43	1197.48	0.30	0.08	0.040	106.00
459	1197.35	1197.40	0.30	0.08	0.040	106.00
460	1197.30	1197.35	0.30	0.08	0.040	106.00
461	1197.26	1197.31	0.30	0.08	0.040	106.00
462	1197.21	1197.26	0.30	0.05	0.040	106.00
463	1197.20	1197.25	0.30	0.05	0.040	106.00
464	1197.18	1197.23	0.30	0.05	0.040	106.00
465	1197.17	1197.22	0.30	0.05	0.040	106.00
466	1197.11	1197.16	0.30	0.05	0.040	106.00
467	1197.04	1197.09	0.30	0.04	0.040	106.00
468	1197.05	1197.10	0.30	0.04	0.040	106.00
469	1196.98	1197.03	0.30	0.04	0.040	106.00
470	1196.90	1196.95	0.30	0.04	0.040	106.00
471	1196.90	1196.95	0.35	0.04	0.040	106.00
472	1196.79	1196.84	0.35	0.04	0.040	106.00
473	1196.76	1196.81	0.35	0.05	0.040	106.00
474	1196.73	1196.78	0.35	0.05	0.040	106.00
475	1196.71	1196.76	0.35	0.05	0.040	106.00
476	1196.68	1196.73	0.35	0.05	0.040	106.00

Table 25: Parameters used for the stream boundary conditions in the Cottonwood Springs models for reaches 477-510.

Reach	Bottom Elevation (m asl)	Top Elevation (m asl)	Width (m)	Slope (m/m)	Rougness Coefficient	Streambed Conductance
477	1196.57	1196.62	0.35	0.05	0.040	106.00
478	1196.54	1196.59	0.35	0.06	0.040	106.00
479	1196.51	1196.56	0.35	0.06	0.040	106.00
480	1196.42	1196.47	0.35	0.06	0.040	106.00
481	1196.33	1196.38	0.35	0.06	0.040	106.00
482	1196.24	1196.29	0.35	0.06	0.040	106.00
483	1196.24	1196.29	0.35	0.06	0.040	106.00
484	1196.22	1196.27	0.35	0.06	0.040	106.00
485	1196.18	1196.23	0.35	0.06	0.040	106.00
486	1196.12	1196.17	0.35	0.06	0.040	106.00
487	1196.10	1196.15	0.35	0.06	0.040	106.00
488	1196.07	1196.12	0.35	0.06	0.040	106.00
489	1195.95	1196.00	0.35	0.12	0.040	106.00
490	1195.95	1196.00	0.35	0.02	0.040	106.00
491	1195.96	1196.01	0.35	0.02	0.040	106.00
492	1195.73	1195.78	0.35	0.12	0.040	106.00
493	1195.44	1195.49	0.40	0.12	0.040	106.00
494	1195.23	1195.28	0.40	0.13	0.040	106.00
495	1195.14	1195.19	0.40	0.13	0.040	106.00
496	1195.05	1195.10	0.40	0.13	0.040	106.00
497	1194.96	1195.01	0.40	0.13	0.040	106.00
498	1194.78	1194.83	0.40	0.13	0.040	106.00
499	1194.67	1194.72	0.40	0.09	0.040	106.00
500	1194.56	1194.61	0.40	0.09	0.040	106.00
501	1194.51	1194.56	0.40	0.09	0.040	106.00
502	1194.45	1194.50	0.40	0.09	0.040	106.00
503	1194.40	1194.45	0.40	0.09	0.040	106.00
504	1194.40	1194.45	0.40	0.11	0.040	106.00
505	1194.20	1194.25	0.40	0.11	0.040	106.00
506	1194.00	1194.05	0.40	0.11	0.040	106.00
507	1193.95	1194.00	0.40	0.11	0.040	106.00
508	1193.90	1193.95	0.40	0.18	0.040	106.00
509	1193.75	1193.80	0.40	0.18	0.040	106.00
510	1193.59	1193.64	0.40	0.18	0.040	106.00

Table 26: Parameters used for the stream boundary conditions in the Cottonwood Springs models for reaches 511-544.

Reach	Bottom Elevation (m asl)	Top Elevation (m asl)	Width (m)	Slope (m/m)	Rougness Coefficient	Streambed Conductance
511	1193.44	1193.49	0.40	0.18	0.040	106.00
512	1193.38	1193.43	0.40	0.09	0.040	106.00
513	1193.32	1193.37	0.40	0.09	0.040	106.00
514	1193.32	1193.37	0.40	0.09	0.040	106.00
515	1193.07	1193.12	0.45	0.09	0.040	106.00
516	1193.03	1193.08	0.45	0.09	0.040	106.00
517	1192.74	1192.79	0.45	0.09	0.040	106.00
518	1192.45	1192.50	0.45	0.09	0.040	106.00
519	1192.42	1192.47	0.45	0.09	0.040	106.00
520	1192.41	1192.46	0.45	0.09	0.040	106.00
521	1192.41	1192.46	0.45	0.09	0.040	106.00
522	1192.40	1192.45	0.45	0.09	0.040	106.00
523	1192.39	1192.44	0.45	0.19	0.040	106.00
524	1192.00	1192.05	0.45	0.19	0.040	106.00
525	1191.93	1191.98	0.45	0.19	0.040	106.00
526	1191.87	1191.92	0.45	0.19	0.040	106.00
527	1191.78	1191.83	0.45	0.09	0.040	106.00
528	1191.69	1191.74	0.45	0.09	0.040	106.00
529	1191.61	1191.66	0.45	0.09	0.040	106.00
530	1191.55	1191.60	0.45	0.09	0.040	106.00
531	1191.48	1191.53	0.45	0.14	0.040	106.00
532	1191.49	1191.54	0.45	0.14	0.040	106.00
533	1191.50	1191.55	0.45	0.14	0.040	106.00
534	1191.16	1191.21	0.45	0.14	0.040	106.00
535	1190.81	1190.86	0.45	0.14	0.040	106.00
536	1190.71	1190.76	0.45	0.06	0.040	106.00
537	1190.71	1190.76	0.45	0.06	0.040	106.00
538	1190.70	1190.75	0.45	0.06	0.040	106.00
539	1190.65	1190.70	0.45	0.06	0.040	106.00
540	1190.65	1190.70	0.45	0.20	0.040	106.00
541	1190.65	1190.70	0.45	0.20	0.040	106.00
542	1190.56	1190.61	0.45	0.20	0.040	106.00
543	1190.33	1190.38	0.45	0.20	0.040	106.00
544	1189.70	1189.75	0.45	0.20	0.040	106.00

Table 27: Parameters used for the stream boundary conditions in the Cottonwood Springs models for reaches 545-578.

Reach	Bottom Elevation (m asl)	Top Elevation (m asl)	Width (m)	Slope (m/m)	Rougness Coefficient	Streambed Conductance
545	1189.66	1189.71	0.45	0.02	0.040	106.00
546	1189.67	1189.72	0.45	0.02	0.040	106.00
547	1189.65	1189.70	0.45	0.02	0.040	106.00
548	1189.65	1189.70	0.45	0.02	0.040	106.00
549	1189.65	1189.70	0.45	0.02	0.040	106.00
550	1189.61	1189.66	0.45	0.02	0.040	106.00
551	1189.59	1189.64	0.45	0.04	0.040	106.00
552	1189.56	1189.61	0.45	0.04	0.040	106.00
553	1189.53	1189.58	0.45	0.04	0.040	106.00
554	1189.48	1189.53	0.45	0.04	0.040	106.00
555	1189.45	1189.50	0.45	0.04	0.040	106.00
556	1189.45	1189.50	0.45	0.06	0.040	106.00
557	1189.32	1189.37	0.45	0.06	0.040	106.00
558	1189.29	1189.34	0.45	0.06	0.040	106.00
559	1189.26	1189.31	0.45	0.06	0.040	106.00
560	1189.23	1189.28	0.45	0.06	0.040	106.00
561	1189.16	1189.21	0.45	0.06	0.040	106.00
562	1189.07	1189.12	0.45	0.16	0.040	106.00
563	1188.79	1188.84	0.45	0.16	0.040	106.00
564	1188.69	1188.74	0.45	0.16	0.040	106.00
565	1188.44	1188.49	0.45	0.16	0.040	106.00
566	1188.19	1188.24	0.45	0.16	0.040	106.00
567	1187.97	1188.02	0.40	0.35	0.040	106.00
568	1187.80	1187.85	0.40	0.35	0.040	106.00
569	1187.81	1187.86	0.40	0.35	0.040	106.00
570	1187.82	1187.87	0.40	0.35	0.040	106.00
571	1186.84	1186.89	0.40	0.35	0.040	106.00
572	1186.79	1186.84	0.40	0.08	0.040	106.00
573	1186.74	1186.79	0.40	0.08	0.040	106.00
574	1186.69	1186.74	0.40	0.08	0.040	106.00
575	1186.65	1186.70	0.40	0.08	0.040	106.00
576	1186.60	1186.65	0.40	0.08	0.040	106.00
577	1186.53	1186.58	0.40	0.06	0.040	106.00
578	1186.47	1186.52	0.40	0.06	0.040	106.00

Table 28: Parameters used for the stream boundary conditions in the Cottonwood Springs models for reaches 579-612.

Reach	Bottom Elevation (m asl)	Top Elevation (m asl)	Width (m)	Slope (m/m)	Rougness Coefficient	Streambed Conductance
579	1186.44	1186.49	0.40	0.06	0.040	106.00
580	1186.40	1186.45	0.40	0.06	0.040	106.00
581	1186.34	1186.39	0.40	0.06	0.040	106.00
582	1186.33	1186.38	0.40	0.02	0.040	106.00
583	1186.32	1186.37	0.40	0.02	0.040	106.00
584	1186.32	1186.37	0.40	0.02	0.040	106.00
585	1186.30	1186.35	0.40	0.02	0.040	106.00
586	1186.28	1186.33	0.40	0.02	0.040	106.00
587	1186.19	1186.24	0.40	0.14	0.040	106.00
588	1186.13	1186.18	0.40	0.14	0.040	106.00
589	1185.91	1185.96	0.40	0.14	0.040	106.00
590	1185.88	1185.93	0.40	0.14	0.040	106.00
591	1185.53	1185.58	0.40	0.14	0.040	106.00
592	1185.56	1185.61	0.40	0.04	0.040	106.00
593	1185.49	1185.54	0.40	0.04	0.040	106.00
594	1185.43	1185.48	0.40	0.04	0.040	106.00
595	1185.36	1185.41	0.40	0.04	0.040	106.00
596	1185.19	1185.24	0.40	0.17	0.040	106.00
597	1185.03	1185.08	0.40	0.17	0.040	106.00
598	1184.86	1184.91	0.40	0.17	0.040	106.00
599	1184.69	1184.74	0.40	0.17	0.040	106.00
600	1184.70	1184.75	0.40	0.01	0.040	106.00
601	1184.70	1184.75	0.40	0.01	0.040	106.00
602	1184.68	1184.73	0.40	0.01	0.040	106.00
603	1184.64	1184.69	0.40	0.01	0.040	106.00
604	1184.63	1184.68	0.40	0.01	0.040	106.00
605	1184.62	1184.67	0.40	0.02	0.040	106.00
606	1184.61	1184.66	0.40	0.02	0.040	106.00
607	1184.57	1184.62	0.40	0.02	0.040	106.00
608	1184.53	1184.58	0.40	0.02	0.040	106.00
609	1184.52	1184.57	0.40	0.02	0.040	106.00
610	1184.47	1184.52	0.40	0.04	0.040	106.00
611	1184.43	1184.48	0.40	0.04	0.040	106.00
612	1184.38	1184.43	0.40	0.04	0.040	106.00

Table 29: Parameters used for the stream boundary conditions in the Cottonwood Springs models for reaches 613-646.

Reach	Bottom Elevation (m asl)	Top Elevation (m asl)	Width (m)	Slope (m/m)	Rougness Coefficient	Streambed Conductance
613	1184.33	1184.38	0.40	0.04	0.040	106.00
614	1184.30	1184.35	0.40	0.04	0.040	106.00
615	1184.07	1184.12	0.40	0.12	0.040	106.00
616	1183.84	1183.89	0.40	0.12	0.040	106.00
617	1183.84	1183.89	0.40	0.12	0.040	106.00
618	1183.84	1183.89	0.40	0.12	0.040	106.00
619	1183.81	1183.86	0.40	0.12	0.040	106.00
620	1183.78	1183.83	0.40	0.12	0.040	106.00
621	1183.75	1183.80	0.40	0.07	0.040	106.00
622	1183.69	1183.74	0.40	0.07	0.040	106.00
623	1183.57	1183.62	0.40	0.07	0.040	106.00
624	1183.46	1183.51	0.40	0.07	0.040	106.00
625	1183.35	1183.40	0.40	0.07	0.040	106.00
626	1183.30	1183.35	0.40	0.02	0.040	106.00
627	1183.24	1183.29	0.40	0.02	0.040	106.00
628	1183.18	1183.23	0.40	0.02	0.040	106.00
629	1183.18	1183.23	0.40	0.02	0.040	106.00
630	1183.20	1183.25	0.40	0.02	0.040	106.00
631	1183.15	1183.20	0.40	0.02	0.040	106.00
632	1183.10	1183.15	0.40	0.02	0.040	106.00
633	1183.08	1183.13	0.40	0.02	0.040	106.00
634	1182.74	1182.79	0.40	0.20	0.040	106.00
635	1182.61	1182.66	0.40	0.20	0.040	106.00
636	1182.59	1182.64	0.40	0.20	0.040	106.00
637	1182.57	1182.62	0.40	0.20	0.040	106.00
638	1182.48	1182.53	0.40	0.06	0.040	106.00
639	1182.48	1182.53	0.40	0.06	0.040	106.00
640	1182.39	1182.44	0.40	0.06	0.040	106.00
641	1182.31	1182.36	0.40	0.06	0.040	106.00
642	1182.30	1182.35	0.40	0.06	0.040	106.00
643	1182.24	1182.29	0.40	0.06	0.040	106.00
644	1182.17	1182.22	0.40	0.06	0.040	106.00
645	1182.02	1182.07	0.40	0.16	0.035	106.00
646	1181.90	1181.95	0.40	0.16	0.035	106.00

Table 30: Parameters used for the stream boundary conditions in the Cottonwood Springs models for reaches 647-680.

Reach	Bottom Elevation (m asl)	Top Elevation (m asl)	Width (m)	Slope (m/m)	Rougness Coefficient	Streambed Conductance
647	1181.71	1181.76	0.40	0.16	0.035	106.00
648	1181.52	1181.57	0.40	0.16	0.035	106.00
649	1181.49	1181.54	0.40	0.16	0.035	106.00
650	1181.45	1181.50	0.40	0.16	0.035	106.00
651	1181.34	1181.39	0.40	0.05	0.035	106.00
652	1181.31	1181.36	0.40	0.05	0.035	106.00
653	1181.30	1181.35	0.40	0.05	0.035	106.00
654	1181.29	1181.34	0.40	0.05	0.035	106.00
655	1181.23	1181.28	0.40	0.06	0.035	106.00
656	1181.17	1181.22	0.40	0.06	0.035	106.00
657	1181.11	1181.16	0.40	0.06	0.035	106.00
658	1180.99	1181.04	0.40	0.06	0.035	106.00
659	1181.00	1181.05	0.40	0.06	0.035	106.00
660	1180.98	1181.03	0.40	0.04	0.035	106.00
661	1180.96	1181.01	0.40	0.04	0.035	106.00
662	1180.93	1180.98	0.40	0.04	0.035	106.00
663	1180.90	1180.95	0.40	0.04	0.035	106.00
664	1180.83	1180.88	0.40	0.17	0.035	106.00
665	1180.75	1180.80	0.40	0.17	0.035	106.00
666	1180.57	1180.62	0.40	0.17	0.035	106.00
667	1180.40	1180.45	0.40	0.17	0.035	106.00
668	1179.90	1179.95	0.40	0.17	0.035	106.00
669	1179.83	1179.88	0.40	0.06	0.035	106.00
670	1179.76	1179.81	0.40	0.06	0.035	106.00
671	1179.69	1179.74	0.40	0.06	0.035	106.00
672	1179.65	1179.70	0.40	0.06	0.035	106.00
673	1179.61	1179.66	0.40	0.06	0.035	106.00
674	1179.59	1179.64	0.40	0.06	0.035	106.00
675	1179.57	1179.62	0.40	0.05	0.035	106.00
676	1179.55	1179.60	0.40	0.05	0.035	106.00
677	1179.51	1179.56	0.40	0.05	0.035	106.00
678	1179.47	1179.52	0.40	0.05	0.035	106.00
679	1179.43	1179.48	0.40	0.05	0.035	106.00
680	1179.38	1179.43	0.40	0.03	0.035	106.00

Table 31: Parameters used for the stream boundary conditions in the Cottonwood Springs models for reaches 681-714.

Reach	Bottom Elevation (m asl)	Top Elevation (m asl)	Width (m)	Slope (m/m)	Rougness Coefficient	Streambed Conductance
681	1179.34	1179.39	0.40	0.03	0.035	106.00
682	1179.30	1179.35	0.40	0.03	0.035	106.00
683	1179.26	1179.31	0.40	0.03	0.035	106.00
684	1179.22	1179.27	0.40	0.04	0.035	106.00
685	1179.17	1179.22	0.40	0.04	0.035	106.00
686	1179.13	1179.18	0.40	0.04	0.035	106.00
687	1179.12	1179.17	0.40	0.04	0.035	106.00
688	1179.06	1179.11	0.40	0.04	0.035	106.00
689	1179.05	1179.10	0.40	0.09	0.035	106.00
690	1178.82	1178.87	0.40	0.09	0.035	106.00
691	1178.69	1178.74	0.40	0.09	0.035	106.00
692	1178.65	1178.70	0.40	0.09	0.035	106.00
693	1178.60	1178.65	0.40	0.09	0.035	106.00
694	1178.59	1178.64	0.40	0.09	0.035	106.00
695	1178.32	1178.37	0.40	0.23	0.035	106.00
696	1178.29	1178.34	0.40	0.23	0.035	106.00
697	1178.06	1178.11	0.40	0.23	0.035	106.00
698	1177.71	1177.76	0.40	0.23	0.035	106.00
699	1177.66	1177.71	0.40	0.07	0.035	106.00
700	1177.62	1177.67	0.40	0.07	0.035	106.00
701	1177.57	1177.62	0.40	0.07	0.035	106.00
702	1177.44	1177.49	0.40	0.07	0.035	106.00
703	1177.43	1177.48	0.40	0.04	0.035	106.00
704	1177.40	1177.45	0.40	0.04	0.035	106.00
705	1177.38	1177.43	0.40	0.04	0.035	106.00
706	1177.35	1177.40	0.40	0.04	0.035	106.00
707	1177.32	1177.37	0.40	0.04	0.035	106.00
708	1177.29	1177.34	0.40	0.04	0.035	106.00
709	1177.21	1177.26	0.40	0.06	0.035	106.00
710	1177.13	1177.18	0.40	0.06	0.035	106.00
711	1177.11	1177.16	0.40	0.06	0.035	106.00
712	1177.10	1177.15	0.40	0.06	0.035	106.00
713	1177.00	1177.05	0.40	0.05	0.035	106.00
714	1176.95	1177.00	0.40	0.05	0.035	106.00

Table 32: Parameters used for the stream boundary conditions in the Cottonwood Springs models for reaches 715-748.

Reach	Bottom Elevation (m asl)	Top Elevation (m asl)	Width (m)	Slope (m/m)	Rougness Coefficient	Streambed Conductance
715	1176.89	1176.94	0.40	0.05	0.035	106.00
716	1176.89	1176.94	0.40	0.05	0.035	106.00
717	1176.85	1176.90	0.40	0.04	0.035	106.00
718	1176.83	1176.88	0.40	0.04	0.035	106.00
719	1176.81	1176.86	0.40	0.04	0.035	106.00
720	1176.79	1176.84	0.40	0.04	0.035	106.00
721	1176.75	1176.80	0.40	0.05	0.035	106.00
722	1176.71	1176.76	0.40	0.05	0.035	106.00
723	1176.67	1176.72	0.40	0.05	0.035	106.00
724	1176.63	1176.68	0.40	0.05	0.035	106.00
725	1176.60	1176.65	0.40	0.05	0.035	106.00
726	1176.56	1176.61	0.40	0.05	0.035	106.00
727	1176.53	1176.58	0.40	0.05	0.035	106.00
728	1176.54	1176.59	0.40	0.03	0.035	106.00
729	1176.47	1176.52	0.40	0.03	0.035	106.00
730	1176.45	1176.50	0.40	0.03	0.035	106.00
731	1176.41	1176.46	0.40	0.03	0.035	106.00
732	1176.37	1176.42	0.40	0.03	0.035	106.00
733	1176.33	1176.38	0.40	0.03	0.035	106.00
734	1176.27	1176.32	0.40	0.03	0.035	106.00
735	1176.20	1176.25	0.40	0.03	0.035	106.00
736	1176.15	1176.20	0.40	0.06	0.035	106.00
737	1176.09	1176.14	0.40	0.06	0.035	106.00
738	1176.02	1176.07	0.40	0.06	0.035	106.00
739	1176.00	1176.05	0.40	0.04	0.035	106.00
740	1175.98	1176.03	0.40	0.04	0.035	106.00
741	1175.86	1175.91	0.40	0.04	0.035	106.00
742	1175.85	1175.90	0.40	0.04	0.035	106.00
743	1175.85	1175.90	0.40	0.04	0.035	106.00
744	1175.77	1175.82	0.40	0.18	0.035	106.00
745	1175.51	1175.56	0.40	0.18	0.035	106.00
746	1175.32	1175.37	0.40	0.18	0.035	106.00
747	1175.13	1175.18	0.40	0.18	0.035	106.00
748	1175.04	1175.09	0.40	0.18	0.035	106.00

Table 33: Parameters used for the stream boundary conditions in the Cottonwood Springs models for reaches 749-782.

Reach	Bottom Elevation (m asl)	Top Elevation (m asl)	Width (m)	Slope (m/m)	Rougness Coefficient	Streambed Conductance
749	1174.95	1175.00	0.40	0.18	0.035	106.00
750	1174.75	1174.80	0.40	0.21	0.035	106.00
751	1174.49	1174.54	0.40	0.21	0.035	106.00
752	1174.33	1174.38	0.40	0.21	0.035	106.00
753	1174.19	1174.24	0.40	0.21	0.035	106.00
754	1174.05	1174.10	0.40	0.21	0.035	106.00
755	1173.96	1174.01	0.40	0.04	0.035	106.00
756	1173.94	1173.99	0.40	0.04	0.035	106.00
757	1173.91	1173.96	0.40	0.04	0.035	106.00
758	1173.89	1173.94	0.40	0.04	0.035	106.00
759	1173.87	1173.92	0.40	0.04	0.035	106.00
760	1173.84	1173.89	0.40	0.04	0.035	106.00
761	1173.77	1173.82	0.40	0.04	0.035	106.00
762	1173.67	1173.72	0.40	0.10	0.035	106.00
763	1173.51	1173.56	0.40	0.10	0.035	106.00
764	1173.46	1173.51	0.40	0.10	0.035	106.00
765	1173.42	1173.47	0.40	0.10	0.035	106.00
766	1173.33	1173.38	0.40	0.10	0.035	106.00
767	1173.24	1173.29	0.40	0.10	0.035	106.00
768	1173.22	1173.27	0.40	0.10	0.035	106.00
769	1173.18	1173.23	0.40	0.12	0.035	106.00
770	1173.09	1173.14	0.40	0.12	0.035	106.00
771	1173.01	1173.06	0.40	0.12	0.035	106.00
772	1172.93	1172.98	0.40	0.12	0.035	106.00
773	1172.95	1173.00	0.40	0.01	0.035	106.00
774	1172.94	1172.99	0.40	0.01	0.035	106.00
775	1172.92	1172.97	0.40	0.01	0.035	106.00
776	1172.90	1172.95	0.40	0.01	0.035	106.00
777	1172.87	1172.92	0.40	0.01	0.035	106.00
778	1172.83	1172.88	0.40	0.02	0.035	106.00
779	1172.80	1172.85	0.40	0.02	0.035	106.00
780	1172.77	1172.82	0.40	0.02	0.035	106.00
781	1172.75	1172.80	0.40	0.02	0.035	106.00
782	1172.74	1172.79	0.40	0.02	0.035	106.00

Table 34: Parameters used for the stream boundary conditions in the Cottonwood Springs models for reaches 783-816.

Reach	Bottom Elevation (m asl)	Top Elevation (m asl)	Width (m)	Slope (m/m)	Rougness Coefficient	Streambed Conductance
783	1172.72	1172.77	0.40	0.02	0.035	106.00
784	1172.70	1172.75	0.40	0.03	0.035	106.00
785	1172.67	1172.72	0.40	0.03	0.035	106.00
786	1172.64	1172.69	0.40	0.03	0.035	106.00
787	1172.61	1172.66	0.40	0.03	0.035	106.00
788	1172.59	1172.64	0.40	0.03	0.035	106.00
789	1172.53	1172.58	0.40	0.06	0.035	106.00
790	1172.46	1172.51	0.40	0.06	0.035	106.00
791	1172.42	1172.47	0.40	0.06	0.035	106.00
792	1172.38	1172.43	0.40	0.06	0.035	106.00
793	1172.35	1172.40	0.40	0.05	0.035	106.00
794	1172.32	1172.37	0.40	0.05	0.035	106.00
795	1172.30	1172.35	0.40	0.05	0.035	106.00
796	1172.28	1172.33	0.40	0.05	0.035	106.00
797	1172.25	1172.30	0.35	0.06	0.035	106.00
798	1172.23	1172.28	0.35	0.06	0.035	106.00
799	1172.13	1172.18	0.35	0.06	0.035	106.00
800	1172.04	1172.09	0.35	0.06	0.035	106.00
801	1172.00	1172.05	0.35	0.02	0.035	106.00
802	1171.98	1172.03	0.35	0.02	0.035	106.00
803	1171.97	1172.02	0.35	0.02	0.035	106.00
804	1171.96	1172.01	0.35	0.02	0.035	106.00
805	1171.96	1172.01	0.35	0.02	0.035	106.00
806	1171.95	1172.00	0.35	0.02	0.035	106.00
807	1171.93	1171.98	0.35	0.02	0.035	106.00
808	1171.93	1171.98	0.35	0.02	0.035	106.00
809	1171.91	1171.96	0.35	0.02	0.035	106.00
810	1171.90	1171.95	0.35	0.02	0.035	106.00
811	1171.81	1171.86	0.35	0.05	0.035	106.00
812	1171.78	1171.83	0.40	0.05	0.035	106.00
813	1171.78	1171.83	0.35	0.05	0.035	106.00
814	1171.72	1171.77	0.35	0.05	0.035	106.00
815	1171.65	1171.70	0.35	0.05	0.035	106.00
816	1171.60	1171.65	0.35	0.05	0.035	106.00

Table 35: Parameters used for the stream boundary conditions in the Cottonwood Springs models for reaches 817-850.

Reach	Bottom Elevation (m asl)	Top Elevation (m asl)	Width (m)	Slope (m/m)	Rougness Coefficient	Streambed Conductance
817	1171.59	1171.64	0.35	0.02	0.035	106.00
818	1171.58	1171.63	0.35	0.02	0.035	106.00
819	1171.58	1171.63	0.35	0.02	0.035	106.00
820	1171.48	1171.53	0.30	0.06	0.035	106.00
821	1171.43	1171.48	0.30	0.06	0.035	106.00
822	1171.38	1171.43	0.30	0.06	0.035	106.00
823	1171.33	1171.38	0.30	0.06	0.035	106.00
824	1171.21	1171.26	0.30	0.06	0.035	106.00
825	1171.24	1171.29	0.30	0.09	0.035	106.00
826	1171.27	1171.32	0.30	0.09	0.035	106.00
827	1171.20	1171.25	0.30	0.09	0.035	106.00
828	1171.00	1171.05	0.30	0.09	0.035	106.00
829	1170.89	1170.94	0.30	0.04	0.035	106.00
830	1170.83	1170.88	0.30	0.04	0.035	106.00
831	1170.81	1170.86	0.30	0.04	0.035	106.00
832	1170.79	1170.84	0.30	0.04	0.035	106.00
833	1170.77	1170.82	0.30	0.04	0.035	106.00
834	1170.74	1170.79	0.30	0.04	0.035	106.00
835	1170.72	1170.77	0.30	0.04	0.035	106.00
836	1170.70	1170.75	0.30	0.04	0.035	106.00
837	1170.50	1170.55	0.30	0.05	0.035	106.00
838	1170.45	1170.50	0.30	0.05	0.035	106.00
839	1170.44	1170.49	0.30	0.05	0.035	106.00
840	1170.42	1170.47	0.30	0.05	0.035	106.00
841	1170.39	1170.44	0.30	0.05	0.035	106.00
842	1170.28	1170.33	0.30	0.04	0.035	106.00
843	1170.26	1170.31	0.30	0.04	0.035	106.00
844	1170.25	1170.30	0.30	0.04	0.035	106.00
845	1170.23	1170.28	0.30	0.04	0.035	106.00
846	1170.21	1170.26	0.30	0.04	0.035	106.00
847	1170.11	1170.16	0.30	0.03	0.035	106.00
848	1170.10	1170.15	0.30	0.03	0.035	106.00
849	1170.09	1170.14	0.30	0.03	0.035	106.00
850	1170.09	1170.14	0.30	0.03	0.035	106.00

Table 36: Parameters used for the stream boundary conditions in the Cottonwood Springs models for reaches 851-884.

Reach	Bottom Elevation (m asl)	Top Elevation (m asl)	Width (m)	Slope (m/m)	Rougness Coefficient	Streambed Conductance
851	1170.08	1170.13	0.30	0.03	0.035	106.00
852	1170.04	1170.09	0.30	0.03	0.035	106.00
853	1170.03	1170.08	0.35	0.02	0.035	106.00
854	1170.03	1170.08	0.35	0.02	0.035	106.00
855	1170.02	1170.07	0.35	0.02	0.035	106.00
856	1169.99	1170.04	0.35	0.02	0.035	106.00
857	1169.95	1170.00	0.35	0.04	0.035	106.00
858	1169.90	1169.95	0.35	0.04	0.035	106.00
859	1169.86	1169.91	0.35	0.04	0.035	106.00
860	1169.85	1169.90	0.35	0.04	0.035	106.00
861	1169.83	1169.88	0.35	0.04	0.035	106.00
862	1169.82	1169.87	0.35	0.04	0.035	106.00
863	1169.72	1169.77	0.35	0.04	0.035	106.00
864	1169.69	1169.74	0.35	0.10	0.035	106.00
865	1169.66	1169.71	0.35	0.10	0.035	106.00
866	1169.42	1169.47	0.35	0.10	0.035	106.00
867	1169.35	1169.40	0.35	0.02	0.035	106.00
868	1169.36	1169.41	0.35	0.02	0.035	106.00
869	1169.36	1169.41	0.35	0.02	0.035	106.00
870	1169.35	1169.40	0.35	0.02	0.035	106.00
871	1169.33	1169.38	0.40	0.02	0.035	106.00
872	1169.27	1169.32	0.40	0.04	0.035	106.00
873	1169.24	1169.29	0.40	0.04	0.035	106.00
874	1169.20	1169.25	0.40	0.04	0.035	106.00
875	1169.21	1169.26	0.40	0.04	0.035	106.00
876	1169.22	1169.27	0.40	0.04	0.035	106.00
877	1169.23	1169.28	0.40	0.04	0.035	106.00
878	1169.09	1169.14	0.40	0.04	0.035	106.00
879	1168.89	1168.94	0.40	0.11	0.035	106.00
880	1168.88	1168.93	0.40	0.11	0.035	106.00
881	1168.27	1168.32	0.45	0.12	0.035	106.00
882	1168.32	1168.37	0.45	0.12	0.035	106.00
883	1168.33	1168.38	0.45	0.12	0.035	106.00
884	1168.25	1168.30	0.45	0.12	0.035	106.00

Table 37: Parameters used for the stream boundary conditions in the Cottonwood Springs models for reaches 885-918.

Reach	Bottom Elevation (m asl)	Top Elevation (m asl)	Width (m)	Slope (m/m)	Rougness Coefficient	Streambed Conductance
885	1168.17	1168.22	0.45	0.12	0.035	106.00
886	1168.12	1168.17	0.45	0.04	0.035	106.00
887	1168.07	1168.12	0.45	0.04	0.035	106.00
888	1168.05	1168.10	0.45	0.04	0.035	106.00
889	1167.98	1168.03	0.45	0.04	0.035	106.00
890	1167.91	1167.96	0.45	0.04	0.035	106.00
891	1167.88	1167.93	0.45	0.04	0.035	106.00
892	1167.85	1167.90	0.45	0.04	0.035	106.00
893	1167.66	1167.71	0.45	0.09	0.035	106.00
894	1167.60	1167.65	0.45	0.09	0.035	106.00
895	1167.53	1167.58	0.45	0.09	0.035	106.00
896	1167.50	1167.55	0.45	0.09	0.035	106.00
897	1167.47	1167.52	0.45	0.09	0.035	106.00
898	1167.44	1167.49	0.45	0.09	0.035	106.00
899	1167.30	1167.35	0.45	0.09	0.035	106.00
900	1167.16	1167.21	0.45	0.09	0.035	106.00
901	1167.18	1167.23	0.45	0.03	0.035	106.00
902	1167.15	1167.20	0.45	0.03	0.035	106.00
903	1167.12	1167.17	0.45	0.03	0.035	106.00
904	1167.05	1167.10	0.45	0.03	0.035	106.00
905	1166.99	1167.04	0.45	0.02	0.035	106.00
906	1166.98	1167.03	0.45	0.02	0.035	106.00
907	1166.98	1167.03	0.45	0.02	0.035	106.00
908	1166.97	1167.02	0.45	0.02	0.035	106.00
909	1166.94	1166.99	0.45	0.11	0.035	106.00
910	1166.91	1166.96	0.45	0.11	0.035	106.00
911	1166.52	1166.57	0.45	0.11	0.035	106.00
912	1166.30	1166.35	0.45	0.11	0.035	106.00
913	1166.30	1166.35	0.45	0.13	0.035	106.00
914	1166.30	1166.35	0.45	0.13	0.035	106.00
915	1166.20	1166.25	0.45	0.13	0.035	106.00
916	1166.16	1166.21	0.45	0.13	0.035	106.00
917	1166.00	1166.05	0.45	0.13	0.035	106.00
918	1165.83	1165.88	0.45	0.13	0.035	106.00

Table 38: Parameters used for the stream boundary conditions in the Cottonwood Springs models for reaches 919-946.

Reach	Bottom Elevation (m asl)	Top Elevation (m asl)	Width (m)	Slope (m/m)	Rougness Coefficient	Streambed Conductance
919	1165.82	1165.87	0.45	0.16	0.035	106.00
920	1165.76	1165.81	0.45	0.16	0.035	106.00
921	1165.20	1165.25	0.45	0.16	0.035	106.00
922	1165.18	1165.23	0.45	0.16	0.035	106.00
923	1164.93	1164.98	0.45	0.07	0.035	106.00
924	1164.94	1164.99	0.45	0.07	0.035	106.00
925	1164.92	1164.97	0.45	0.07	0.035	106.00
926	1164.87	1164.92	0.45	0.04	0.035	106.00
927	1164.83	1164.88	0.45	0.04	0.035	106.00
928	1164.80	1164.85	0.45	0.04	0.035	106.00
929	1164.77	1164.82	0.45	0.05	0.035	106.00
930	1164.70	1164.75	0.45	0.05	0.035	106.00
931	1164.71	1164.76	0.45	0.05	0.035	106.00
932	1164.72	1164.77	0.45	0.05	0.035	106.00
933	1164.60	1164.65	0.45	0.05	0.035	106.00
934	1164.56	1164.61	0.45	0.02	0.035	106.00
935	1164.56	1164.61	0.45	0.02	0.035	106.00
936	1164.56	1164.61	0.45	0.02	0.035	106.00
937	1164.49	1164.54	0.45	0.08	0.035	106.00
938	1164.46	1164.51	0.45	0.08	0.035	106.00
939	1164.44	1164.49	0.45	0.08	0.035	106.00
940	1164.21	1164.26	0.45	0.08	0.035	106.00
941	1164.16	1164.21	0.45	0.08	0.035	106.00
942	1164.14	1164.19	0.45	0.04	0.035	106.00
943	1164.11	1164.16	0.45	0.04	0.035	106.00
944	1164.07	1164.12	0.45	0.04	0.035	106.00
945	1164.03	1164.08	0.45	0.04	0.035	106.00
946	1164.00	1164.05	0.45	0.04	0.035	106.00

APPENDIX B

Surveyed channel cross sections at Cottonwood Creek used to estimate channel morphologic parameters. Vertical exaggeration is 3.2 X.

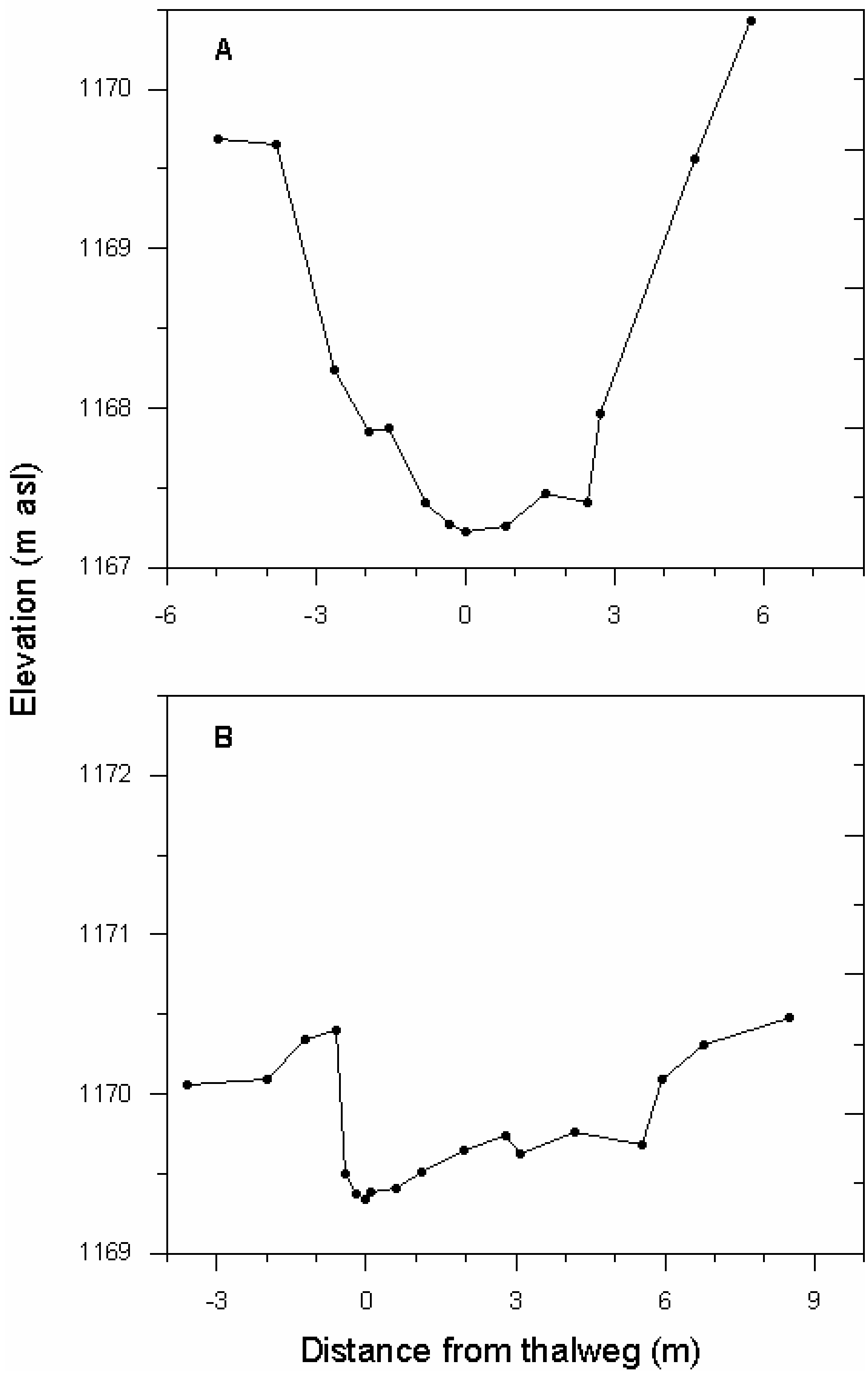

Figure 24: Surveyed channel cross sections at Cottonwood Creek; (A) section 1, (B) section 2.

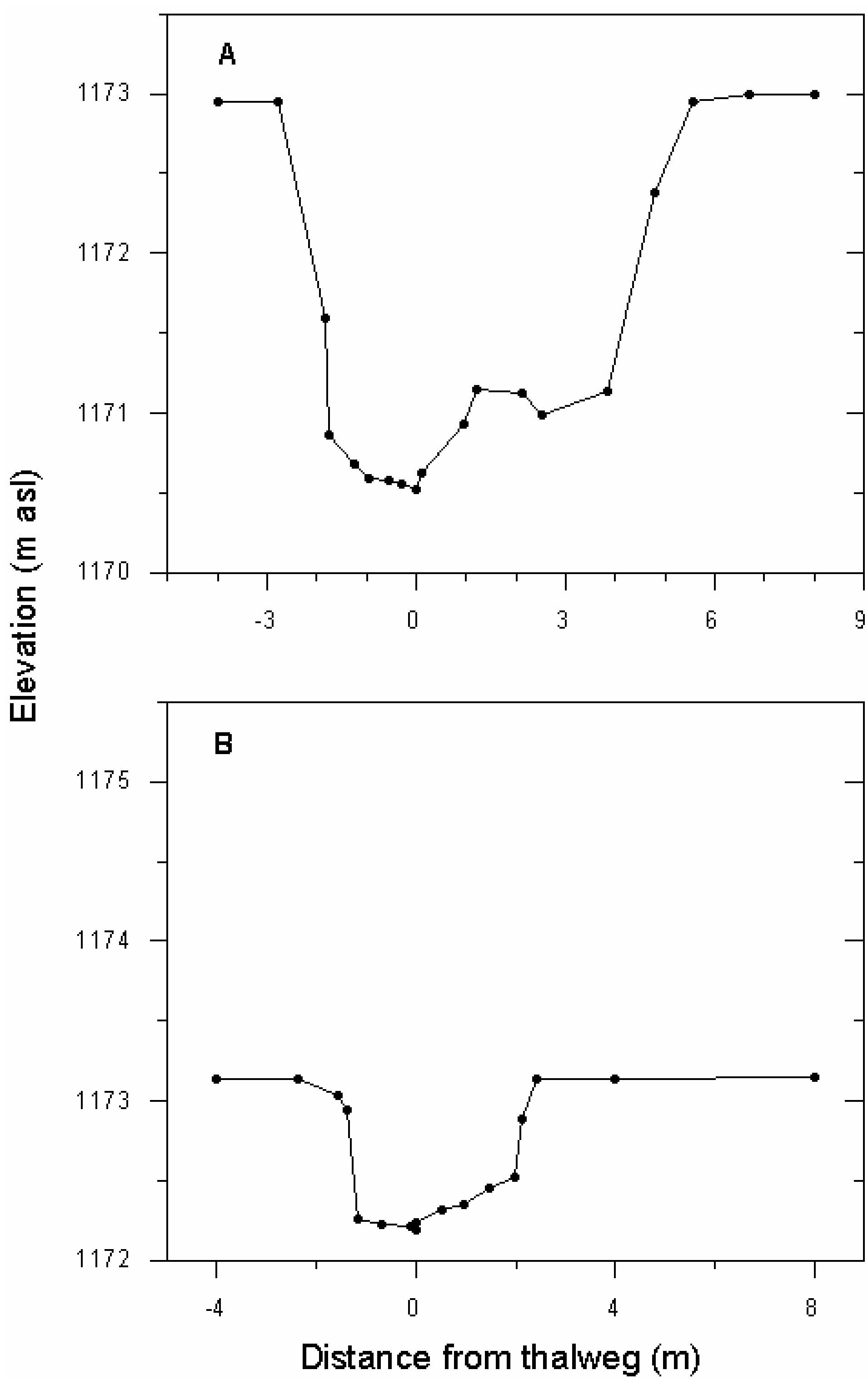

Figure 25: Surveyed channel cross sections at Cottonwood Creek; (A) section 3, (B) section 4.

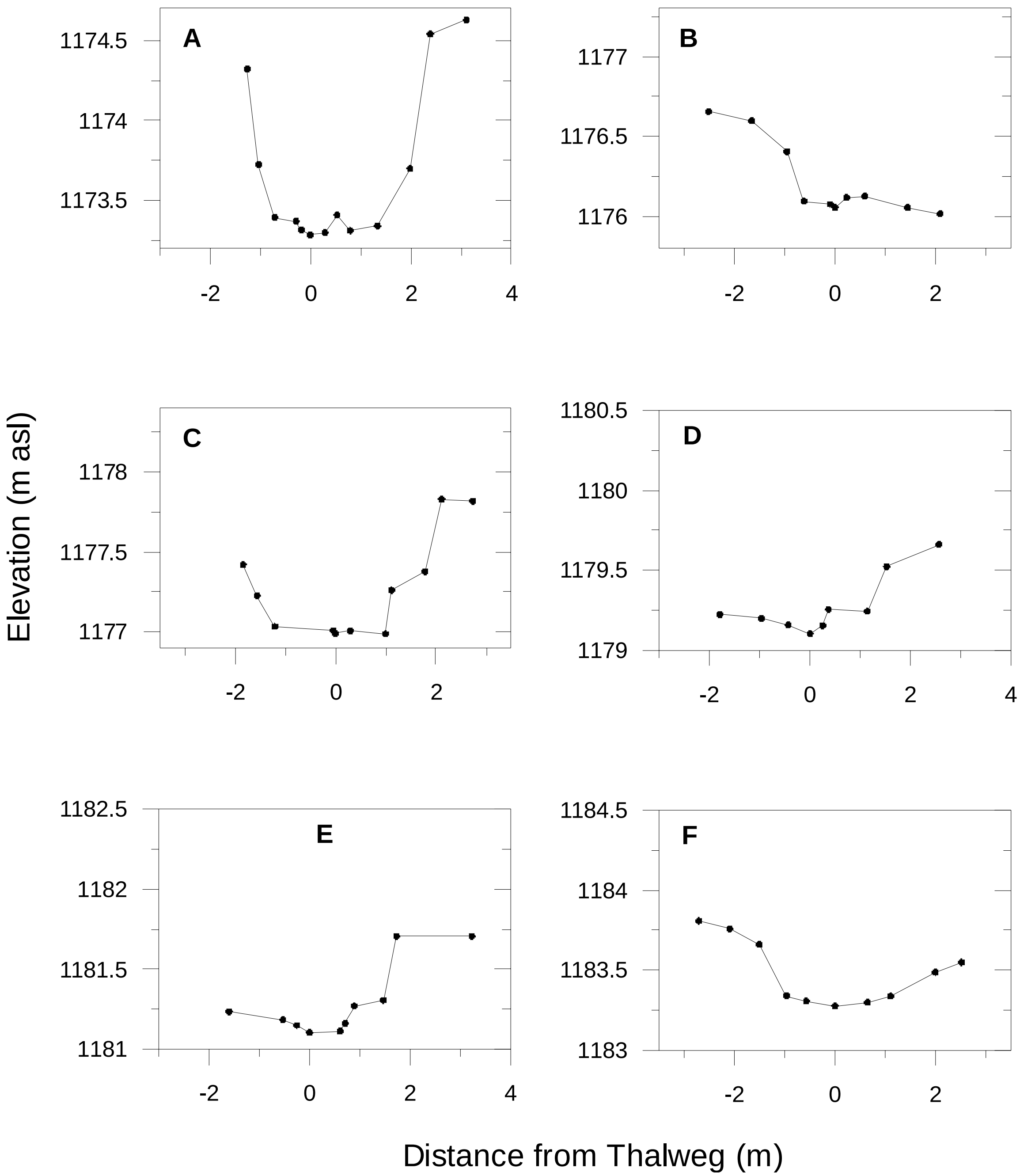

Figure 26: Surveyed channel cross sections at Cottonwood Creek; (A) section 5, (B) section 6, (C) section 7, (D) section 8, (E) section 9, (F) section 10.

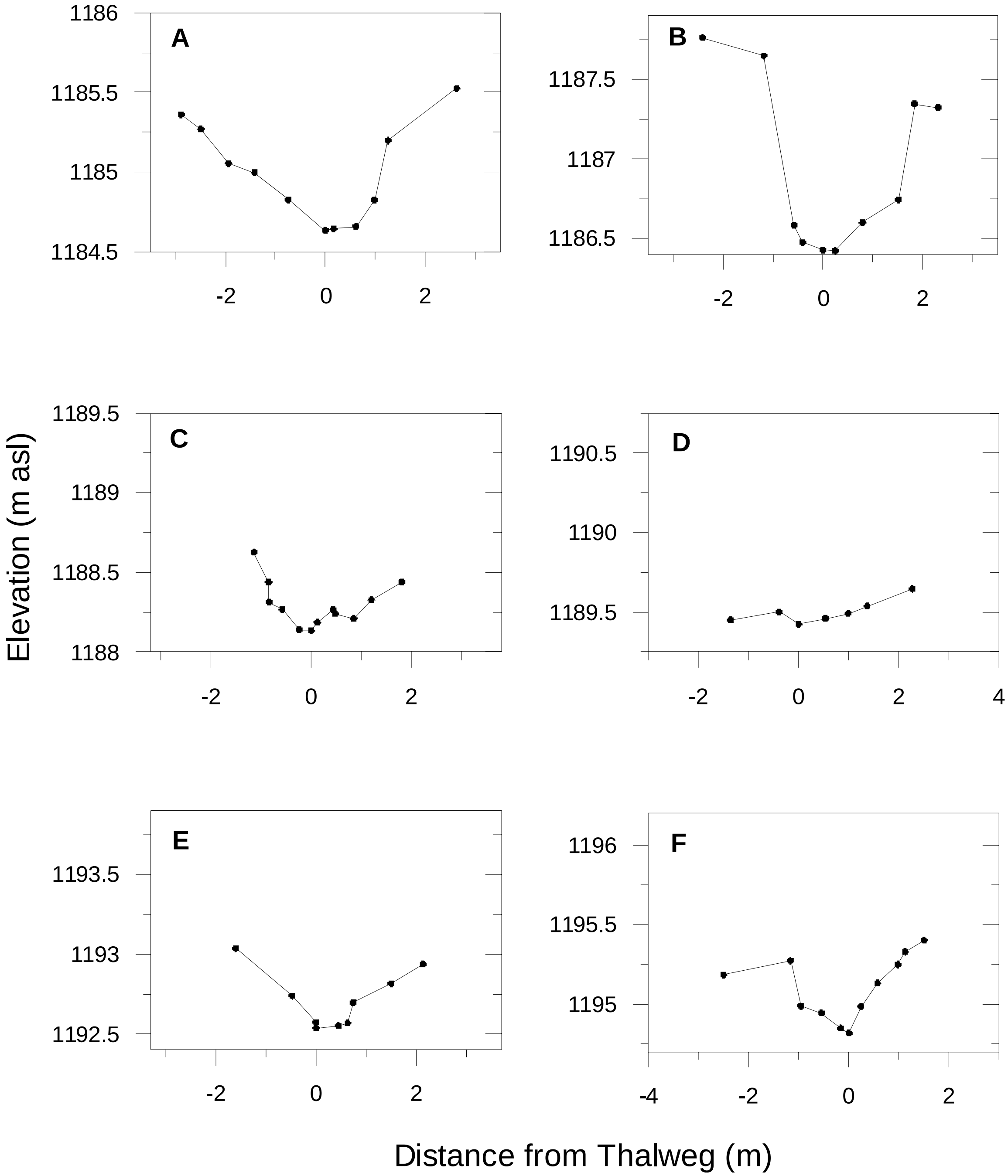

Figure 27: Surveyed channel cross sections at Cottonwood Creek; (A) section 11, (B) section 12, (C) section 13, (D) section 14, (E) section 15, (F) section 16.

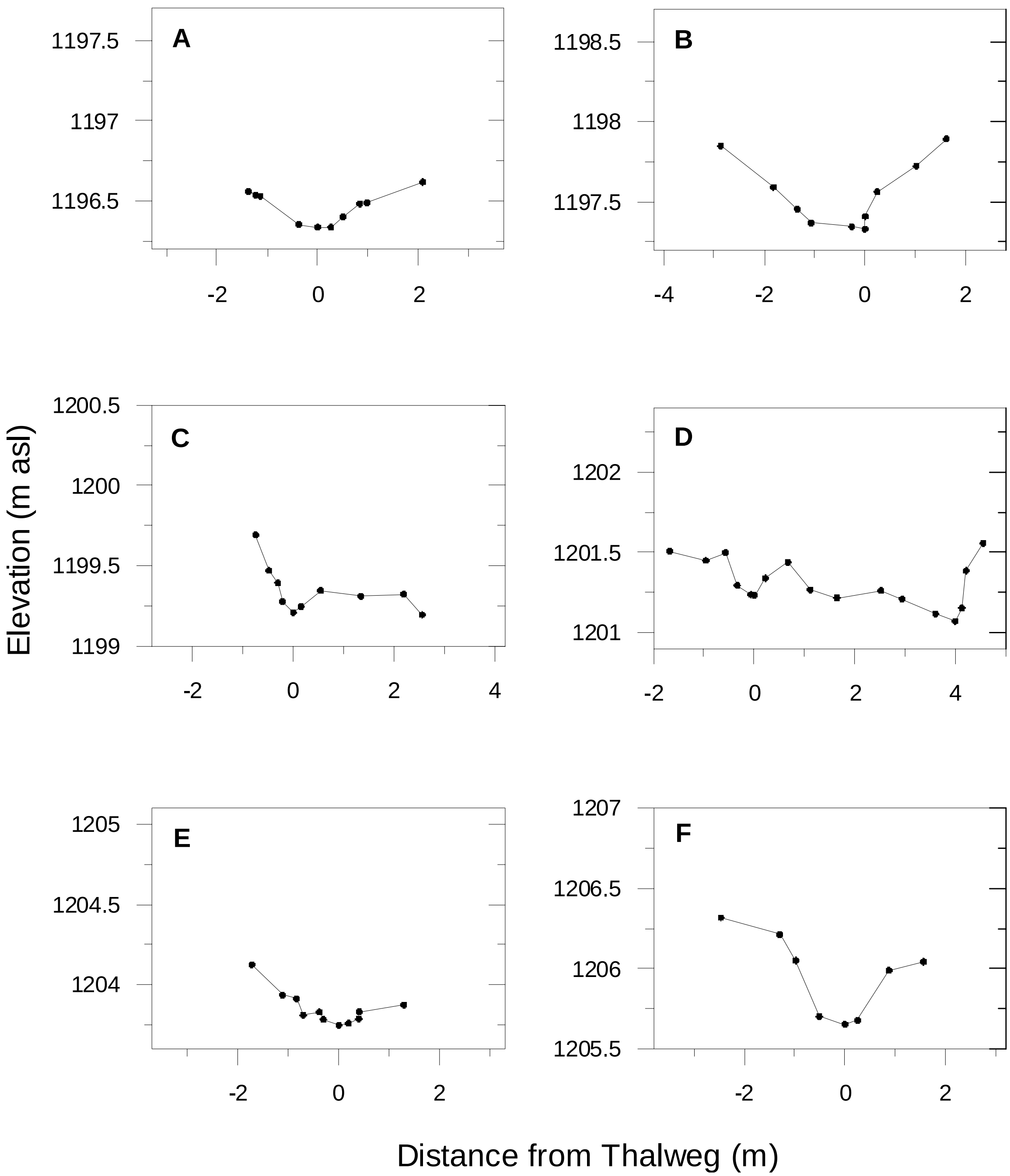

Figure 28: Surveyed channel cross sections at Cottonwood Creek; (A) section 17, (B) section 18, (C) section 19, (D) section 20, (E) section 21, (F) section 22.

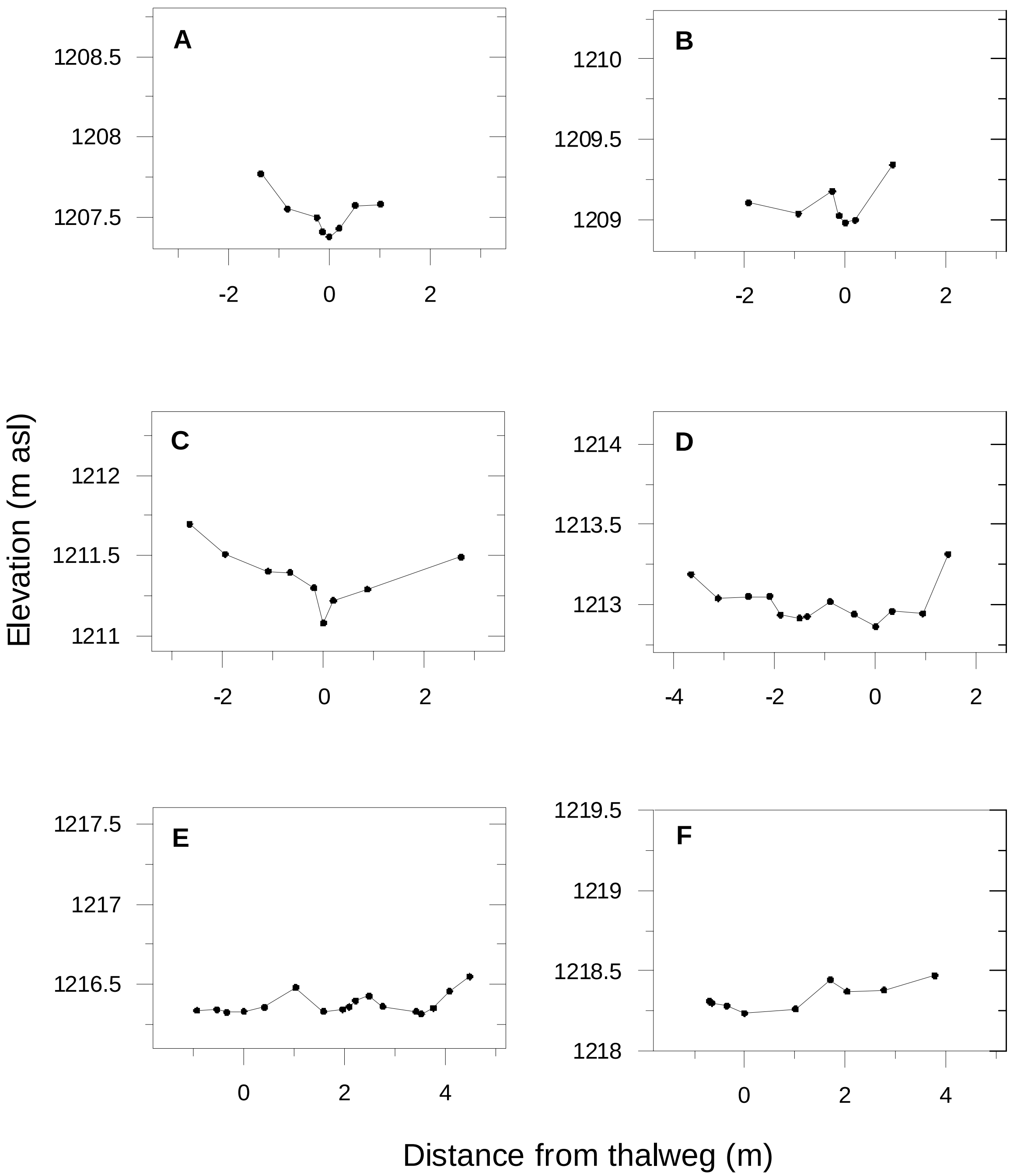

Figure 29: Surveyed channel cross sections at Cottonwood Creek; (A) section 23, (B) section 24, (C) section 25, (D) section 26, (E) section 27, (F) section 28.

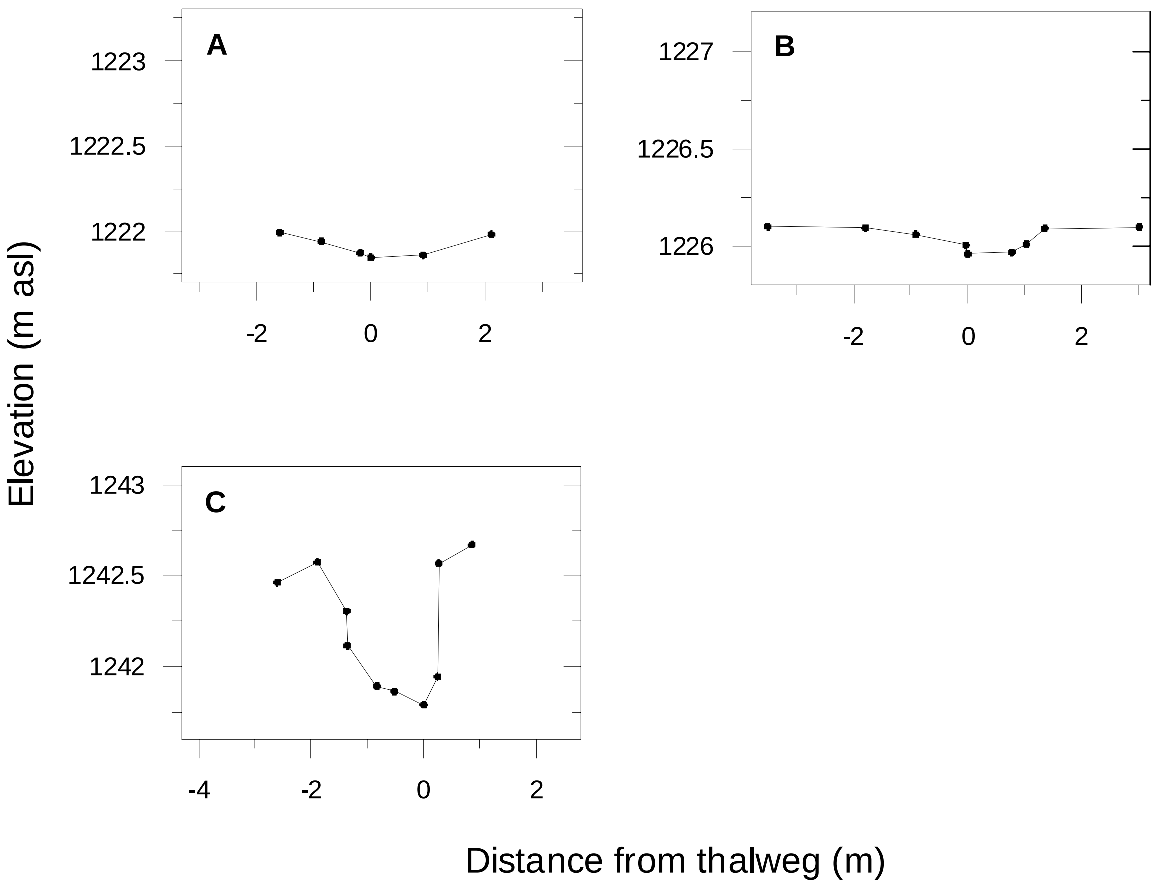

Figure 30: Surveyed channel cross sections at Cottonwood Creek; (A) section 29, (B) section 30, (C) section 31.

APPENDIX C

Grain-size distributions of dominantly sand-sized samples from Cottonwood Springs.

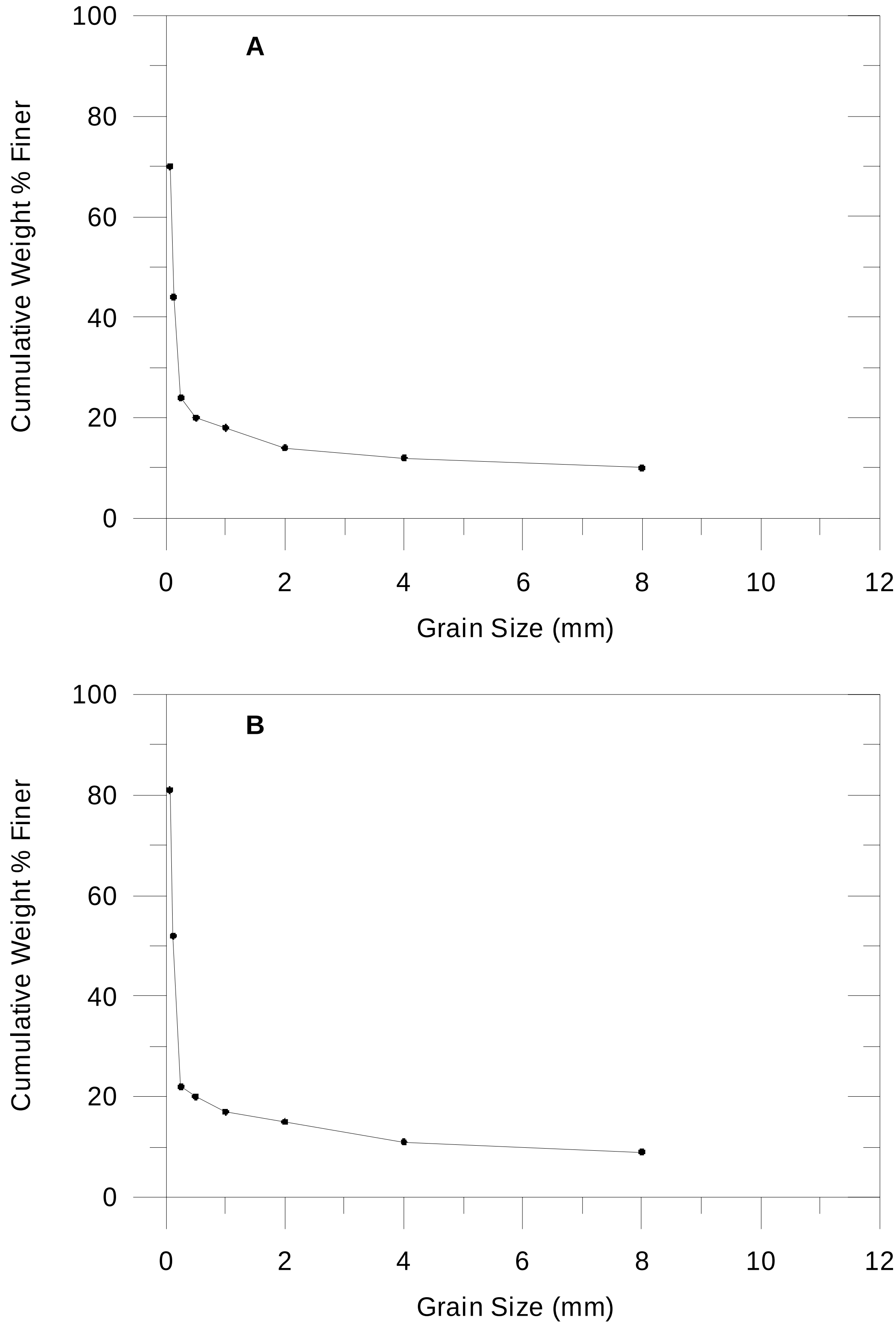

Figure 31: Grain-size distribution curves used to determine the d_{50} grain-size for samples from (A) Qs1 at well DS, and (B) Qt1 near discharge station 9 (see Fig. 6 and Plate 1a).

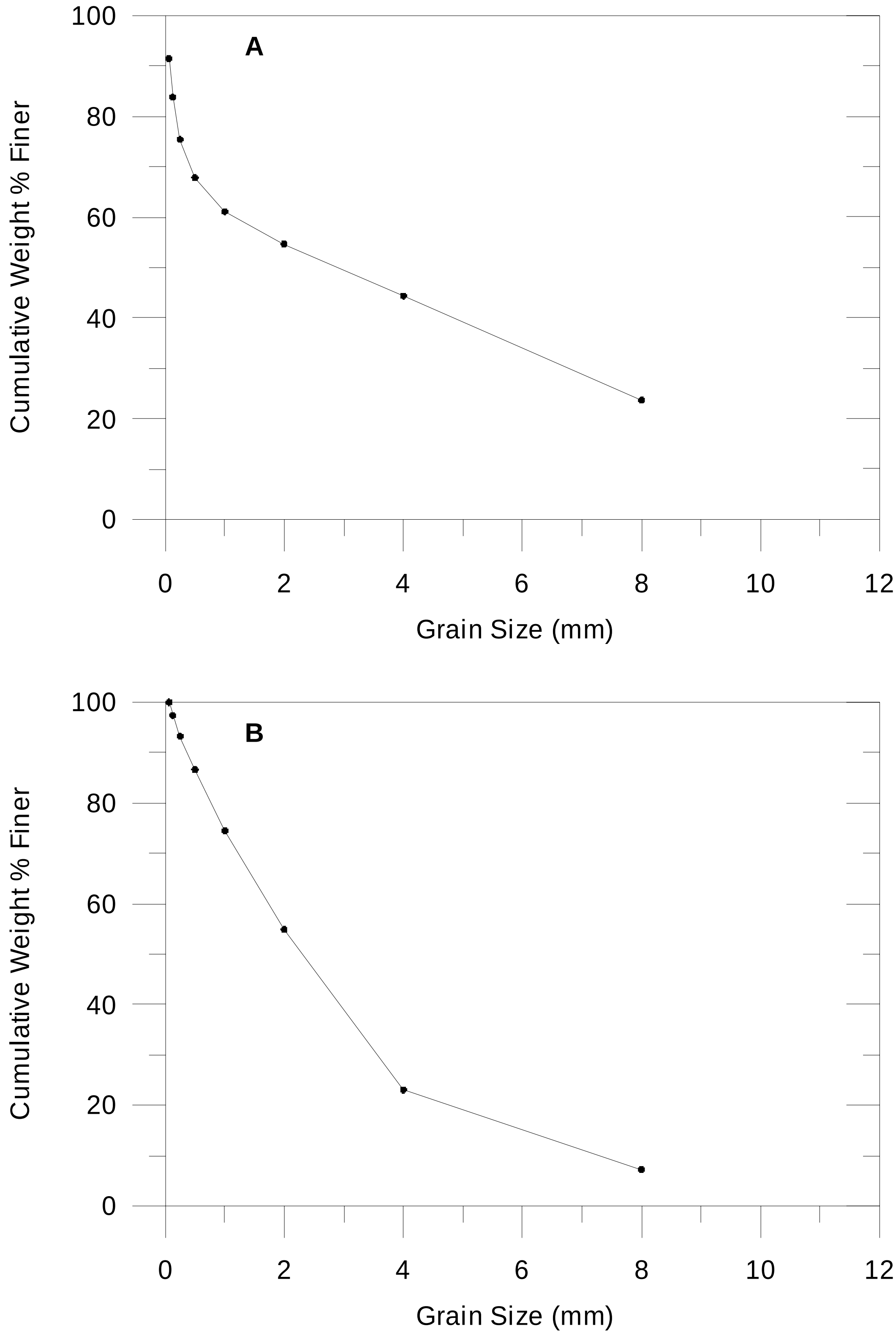

Figure 32: Grain-size distribution curves used to determine the d_{50} grain-size for samples from (A) Qs2 at well DW, and (B) Qt2 near USGS gauge (see Fig. 6 and Plate 1a).

APPENDIX D

Stream discharge measurements at Cottonwood Springs discharge stations.

Table 39: Stream discharge measurements at Cottonwood Springs discharge stations 1-10. Measurements are in m^3/day. See Fig. 6 and Plate 1a for locations.

Station #	1	2	3	4	5	6	7	8	9	10
2/9/2003	-	34.8	3.8	7.4	-	-	-	-	-	-
3/21/2003	-	37.6	3.8	4.0	32.2	-	27.8	27.9	3.0	2.3
4/26/2003	-	16.2	0.0	0.7	5.5	-	2.0	2.1	0.0	0.7
6/7/2003	-	0.0	0.0	0.0	0.0	-	0.0	0.0	0.0	0.0
7/20/2003	-	0.0	0.0	0.0	0.0	-	0.0	0.0	0.0	0.0
9/12/2003	5.5	0.0	0.0	0.0	0.0	3.9	0.0	0.0	0.0	0.0
10/23/2003	5.3	0.0	0.0	0.7	2.7	4.2	0.0	0.0	0.0	0.0
1/16/2004	-	33.1	0.0	10.6	36.7	-	11.0	5.3	1.3	0.7
4/18/2004	-	13.8	0.0	0.7	2.4	-	14.8	-	0.0	0.7